AFRL-ML-WP-TR-2001-4100

EVALUATION OF ENVIROSTRIP FOR DEPAINTING THIN-SKINNED ALUMINUM ALLOYS

BARRY S. SPIGEL
JANET BUCHINGHAM
CRAIG McCLUNG

SOUTHWEST RESEARCH INSTITUTE
6220 CULEBRA ROAD
P.O. DRAWER 28510
SAN ANTONIO, TEXAS 78228-0510

OCTOBER 2000

FINAL REPORT FOR PERIOD 01 JULY 1998 – 30 JUNE 1999

Approved for public release; distribution unlimited.

MATERIALS AND MANUFACTURING DIRECTORATE
AIR FORCE RESEARCH LABORATORY
AIR FORCE MATERIEL COMMAND
WRIGHT-PATTERSON AIR FORCE BASE, OH 45433-7750

NOTICE

When Government drawings, specifications, or other data are used for any purpose other than in connection with a definitely related Government procurement operation, the United States Government thereby incurs no responsibility nor any obligation whatsoever; and the fact that the government may have formulated, furnished, or in any way supplied the said drawings, specifications, or other data, is not to be regarded by implication or otherwise as in any manner licensing the holder or any other person or corporation, or conveying any rights or permission to manufacture, use, or sell any patented invention that may in any way be related thereto.

This report has been reviewed by the Office of Public Affairs (ASC/PA) and is releasable to the National Technical Information Service (NTIS). At NTIS, it will be available to the general public, including foreign nations.

This technical report has been reviewed and is approved for publication.

Melvin L. Nowlin

MELVIN L. NOWLIN, MAJ USAF
Project Engineer
Coatings Technology Integration Office
Logistics Systems Support Branch
Systems Support Division

Stephan Wolanczyk

STEPHAN M. WOLANCZYK
Acting Chief
Logistics Systems Support Branch
Systems Support Division

Gary A. Kepple

GARY A. KEPPLE
Assistant Chief
System Support Division
Materials & Manufacturing Directorate

If your address has changed, if you wish to be removed from our mailing list, or if the addressee is no longer employed by your organization please notify AFRL/MLMS, Bldg. 653, 2977 P St., Suite 6, W-PAFB, OH 45433-7739 to help us maintain a current mailing list.

Copies of this report should not be returned unless return is required by security considerations, contractual obligations, or notice on a specific document.

REPORT DOCUMENTATION PAGE

Form Approved
OMB No. 074-0188

1. AGENCY USE ONLY (Leave blank)	2. REPORT DATE	3. REPORT TYPE AND DATES COVERED
	OCTOBER 2000	Final, 07/01/1998 – 06/30/1999

4. TITLE AND SUBTITLE
EVALUATION OF ENVIROSTRIP FOR DEPAINTING THIN-SKINNED ALUMINUM ALLOYS

5. FUNDING NUMBERS
C: F09603-95-D-0176
PE: N/A
PN: N/A
TN: N/A
WU: N/A

6. AUTHOR(S)
BARRY S. SPIGEL
JANET BUCHINGHAM
CRAIG McCLUNG

7. PERFORMING ORGANIZATION NAME(S) AND ADDRESS(ES)
SOUTHWEST RESEARCH INSTITUTE
6220 CULEBRA ROAD
P.O. DRAWER 28510
SAN ANTONIO, TEXAS 78228-0510

8. PERFORMING ORGANIZATION REPORT NUMBER

9. SPONSORING / MONITORING AGENCY NAME(S) AND ADDRESS(ES)
MATERIALS AND MANUFACTURING DIRECTORATE
AIR FORCE RESEARCH LABORATORY
AIR FORCE MATERIEL COMMAND
WRIGHT-PATTERSON AIR FORCE BASE, OH 45433-7750
POC: Major Melvin L. Nowlin, AFRL/MLSSO, (937) 255-0943

10. SPONSORING / MONITORING AGENCY REPORT NUMBER
AFRL-ML-WP-TR-2001-4100

11. SUPPLEMENTARY NOTES

12a. DISTRIBUTION / AVAILABILITY STATEMENT
Approved for public release; distribution unlimited.

12b. DISTRIBUTION CODE

13. ABSTRACT *(Maximum 200 Words)*

An Envirostrip™ wheat starch process was evaluated versus Type V and Polymedia Lite™ plastic media paint removal processes on 0.32-inch aluminum substrates. While some small and statistically significant differences were seen in the mechanical properties of the substrates receiving the three treatments, they were judged to be within the variations expected within the procedures, and not judged to be of engineering significance.

14. SUBJECT TERMS	15. NUMBER OF PAGES
Type V media, PMB, paint removal, wheat starch, Envirostrip, Polymedia Lite, and dry media blasting	114
	16. PRICE CODE

17. SECURITY CLASSIFICATION OF REPORT	18. SECURITY CLASSIFICATION OF THIS PAGE	19. SECURITY CLASSIFICATION OF ABSTRACT	20. LIMITATION OF ABSTRACT
Unclassified	Unclassified	Unclassified	SAR

NSN 7540-01-280-5500

Standard Form 298 (Rev. 2-89)
Prescribed by ANSI Std. Z39-18
298-102

TABLE OF CONTENTS

LIST OF FIGURES iv
LIST OF TABLES vi
EXECUTIVE SUMMARY vii

1. INTRODUCTION 1

2. TEST PROCEDURES AND SPECIMEN 1
   2.1 Test Procedures 1
   2.2 Test Panel and Test Specimen Identification System 2
   2.3 Specimen Dimensions and Test Procedures 3
      2.3.1 Tensile Test Specimens 3
      2.3.2 Fatigue Test Specimens 3
      2.3.3 Fatigue Crack Growth Rate Test 3
   2.4 Envirostrip™ Blasting Parameters 4
   2.5 Statistical Analysis of Test Data 5

3. TENSILE TEST RESULTS 10

4. FATIGUE TEST RESULTS 27

5. FATIGUE CRACK GROWTH RATE (FCGR) TEST RESULTS 38

6. DAMAGE ASSESSMENT TEST RESULTS 57
   6.1 Residual Stress Saturation 57
   6.2 Surface Profile Roughness 58

7. CONCLUSIONS/RECOMMENDATIONS 67

8. REFERENCES 70

APPENDIX A: Letter from CAE to CTIO Specifying the Envirostrip™ Blast Process Parameters A-1

APPENDIX B: Discussion of the Fatigue performance of Blasted 0.032-inch Thick Aluminum Alloys B-1

LIST OF FIGURES

Figure 2.1 Cutting Plan for Panel XB-1 6
Figure 2.2 Cutting Plan for Panel XB-2 6
Figure 2.3 Cutting Plan for Panel XB-3 7
Figure 2.4 Cutting Plan for XB-4 7
Figure 2.5 Cutting Plan for XB-5 8
Figure 2.6 Drawing of Tension Test Specimen 8
Figure 2.7 Drawing of Axial Fatigue Test Specimen 9
Figure 2.8 Drawing of M(T) Fatigue Crack Growth Rate Specimen 9
Figure 3.1 Scatter, Mean, and 90% Confidence Intervals of Offset Yield Stress for Bare 7075-T6 15
Figure 3.2 Scatter, Mean, and 90% Confidence Intervals of Offset Yield Stress for Clad 7075-T6 16
Figure 3.3 Scatter, Mean, and 90% Confidence Intervals of Offset Yield Stress for Bare 2024-T3 17
Figure 3.4 Scatter, Mean, and 90% Confidence Intervals of Offset Yield Stress for Clad 2024-T3 18
Figure 3.5 Scatter, Mean, and 90% Confidence Intervals of Ultimate Strength for Bare 7075-T6 19
Figure 3.6 Scatter, Mean, and 90% Confidence Intervals of Ultimate Strength for Clad 7075-T6 20
Figure 3.7 Scatter, Mean, and 90% Confidence Intervals of Ultimate Strength for Bare 2024-T3 21
Figure 3.8 Scatter, Mean, and 90% Confidence Intervals of Ultimate Strength for Clad 2024-T3 22
Figure 3.9 Scatter, Mean, and 90% Confidence Intervals of Peak Elongation for Bare 7075-T6 23
Figure 3.10 Scatter, Mean, and 90% Confidence Intervals of Peak Elongation for Clad 7075-T6 24
Figure 3.11 Scatter, Mean, and 90% Confidence Intervals of Peak Elongation for Bare 2024-T3 25
Figure 3.12 Scatter, Mean, and 90% Confidence Intervals of Peak Elongation for Clad 2024-T3 26
Figure 4.1 Scatter, Mean, and 90% Confidence Intervals of Cycles to Failure for Bare 7075-T6 34
Figure 4.2 Scatter, Mean, and 90% Confidence Intervals of Cycles to Failure for Clad 7075-T6 35
Figure 4.3 Scatter, Mean, and 90% Confidence Intervals of Cycles to Failure for Bare 2024-T3 36
Figure 4.4 Scatter, Mean, and 90% Confidence Intervals of Cycles to Failure for Clad 2024-T3 37

Figure 5.1 FCGR Test Results for Bare 7075-T6 Control Specimens 45
Figure 5.2 FCGR Test Results for Bare 7075-T6 Blasted Specimens 46
Figure 5.3 FCGR Test Results for Clad 7075-T6 Control Specimens 47
Figure 5.4 FCGR Test Results for Clad 7075-T6 Blasted Specimens 48
Figure 5.5 FCGR Test Results for Bare 2024-T3 Control Specimens 49
Figure 5.6 FCGR Test Results for Bare 2024-T3 Blasted Specimens 50
Figure 5.7 FCGR Test Results for Clad 2024-T3 Control Specimens 51
Figure 5.8 FCGR Test Results for Clad 2024-T3 Blasted Specimens 52
Figure 5.9 Comparison of Control and Blasted FCGR Curves for Bare 7075-T6 53
Figure 5.10 Comparison of Control and Blasted FCGR Curves for Clad 7075-T6 54
Figure 5.11 Comparison of Control and Blasted FCGR Curves for Bare 2024-T3 55
Figure 5.12 Comparison of Control and Blasted FCGR Curves for Clad 2024-T3 56
Figure 6.1 Almen Arc Height Saturation Curves for Type V, Polymedia-Lite™, and Envirostrip™ on 0.032-inch Bare 2024-T3 64
Figure 6.2 Surface Roughness Per Blast Cycle for Type V, Polymedia-Lite™, and Envirostrip™ on Bare 2024-T3 65
Figure 6.3 Surface Roughness Per Blast Cycle for Type V, Polymedia-Lite™, and Envirostrip™ on Clad 2024-T3 66

LIST OF TABLES

Table 2.1 Listing of Aluminum Sheet Materials and Assigned I.D. Code Letters 2
Table 3.1 Tensile Test Results for Bare 7075-T6 12
Table 3.2 Tensile Test Results for Clad 7075-T6 12
Table 3.3 Tensile Test Results for Bare 2024-T3 13
Table 3.4 Tensile Test Results for Clad 2024-T3 13
Table 3.5 Summary of Descriptive Statistics for Tensile Tests for Envirostrip™ 14
Table 3.6 Tensile Test Engineering Summary for Envirostrip™ 14
Table 4.1 Fatigue Test Results for Bare 7075-T6 29
Table 4.2 Fatigue Test Results for Clad 7075-T6 30
Table 4.3 Fatigue Test Results for Bare 2024-T3 31
Table 4.4 Fatigue Test Results for Clad 2024-T3 32
Table 4.5 Fatigue Test Data and Statistical Summary for Envirostrip™ 33
Table 5.1 Fatigue Crack Growth Rate Data and Statistical Analysis Results for 7075-T6 Bare 40
Table 5.2 Fatigue Crack Growth Rate Data and Statistical Analysis Results for 7075-T6 Clad. 41
Table 5.3 Fatigue Crack Growth Rate Data and Statistical Analysis Results for 2024-T3 Bare 42
Table 5.4 Fatigue Crack Growth Rate Data and Statistical Analysis Results for 2024-T3 Clad 43
Table 5.5 FCGR Engineering Summary for Envirostrip™, Polymedia-Lite™, and Type V 44
Table 6.1 Residual Stress Arc Heights of 0.032-inch-thick Bare 2024-T3 After Blasting with Dry Media 61
Table 6.2 Surface Profile Roughness Measurements for Bare 2024-T3 Using Type V, Polymedia-Lite™, and Envirostrip 61
Table 6.3 Surface Profile Roughness Measurements for Clad 2024-T3 Using Type V, Polymedia-Lite™, and Envirostrip 62
Table 6.4 Surface Roughness of 0.032-inch Panels Blasted with Envirostrip™ 63

EXECUTIVE SUMMARY

1.0 Introduction

The Flight Training System Program Office and the Air Education Training Command (AETC) currently use a Type V acrylic dry media blasting (DMB) process for the removal of coatings from their aircraft. With the introduction of the T-1A and T-6 aircraft, the manufacturer has recommended a wheatstarch-based DMB process for the T-6, and has further recommended a one-time use only of the Type V DMB process for the T-1A. These recommendations could have major impacts on facilities, schedule, operational cost, and waste disposal for all AETC aircraft. The Program Office and AETC had to determine if there was a requirement or sufficient technical reason beyond the aircraft manufacturer's recommendations to change from a Type V DMB process to a wheatstarch-based process for the T-1A or T-6.

2.0 Approach

Southwest Research Institute (SwRI), under the direction of the US Air Force Coatings Technology Integration Office (CTIO), investigated the effects of an Envirostrip™ wheatstarch process on the same 0.032-inch-thick aluminum substrates that were used to evaluate Type V and Polymedia-Lite™ DMB processes. The aluminum substrate testing included tension, constant-amplitude fatigue, and constant-amplitude fatigue crack growth rate. The test data were analyzed using analysis of variance (ANOVA) techniques wherein the average mechanical property of the Control (unblasted) specimens was compared to the average mechanical property of the Blasted specimens. All statistical tests were made at the ten-percent level of significance. Additional material damage assessment tests included erosion of cladding after blasting, surface profile/roughness measurements, and residual stress/peak saturation data development. The Envirostrip™ test results were compared to test results using Type V and Polymedia-Lite™.

3.0 Results

The tensile test data indicated no degradation of material properties due to stripping with the Envirostrip™ process. The tensile yield stress and ultimate strength data were very precise; a difference of 3 ksi (or less than 4%) in the average measured properties resulted in a statistically significant effect. This difference was within accepted variation due to experimental error and material variability, and for these reasons may not be of practical significance. There were no statistically significant differences in the average elongation for bare and clad 7075-T6 and clad 2024-T3. There was a statistically significant increase in the elongation for bare 2024-T3, but the difference was only 1%. This was also within accepted test variation and may not be of practical significance.

The majority of statistical results for fatigue crack growth rates indicated differences between the Control and Blasted groups. However, the variability in the 7075-T6 and 2024-

T3 materials were generally below the average of the ASTM guidelines on reproducibility, and it was difficult to distinguish any differences in crack growth between Control and Blasted data sets.

The damage assessment test results were: (1) Test specimens blasted with Envirostrip™ reached saturated stress levels after seven blast cycles. The Almen arc height was approximately 0.0058 inch. In contrast, specimens blasted with Polymedia-Lite™ reached saturation after four blast cycles at an arc height of 0.0050 inch, although the number rose slightly to 0.0057 inch after the seventh blast cycle. Specimens blasted with Type V reached saturation after four blast cycles at an arc height of 0.0080 inch. (2) Experimental data indicated that Envirostrip™ did not change the surface roughness of bare 7075-T6 or bare 2024-T3. The roughness on clad 2024-T3 was approximately 70μin after four blast cycles, which was comparable to earlier results with Polymedia-Lite™. Tests on clad 7075-T6 yielded similar results, with the roughness after four blast cycles reaching 80μin.

There was no statistically significant difference in the average fatigue lives from Control to Blasted specimens for bare 7075-T6. There were, however, statistically significant decreases in fatigue lives for clad 7075-T6, and for bare and clad 2024-T3. Unlike the tensile test results, the debits in the fatigue lives were significant from both statistical and engineering points of view. The substantial decreases in fatigue lives prompted further investigations to explore why the debits were observed for the Envirostrip process. These investigations indicated that the fatigue life behavior of blasted surfaces could be understood in terms of the competing effects of beneficial compressive surface residual stresses and harmful surface roughness. The Envirostrip™ blasting process had the most shallow (least beneficial) compressive residual stresses than either Type V or Polymedia-Lite™, and the shallow residual stresses may have been more susceptible to stress relaxation during fatigue cycling. The Envirostrip™ process exhibited higher and more damaging levels of surface roughness than Polymedia-Lite™, but were significantly less than the roughness levels resulting from Type V. No definitive conclusions could be reached about the factors affecting fatigue performance of dry media blasted aluminum alloys, but the available information supported the hypothesis that fatigue performance was influenced by the beneficial effects of compressive residual stresses and the deleterious effects of surface roughness.

4.0 Conclusions/Recommendations

In conclusion, statistical analyses of the tensile and FCGR test results for the Envirostrip process indicated degradation for some material properties; however, the differences were within practical test variation due to experimental error and material variability. Statistical analyses of the fatigue test results indicated degradation for fatigue lives; but the concomitant effects of residual stresses and surface roughness may have influenced the fatigue behavior. These material property test results alone may not be sufficient evidence to change the current AETC DMB process.

Further work would be required to confirm or deny the fatigue life hypothesis, or, if desired, to develop a more fundamental understanding of the problem. No Almen strip

deflection/residual stress tests were conducted with either clad 2024-T3 material or bare or clad 7075-T6, and these would be useful to characterize the residual stresses in the clad layer. It could be particularly interesting to evaluate the residual stresses before and after fatigue cycling, perhaps with Almen strip tests, to make some assessment of the residual stress relaxation due to cycling. A more systematic treatment of the problem could also be performed comparing the residual stresses and the fatigue performance of clad material in the as-blasted condition with blasted material that has been stress relieved (to remove residual stresses) or electropolished (to remove surface roughness). Related to this is the potential impact of the sanding, priming, and repainting operation on the surface roughness of blasted material, and hence on the fatigue performance. Finally, just as shot-peening parameters can be adjusted to optimize the depth and magnitude of the beneficial residual stresses while minimizing surface damage, it may be possible to optimize the blasting parameters in such a way as to improve their post-blast fatigue performance.

1. INTRODUCTION

The Flight Training System Program Office and the Air Education Training Command (AETC) currently use a Type V acrylic dry media blasting (DMB) process for the removal of coatings from their aircraft. With the introduction of the T-1A and T-6 aircraft, the manufacturer has recommended a wheatstarch-based DMB process for the T-6, and has further recommended a one-time use only of Type V for the T-1A. These recommendations could have major impacts on facilities, schedule, operational cost, and waste disposal for all AETC aircraft. The Program Office and AETC had to determine if there was a requirement or sufficient technical reason beyond the aircraft manufacturer's recommendations to change from a Type V DMB process to a wheatstarch-based process for the T-1A or T-6.

Type V can quickly remove paint from a substrate, but it may induce undesirable stress states on the surface of an aluminum panel (as measured by Almen arc heights).[1] Envirostrip™ may not induce as severe a residual stress state, but it generally has a slower coating removal rate and tends to be hygroscopic. Polymedia-Lite™ was introduced to address the disadvantages of Type V and Envirostrip™ and was shown to have strip rates similar to Type V and affect the aluminum surface similar to Envirostrip™.[2]

However, a thorough evaluation of the effects of Envirostrip™ on thin-skinned aluminum substrates had not been conducted. Southwest Research Institute (SwRI), under the direction of the US Air Force Coatings Technology Integration Office (CTIO), investigated the effects of an Envirostrip™ DMB process on the same 0.032-inch-thick aluminum substrates that were used to evaluate Type V and Polymedia-Lite™ DMB processes. The aluminum substrate testing included tension, constant-amplitude fatigue, and constant-amplitude fatigue crack growth rate. Additional material damage assessment tests included erosion of cladding after blasting, surface profile/roughness measurements, and residual stress/peak saturation data development. The Envirostrip™ test results were compared to test results using Type V and Polymedia-Lite™.

2. TEST PROCEDURES AND SPECIMEN

2.1 Test Procedures

The test matrix for the 0.032-inch-thick aluminum alloys is shown in Table 2.1. The tensile, fatigue, and fatigue crack growth rate (FCGR) properties were determined. Replicate baseline and blasted specimens were evaluated for each test method for a total of 192 tests. It is noted that throughout this report, the generic term "blasted," when used by itself, refers to dry media blasting with either Type V, Polymedia-Lite™, or Envirostrip™.

Table 2.1 Listing of Aluminum Sheet Materials and Assigned I.D. Code Letters

Material I.D. Code	Test Material	Number and Type of Tests					
		Control Specimens			Blasted Specimens		
		Tension	Fatigue	FCGR	Tension	Fatigue	FCGR
K	7075-T6 Bare	4	10	10	4	10	10
L	7075-T6 Clad	4	10	10	4	10	10
M	2024-T3 Bare	4	10	10	4	10	10
N	2024-T3 Clad	4	10	10	4	10	10
Totals		16	40	40	16	40	40

2.2 Test Panel and Test Specimen Identification System

A listing of the 0.032-inch-thick aluminum sheet materials and their identification code letters is shown in Table 2.1. The materials were procured in 4 X 12-foot sheets and sheared into 16 X 24-inch test panels by the aluminum supplier. The test panel codes consisted of an XX-X format where:

First X: Material ID Code (per Table 2.1)
Second X: Letter Code, C = Control or B = Blasted
Dash X: Panel Number

The test specimen layout, including several spare coupons, and identification system for each specimen is shown in Figures 2.1 through 2.5. All specimens were excised from the sheet where the specimen's lengthwise orientation was parallel with the rolling direction of each material. The test identification system consisted of an XXXX-X format where:

First X: Media Type, W = Envirostrip™
Second X: Material ID Code (per Table 2.1)
Third X: Condition Code B=Blasted
(Code missing from control specimens)
Fourth X: Letter Code, D = da/dN (fatigue crack growth rate)
F = fatigue
T = tension
Dash X: Specimen Number

2.3 Specimen Dimensions and Test Procedures

2.3.1 Tensile Test Specimens

Tension tests were performed in ambient laboratory air per ASTM Standard B557. The test specimen geometry is shown in Figure 2.6. Four tests from each Control and Blasted panel were conducted for a total of 32 tests. The properties that were determined included yield stress (0.2% offset), ultimate tensile strength, and percent elongation.

2.3.2 Fatigue Test Specimens

Constant-amplitude fatigue tests were performed in ambient laboratory air per ASTM Standard E466. All tests were performed at a stress ratio R of 0.1 and a frequency of 10 Hz. After machining, and prior to testing, the radii and reduced section edges of the test specimens were polished with 600-grit paper to remove nicks, scratches, and other machining marks. The specimens were inspected with a zoom-stereomicroscope (7X to 30X) to insure the quality of the polishing operations.

The test fixtures used clamping grips that provided forward or backward adjustment of the test specimen for alignment purposes. Threaded bolts drilled through the center to accommodate an alignment pin that also passed through the grip end of the test specimen accomplished this. The bolts were rounded on the internal ends and engaged grip platens machined with matching spherical seats. This feature also promoted even gripping of the test specimen. Additional clamping force was achieved by tightening four through-the-grip bolts. The alignment was checked with specimens prepared with two sets of back-to-back strain gages mounted on each side of the specimen's test section.

Following the alignment procedures, the initial fatigue tests were performed on Control specimens to experimentally determine the stress range that produced total specimen failure after approximately 100,000 sinusoidal load cycles at an R of 0.1. The established stress range was then applied to at least ten specimens taken from the designated Control and Blasted panels. All the fatigue specimens were tested utilizing the identical testing system and established procedures.

A drawing of the test specimen geometry is shown in Figure 2.7.

2.3.3 Fatigue Crack Growth Rate Test

Constant-amplitude FCGR tests were performed in ambient laboratory air per ASTM E647. The tests were conducted at an R of 0.1 and a frequency of 10 Hz. The center crack test specimens were machined in accordance with the drawing shown in Figure 2.8. Two MTS closed-loop servo-hydraulic testing systems were utilized for the tests. The test systems

were calibrated using standards traceable to the National Institute of Standards and Technology. Alignment was verified on each test frame prior to starting the fatigue testing.

The crack measurements were made using the indirect DC potential drop technique developed by Hartrun Corporation. The technique incorporated Krak-Gages that were thin, brittle, metallic foils bonded to an equally brittle, non-conducting backing, and were similar to a conventional strain-gage. The Krak-Gages were bonded to a test specimen surface and simultaneously cracked along with the cracking in the test coupon. With application of a constant gage current, an increase in crack length increased the resistance of the gage resulting in an increase in the gage output voltage. The gages were designed to provide a linear relationship between crack length and output voltage. Excitation, conditioning, and calibration of the gages were accomplished with Model No. 1288 Fractomat amplifiers. The tests were controlled and data was acquired using Fracture Technology Associates software.

The testing of the 0.032-inch thick sheets of material required Part No. B30 Krak-Gages be mounted on only one side of the test specimen. Two gages, one on each side of the centerline, were used. Gages on Blasted specimens were mounted on the non-Blasted side. Control and Blasted specimens were prepared and tested utilizing the automated system described.

Ten tests were planned for Control and Blasted panels taken from each test media. The test data covered a stress intensity range (ΔK) from approximately 6.4 to 16 ksi-$\sqrt{\text{inch}}$. This provided an overlap at each end of the data to be analyzed; that is, the analysis included ΔK values ranging from 7 to 15 ksi-$\sqrt{\text{inch}}$. Visual crack measurements were included during each test to verify the automatically determined crack lengths. These measurements were made, as a minimum, at the beginning of the test (following precracking). SwRI's experience with the Krak-Gage/Fractomat System has shown crack length measurement accuracy well within the validity requirements of ASTM E647. Test results that did not meet all the validity requirements of ASTM E647 were discarded and a retest was initiated.

The test data were reported in a tabular format that included crack length, cycles, *da/dN*, ΔK, and all other information pertinent to ASTM E647. Plots of *da/dN* versus ΔK were provided along with summary plots that compare data from each group of tests.

2.4 Envirostrip™ Blasting Parameters

A study of Envirostrip™ performance characteristics by the media vendor demonstrated a coating removal rate of 0.75 square feet/minute on clad aluminum at a nozzle pressure of 40 psi, a stand-off distance of 3 inches, and a traverse velocity of the nozzle across the panel at 1.8 inches/second. A coating removal rate of 0.83 square feet/minute was achieved on bare aluminum using the same pressure and stand-off distance, but at a faster traverse velocity of 2.0 inches/second. The letter specifying these parameters from CAE

Electronics Ltd. to the CTIO is given in Appendix A. In accordance with this letter, SwRI used the following stripping parameters:

Nozzle Diameter:	0.5 inch
Nozzle Pressure:	40 psi
Stand-Off Distance:	3 inches
Angle of Attack:	45 degrees
Media Flow Rate:	12 lb/min

The test panels were placed on a stand in front of an X-Y positioner. The nozzle was attached to the X-Y positioner and oriented at 45 degrees to the panel face. A 1.8 inch/second traverse velocity was used on the clad aluminum substrates and a 2.0 inch/second velocity was used on the bare aluminum. Since the panels were not painted, SwRI was unable to verify either the 0.75 or 0.83 square feet/minute strip rates.

The test panels were not prepared in any way; the panels were neither etched nor sanded in preparation for painting, nor were they painted. The media was applied to the as-received panels. This represented a worst-case condition to have the panels completely unprepared.

2.5 Statistical Analysis of Test Data

The test data were analyzed to determine if any statistically significant change in mechanical properties existed when comparing results from Control specimens to those obtained from Blasted specimens. Test data were analyzed using classical analyses of variance (ANOVA) techniques wherein the average mechanical property of the Control specimens was compared to the average mechanical property of the Blasted specimens. All statistical tests were made at the 10% level of significance.

ANOVA results were tabulated, and graphical plots of 90% confidence intervals about the average response for the Control and Blast cycles were generated.

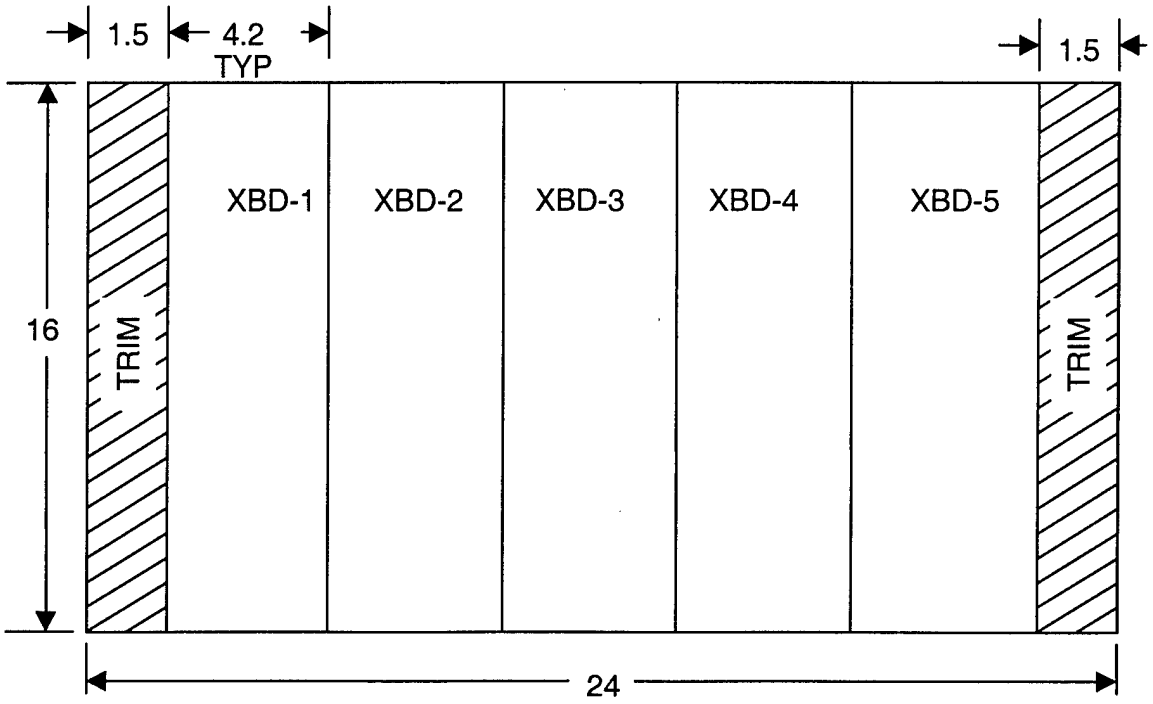

Figure 2.1 Cutting Plan for Panel XB-1

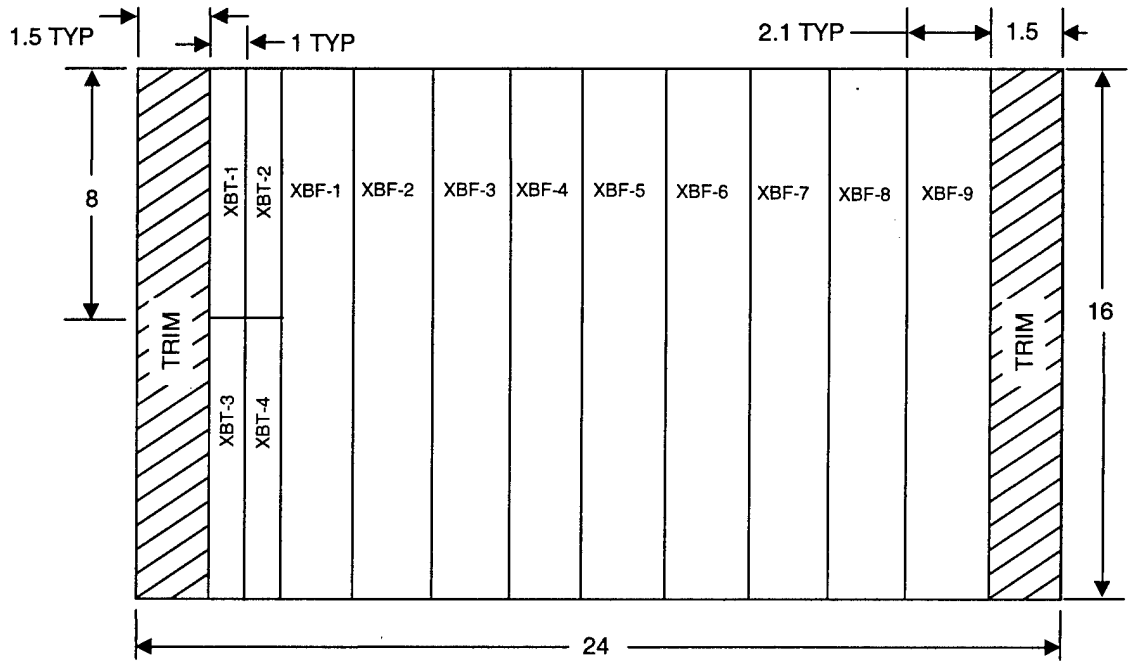

Figure 2.2 Cutting Plan for Panel XB-2

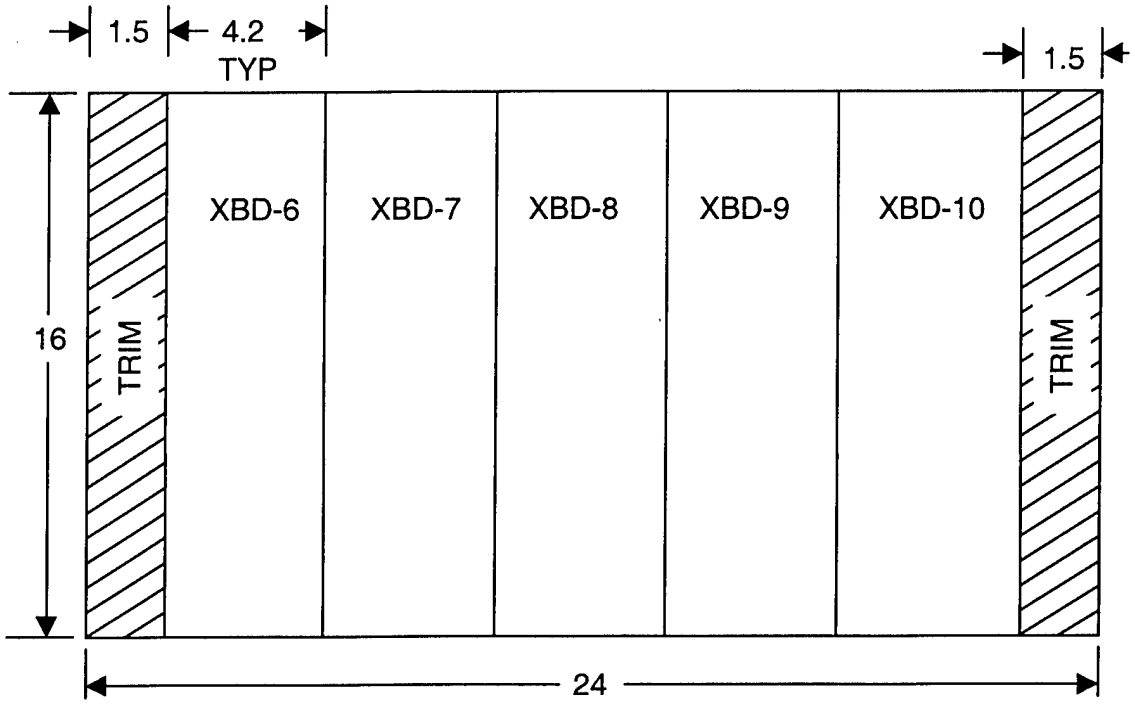

Figure 2.3 Cutting Plan for Panel XB-3

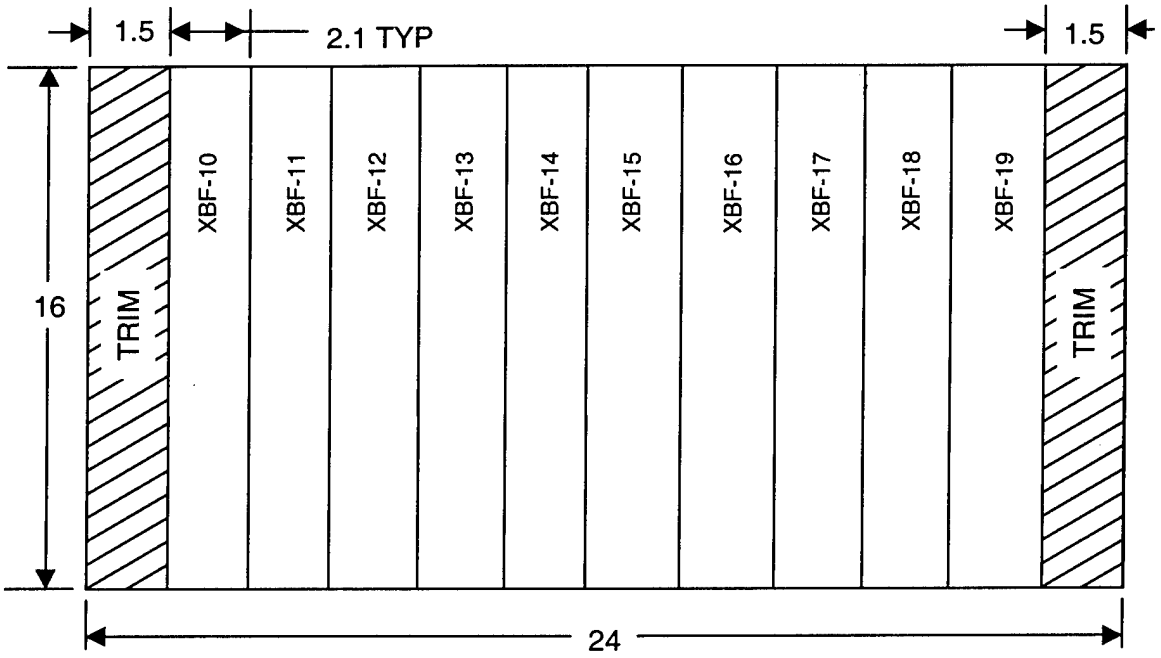

Figure 2.4 Cutting Plan for XB-4

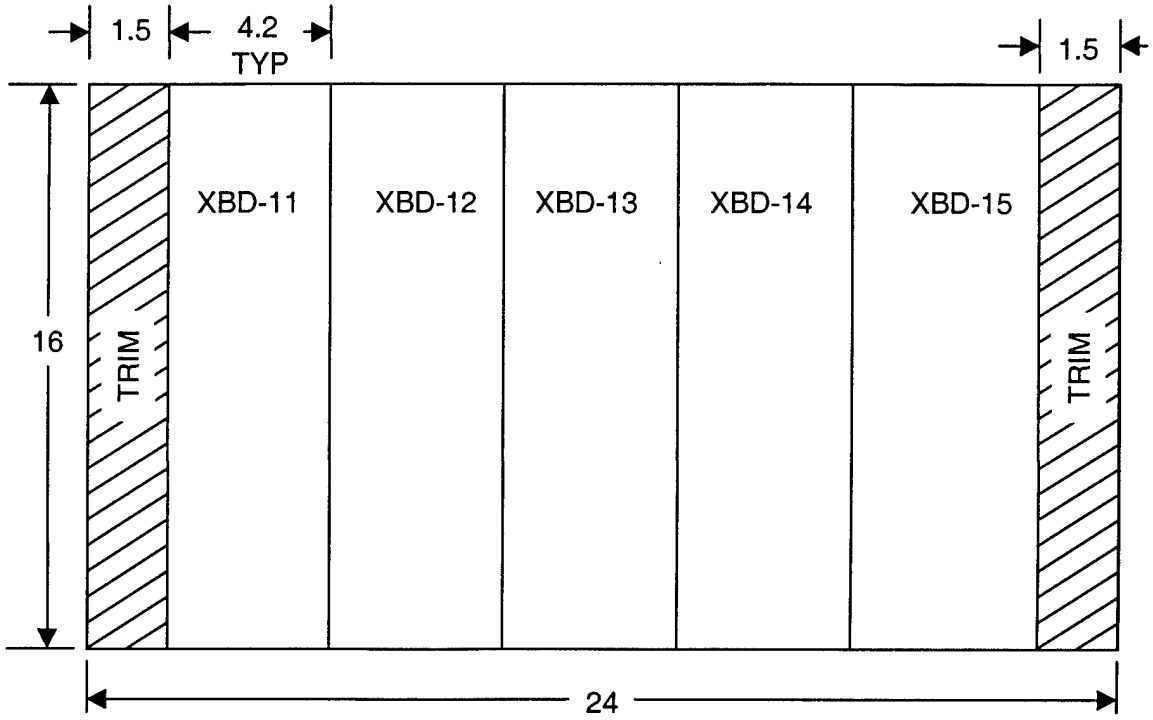

Figure 2.5 Cutting Plan for XB-5

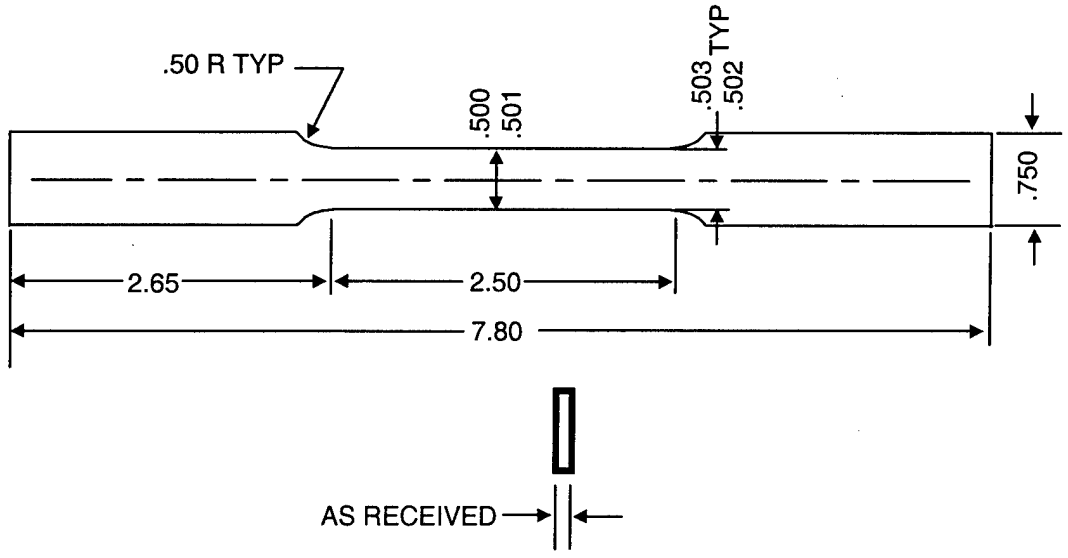

Figure 2.6 Drawing of Tension Test Specimen

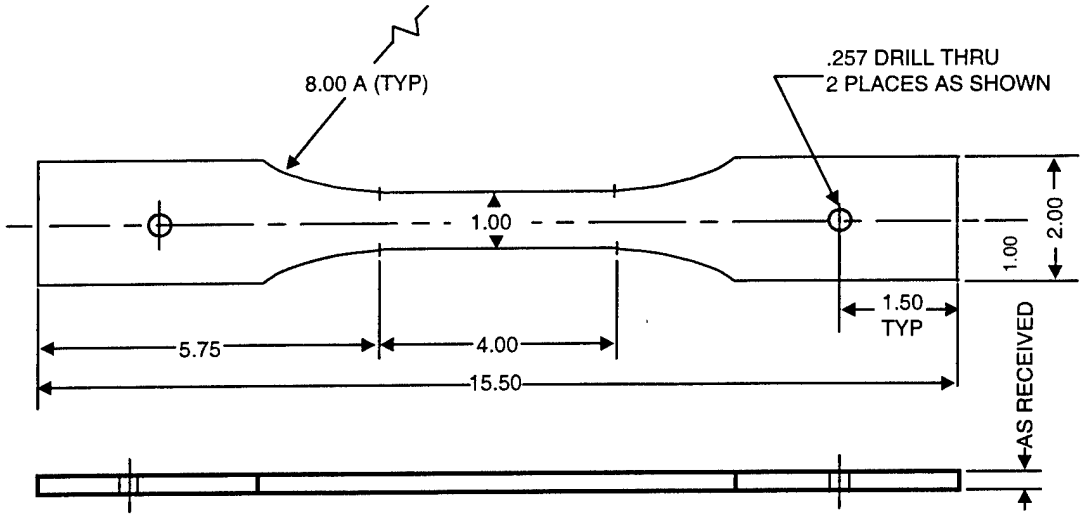

Figure 2.7 Drawing of Axial Fatigue Test Specimen

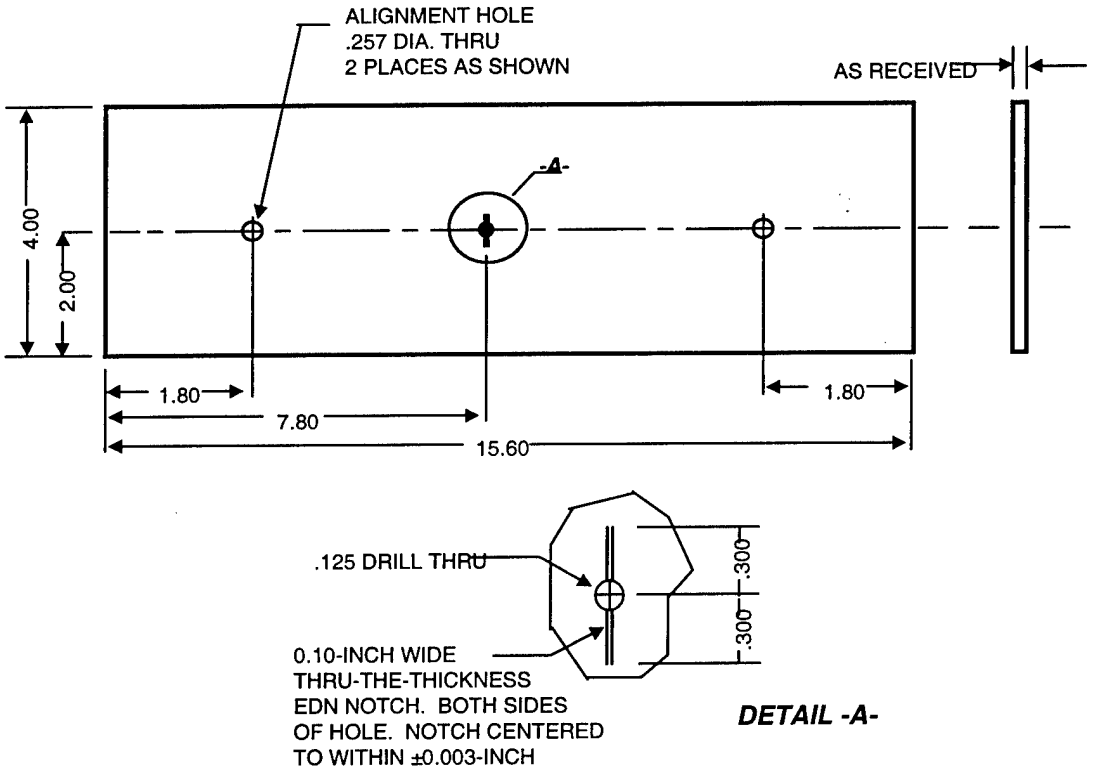

Figure 2.8 Drawing of M(T) Fatigue Crack Growth Rate Specimen

3. TENSILE TEST RESULTS

The tensile tests measured the ultimate strength, the peak elongation, and the 0.2% offset yield stress of the Control and Blasted specimens. Tabulated results for the bare and clad 7075-T6 are given in Table 3.1 and 3.2, respectively, and the results for the bare and clad 2024-T3 are given in Table 3.3 and 3.4, respectively. A summary of the descriptive statistics for the tensile test results is shown in Table 3.5, and the statistical comparison of the Control and Blasted specimens is given in Table 3.6. There was a statistically significant decrease in both the yield and ultimate stress for all materials. In addition, there was a statistically significant increase in the peak elongation of bare 2024-T3.

Figure 3.1 shows the scatter of the yield stress for Control and Blasted for bare 7075-T6, the means of each group, and the 90% confidence intervals about the mean computed from the ANOVA for each group. Similar plots of the yield stress for clad 7075-T6, bare 2024-T3, and clad 2024-T3 are given in Figures 3.2, 3.3, and 3.4, respectively. The confidence intervals demonstrate the range of yield stress at which the average of a set of data of the Control and Blasted groups would fall. If there are common ranges of yield stress wherein the two confidence intervals overlap, i.e., the average yield stresses are equal, one would conclude that there is no statistically significant difference in the average yield stresses across the two groups at the 10% level of significance. Therefore, in Figure 3.1, the confidence intervals do not overlap, and there is a statistically significant decrease in the average yield stress from Control to Blasted for bare 7075-T6.

Figures 3.5 through 3.8 show the scatter, means, and 90% confidence intervals about the mean for the ultimate tensile strength for the four aluminum alloys. One can easily observe that the confidence intervals do not overlap, and that there is a statistically significant decrease in the average ultimate strengths from Control to Blasted for all of the alloys. Figures 3.9 through 3.12 show the scatter, means and 90% confidence intervals for the percent elongation. In this case, the confidence intervals do overlap for bare and clad 7075-T6 and the clad 2024-T3. One can state that there is not a statistically significant difference in the average percent elongation across these Control and Blasted groups. For bare 2024-T3, there is a statistically significant increase in the elongation between the Control and Blasted groups.

It is tempting to state that, based on these statistical results, Envirostrip™ causes a significant decrease in the yield and ultimate stresses of 7075-T6 and 2024-T3 alloys. However, such a statement may be erroneous because these statistically significant results do not necessarily agree with a practical perspective of the data. From Table 3.5, it is seen that the differences in the means of the Control and Blasted yield stresses are, at most, 3 ksi or less than 4%, which is within practical variation due to experimental error or material variability. It is also noted that the coefficients of variation are less than 3%. This is testimony to the precision of the data and the ability to replicate the yield stress measurements over the four observations. The small variability in the data was such that even a 3-ksi difference in the means became statistically significant at a 10% level of significance. This same argument is valid for the statistically significant decrease in ultimate

stress; the difference between the Control and Blasted averages was no greater than 2 ksi and the coefficients of variation are 0.6% or less. Table 3.6 provides an engineering summary to reflect that the variation in the test results was within experimental error and material variability.

It is noted that similar statements were made about tensile test results after blasting with Polymedia-Lite™ [2]. The differences in average yield and ultimate strengths in that study were only 1 ksi and the coefficients of variation were less than 0.5%. The ANOVA results in Reference 2 identified both statistically significant increases and decreases between the averages, depending upon which material group one was concerned with. No trend was present in that data.

In summary, although there were statistically significant decreases in tensile yield strength and ultimate strength, the differences between Control and Blasted averages were within the variability of the test.

Table 3.1 Tensile Test Results for Bare 7075-T6

Tensile Test Results for Bare 7075-T6							
CONTROLS:							
Specimen Number	Width	Thickness	Area	Peak Load	Ultimate Strength	Peak Elongation	Offset Yield Stress
	(in)	(in)	(sq in)	(lb)	(psi)	(%)	(psi)
KCT-1	0.497	0.032	0.016	1347	85.23	13.10	82.62
KCT-2	0.502	0.032	0.016	1372	85.93	12.65	78.69
KCT-3	0.502	0.032	0.016	1363	85.39	11.35	77.94
KCT-4	0.499	0.032	0.016	1350	85.10	12.20	78.01
Average					85.41	12.33	79.31
Std Dev					0.37	0.75	2.23
FOURTH CYCLE:							
Specimen Number	Width	Thickness	Area	Peak Load	Ultimate Strength	Peak Elongation	Offset Yield Stress
	(in)	(in)	(sq in)	(lb)	(psi)	(%)	(psi)
WKBT-1	0.499	0.032	0.016	1338	83.81	12.35	75.90
WKBT-2	0.498	0.032	0.016	1334	83.72	12.80	75.92
WKBT-3	0.501	0.032	0.016	1335	83.22	12.75	75.89
WKBT-4	0.499	0.032	0.016	1338	83.86	12.30	76.53
Average					83.65	12.55	76.06
Std Dev					0.29	0.26	0.31

Table 3.2 Tensile Test Results for Clad 7075-T6

Tensile Test Results for Clad 7075-T6							
CONTROLS:							
Specimen Number	Width	Thickness	Area	Peak Load	Ultimate Strength	Peak Elongation	Offset Yield Stress
	(in)	(in)	(sq in)	(lb)	(psi)	(%)	(psi)
LCT-1	0.483	0.032	0.015	1208	77.69	14.20	70.17
LCT-2	0.480	0.032	0.015	1208	78.38	13.05	70.24
LCT-3	0.497	0.032	0.016	1249	78.52	14.00	68.02
LCT-4	0.478	0.032	0.015	1205	78.52	14.55	70.29
Average					78.28	13.95	69.68
Std Dev					0.40	0.64	1.11
FOURTH CYCLE:							
Specimen Number	Width	Thickness	Area	Peak Load	Ultimate Strength	Peak Elongation	Offset Yield Stress
	(in)	(in)	(sq in)	(lb)	(psi)	(%)	(psi)
WLBT-1	0.499	0.032	0.0160	1227	76.36	14.45	68.12
WLBT-2	0.499	0.032	0.0160	1225	76.43	13.45	67.92
WLBT-3	0.501	0.032	0.0160	1233	76.45	13.20	68.12
WLBT-4	0.500	0.032	0.0160	1229	76.26	13.65	67.95
Average					76.38	13.69	68.03
Std Dev					0.09	0.54	0.11

Table 3.3 Tensile Test Results for Bare 2024-T3

Tensile Test Results for Bare 2023-T3							
CONTROLS:							
Specimen Number	Width	Thickness	Area	Peak Load	Ultimate Strength	Peak Elongation	Offset Yield Stress
	(in)	(in)	(sq in)	(lb)	(psi)	(%)	(psi)
MCT-1	0.480	0.032	0.015	1115	72.83	16.50	53.67
MCT-2	0.483	0.032	0.015	1122	72.81	17.40	53.93
MCT-3	0.480	0.032	0.015	1117	72.96	17.20	53.89
MCT-4	0.490	0.032	0.016	1132	72.73	16.60	54.26
Average					72.83	16.93	53.94
Std Dev					0.10	0.44	0.24
FOURTH CYCLE:							
Specimen Number	Width	Thickness	Area	Peak Load	Ultimate Strength	Peak Elongation	Offset Yield Stress
	(in)	(in)	(sq in)	(lb)	(psi)	(%)	(psi)
WMBT-1	0.501	0.032	0.016	1154	71.82	17.45	52.53
WMBT-2	0.501	0.032	0.016	1159	72.25	18.60	52.87
WMBT-3	0.497	0.032	0.016	1150	72.28	18.25	52.62
WMBT-4	0.492	0.032	0.016	1139	72.39	17.95	52.66
Average					72.19	18.06	52.67
Std Dev					0.25	0.49	0.14

Table 3.4 Tensile Test Results for Clad 2024-T3

Tensile Test Results for Clad 2023-T3							
CONTROLS:							
Specimen Number	Width	Thickness	Area	Peak Load	Ultimate Strength	Peak Elongation	Offset Yield Stress
	(in)	(in)	(sq in)	(lb)	(psi)	(%)	(psi)
NCT-1	0.486	0.032	0.016	1045	67.38	[1]	50.04
NCT-2	0.497	0.032	0.016	1063	67.02	16.80	50.97
NCT-3	0.499	0.032	0.016	1069	66.76	17.65	50.38
NCT-4	0.501	0.032	0.016	1066	66.49	15.65	50.52
Average					66.91	16.70	50.48
Std Dev					0.38	1.00	0.39
Comment:	1. Specimen failed outside of gage section.						
FOURTH CYCLE:							
Specimen Number	Width	Thickness	Area	Peak Load	Ultimate Strength	Peak Elongation	Offset Yield Stress
	(in)	(in)	(sq in)	(lb)	(psi)	(%)	(psi)
WNBT-1	0.500	0.032	0.016	1055	65.61	15.95	49.00
WNBT-2	0.499	0.032	0.016	1058	65.93	17.70	48.93
WNBT-3	0.501	0.032	0.016	1064	65.96	17.40	48.90
WNBT-4	0.500	0.032	0.016	1066	66.21	16.70	48.79
Average					65.93	16.94	48.91
Std Dev					0.25	0.78	0.09

Table 3.5 Summary of Descriptive Statistics for Tensile Tests for Envirostrip™

Material	Control Specimens						Blasted Specimens					
	Yield Stress 0.2% Offset		Ultimate Strength		Elongation		Yield Stress 0.2% Offset		Ultimate Strength		Elongation	
	Avg (ksi)	COV (%)	Avg (ksi)	COV (%)	Avg (ksi)	COV (%)	Avg (ksi)	COV (%)	Avg (ksi)	COV (%)	Avg (ksi)	COV (%)
7075-T6 Bare	79.32	2.8	85.41	0.4	12.33	6.1	76.06	0.4	83.65	0.3	12.55	2.1
7075-T6 Clad	69.68	1.6	78.28	0.5	13.95	4.6	68.03	0.2	76.38	0.1	13.69	3.9
2024-T3 Bare	53.94	0.4	72.83	0.1	16.93	2.6	52.67	0.3	72.19	0.3	18.06	2.7
2024-T3 Clad	50.48	0.8	66.91	0.6	16.70	6.0	48.91	0.2	65.93	0.4	16.94	4.6

Table 3.6 Tensile Test Engineering Summary for Envirostrip™

Material	Statistical Significance			Engineering Summary		
	Yield Stress	Ultimate Strength	Elongation	Yield Stress	Ultimate Strength	Elongation
7075-T6 Bare	S ↓	S ↓	NS	NPS	NPS	NS
7075-T6 Clad	S ↓	S ↓	NS	NPS	NPS	NS
2024-T3 Bare	S ↓	S ↓	S ↑	NPS	NPS	NPS
2024-T3 Clad	S ↓	S ↓	NS	NPS	NPS	NS

S ↑ = Statistically significant increase in the average response from Control to Envirostrip™ specimens at the 10% level of significance.

S ↓ = Statistically significant decrease in the average response from Control to Envirostrip™ specimens at the 10% level of significance.

NS = No statistically significant difference in averages at a 10% level of significance.

NPS = Statistically significant difference in the average response, but not practically significant, because difference was within test and material variability.

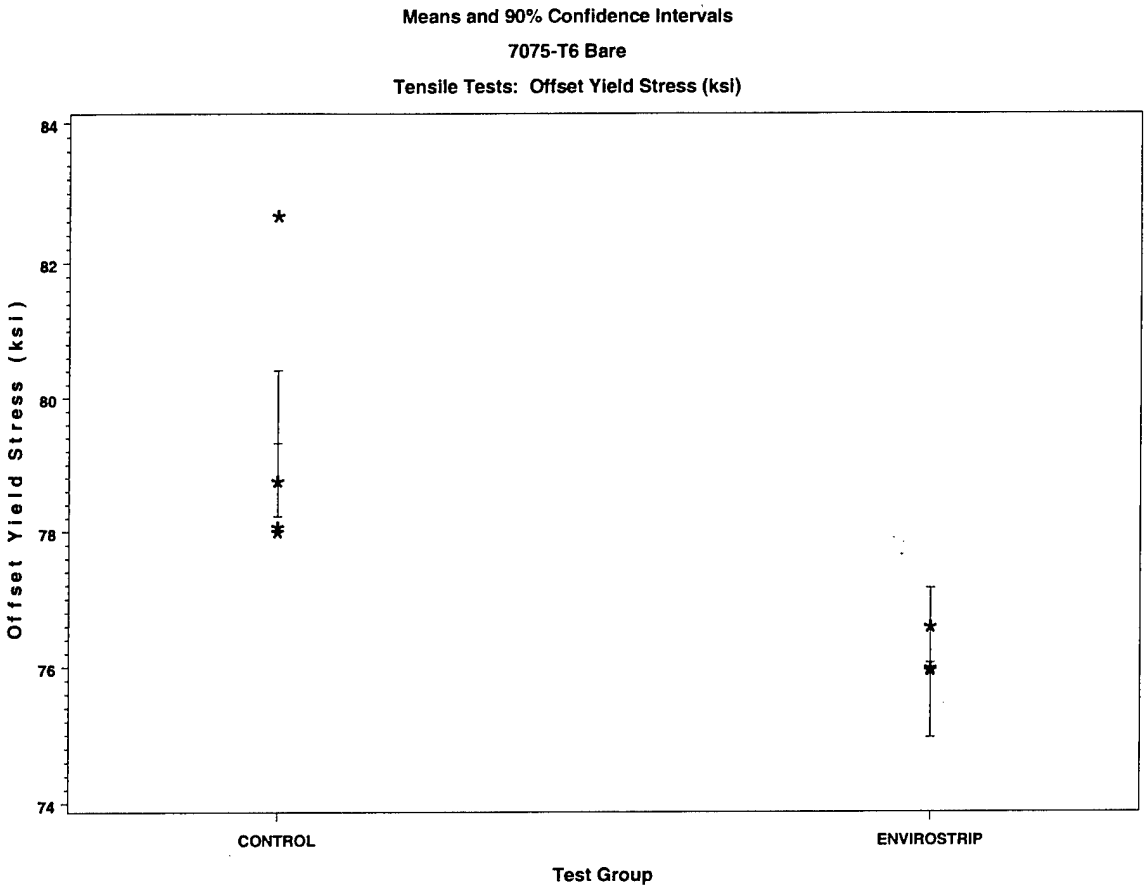

Figure 3.1 Scatter, Mean, and 90 Percent Confidence Intervals of Offset Yield Stress for Bare 7075-T6

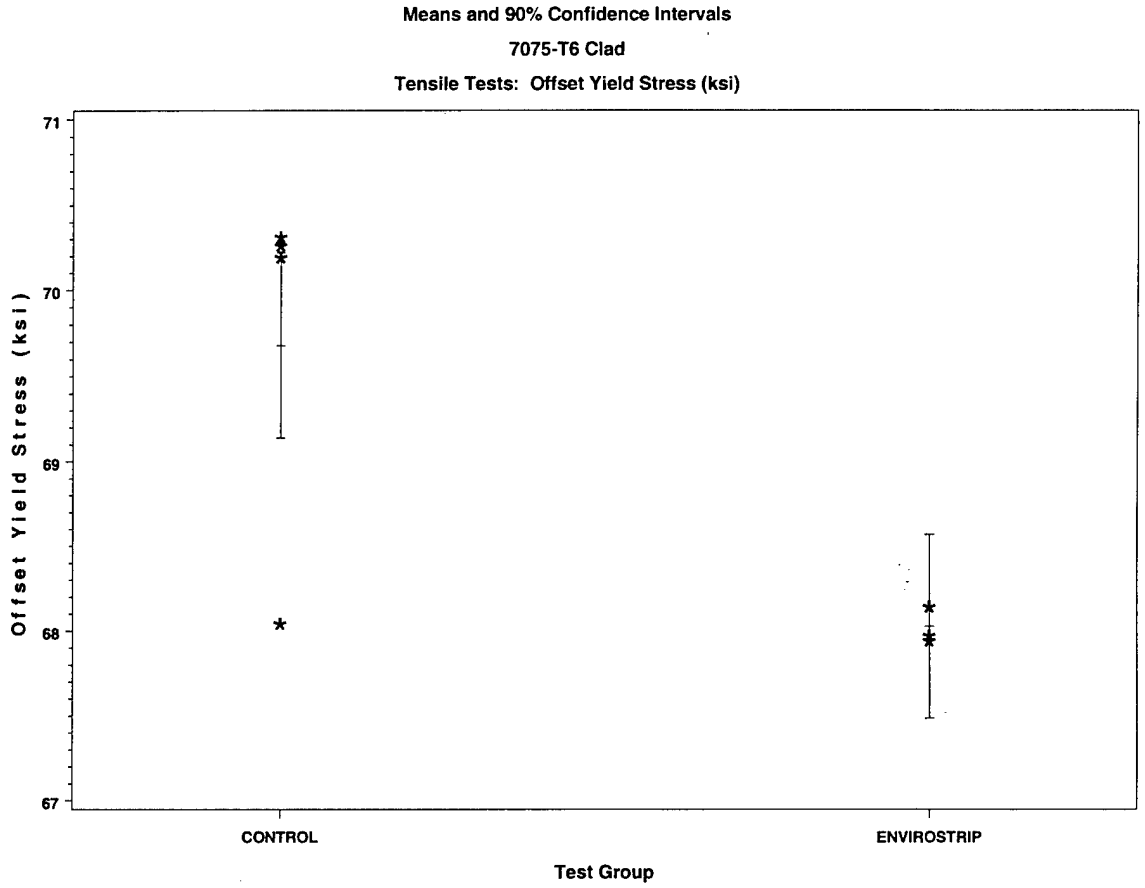

Figure 3.2 Scatter, Mean, and 90 Percent Confidence Intervals of Offset Yield Stress for Clad 7075-T6

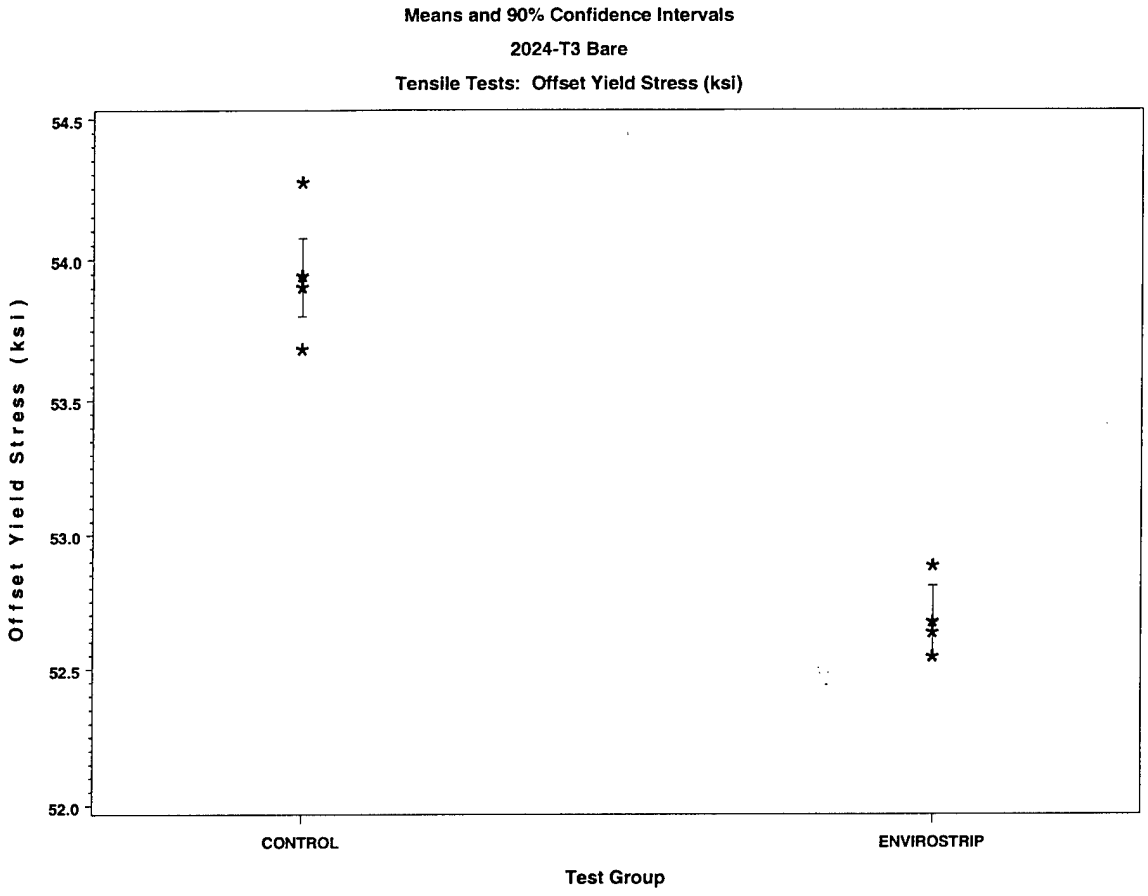

Figure 3.3 Scatter, Mean, and 90 Percent Confidence Intervals of Offset Yield Stress for Bare 2024-T3

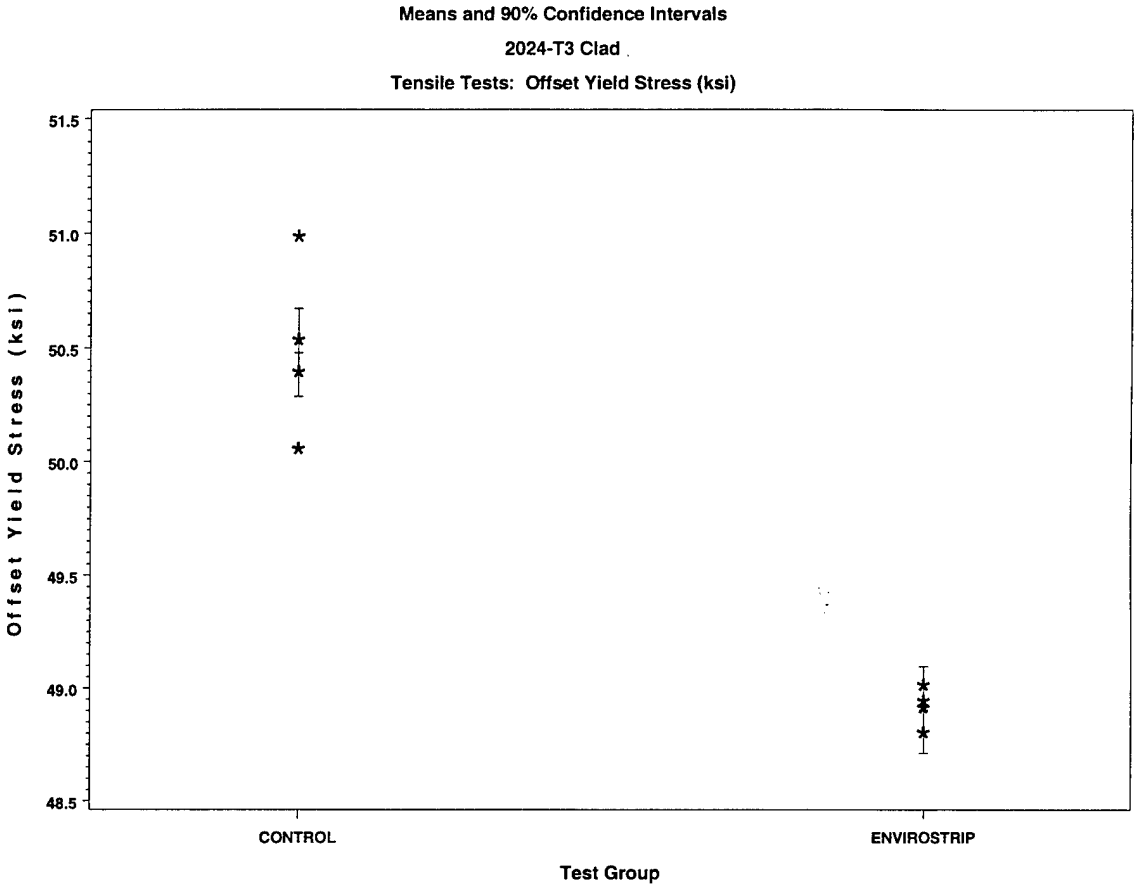

Figure 3.4 Scatter, Mean, and 90 Percent Confidence Intervals of Offset Yield Stress for Clad 2024-T3

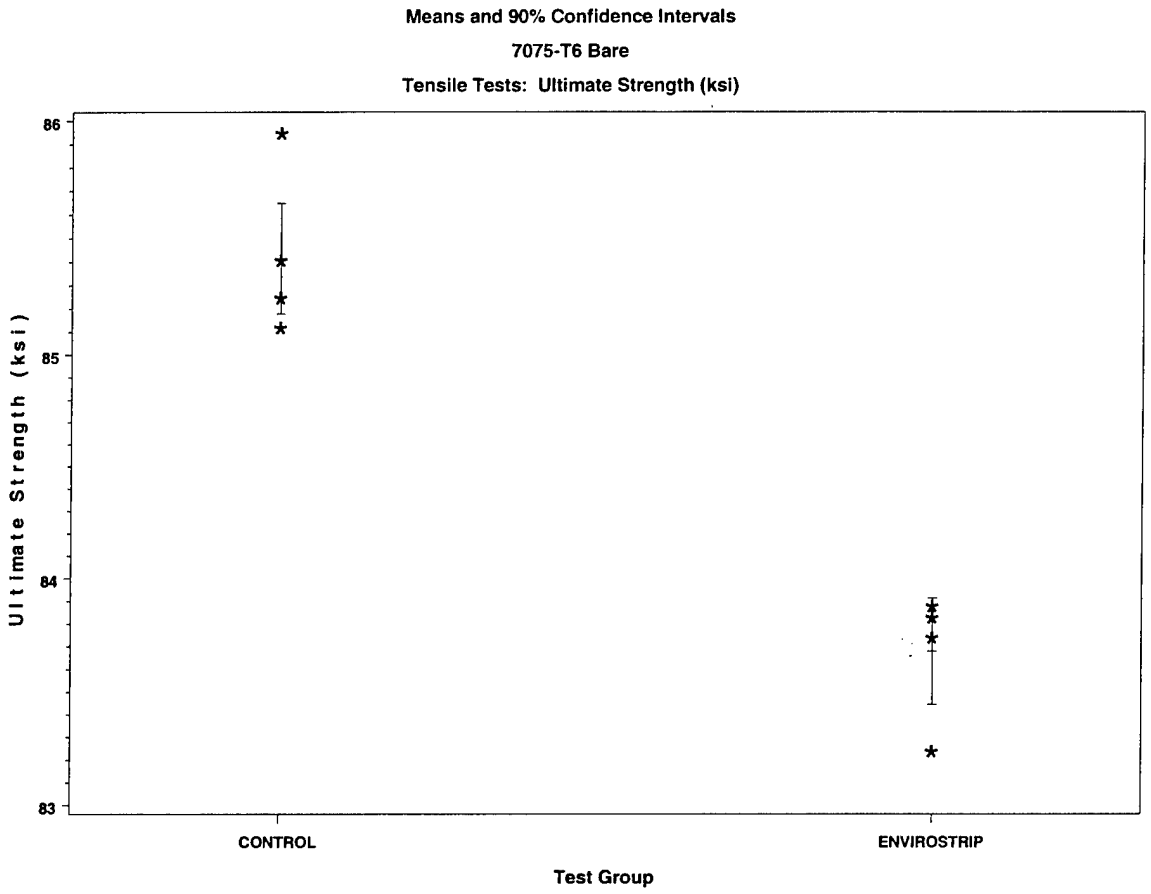

Figure 3.5 Scatter, Mean, and 90 Percent Confidence Intervals of Ultimate Strength for Bare 7075-T6

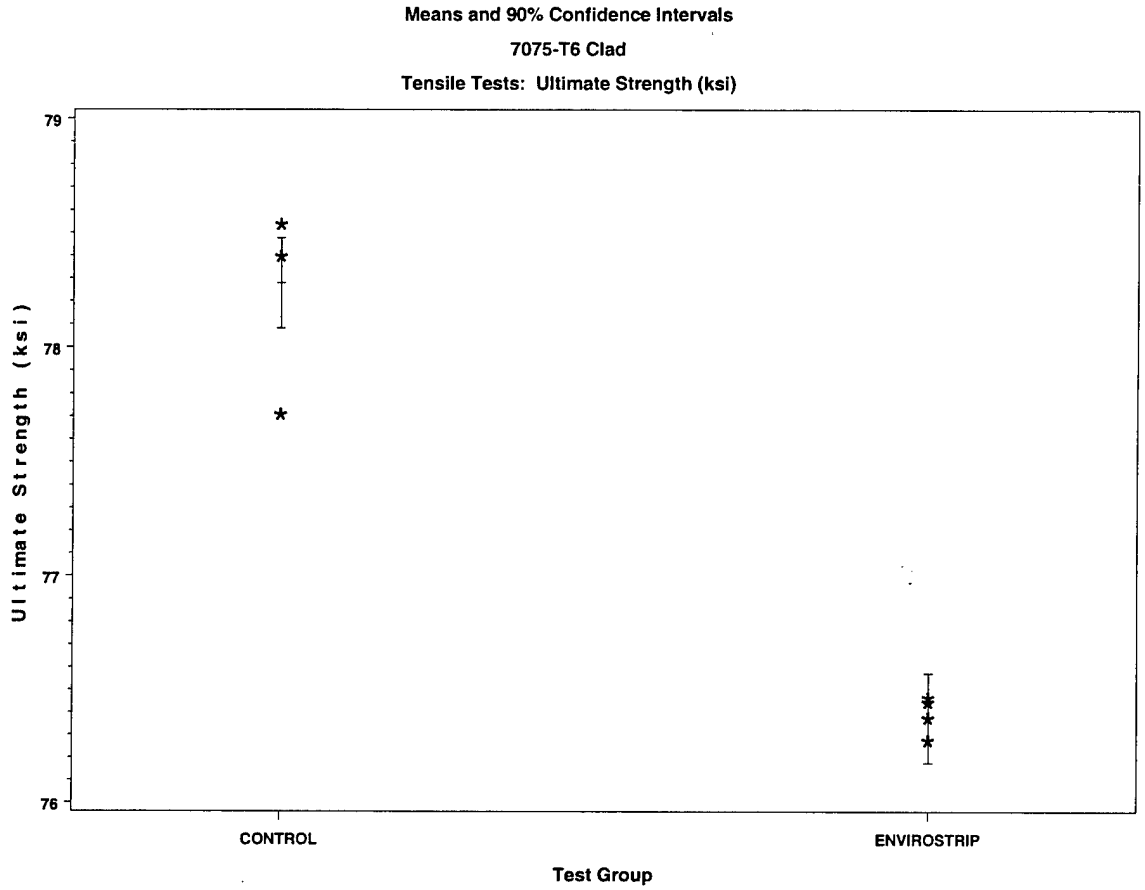

Figure 3.6 Scatter, Mean, and 90 Percent Confidence Intervals of Ultimate Strength for Clad 7075-T6

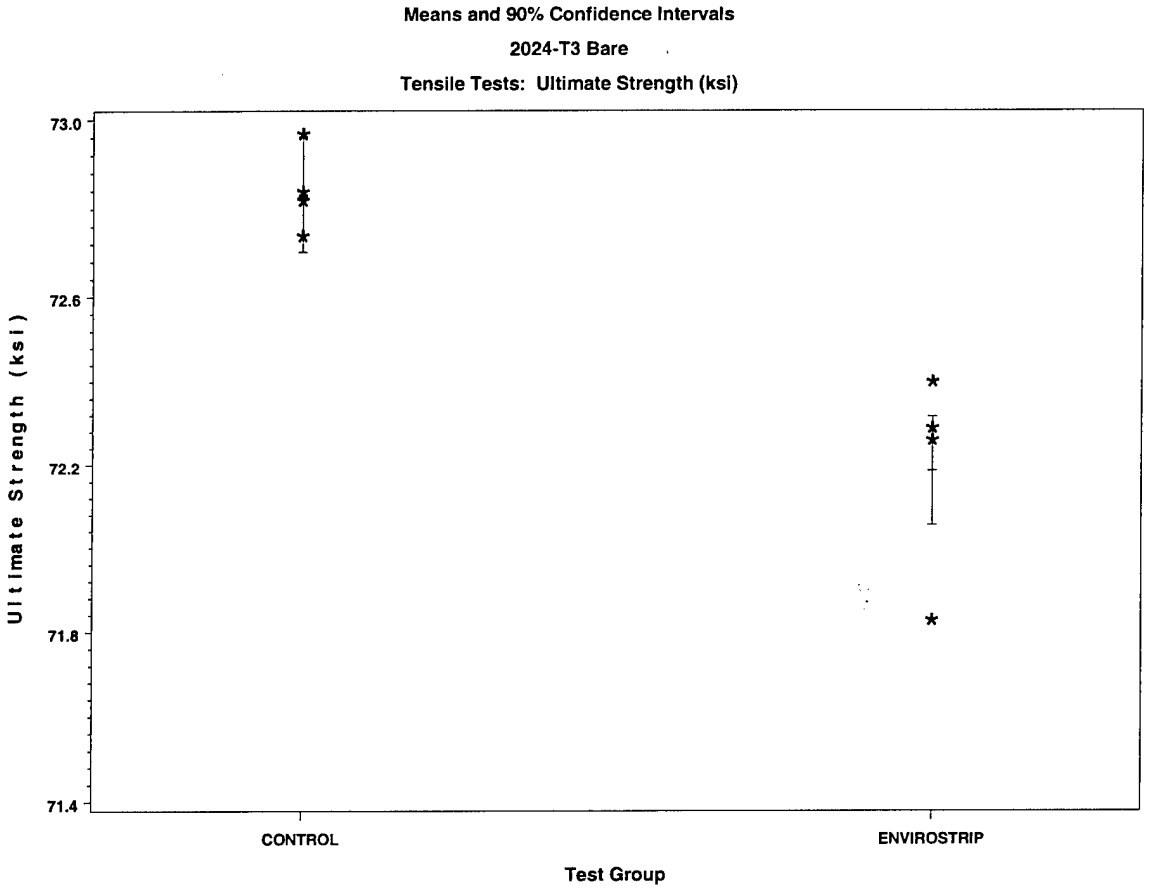

Figure 3.7 Scatter, Mean, and 90 Percent Confidence Intervals of Ultimate Strength for Bare 2024-T3

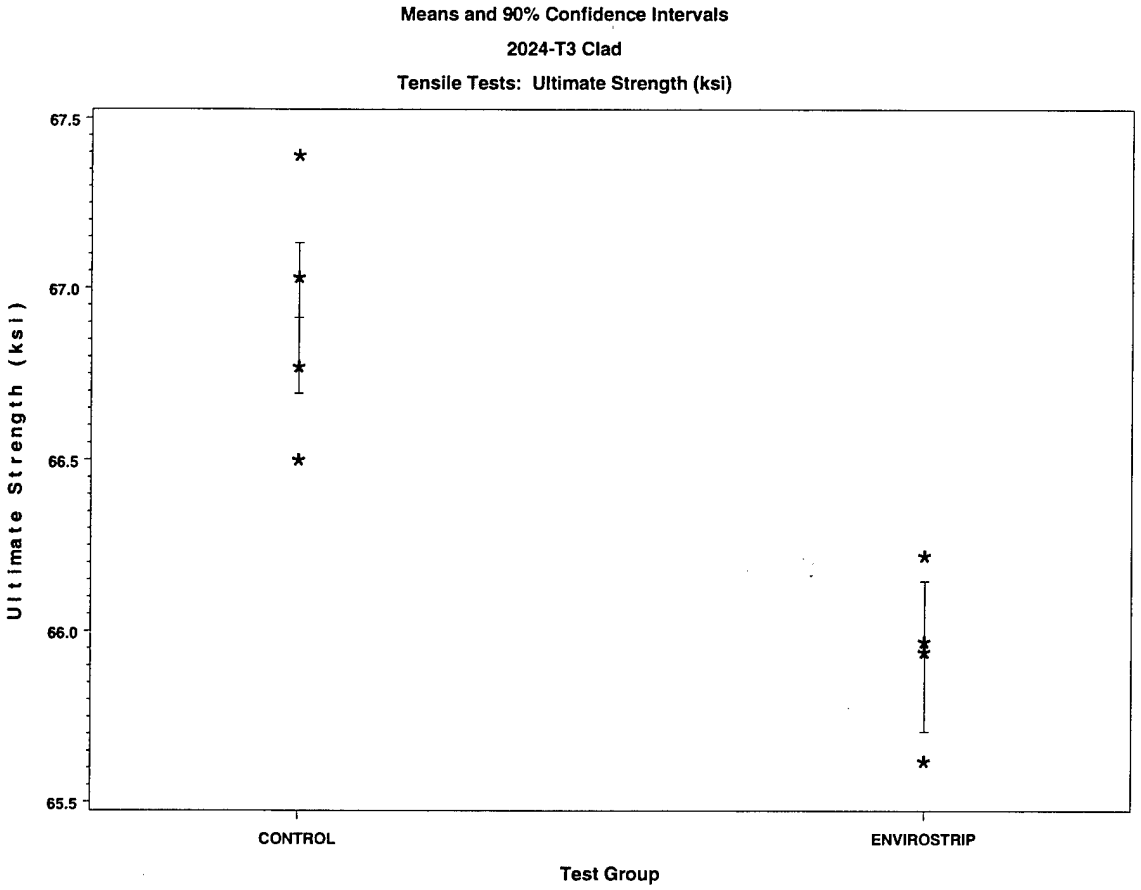

Figure 3.8 Scatter, Mean, and 90 Percent Confidence Intervals of Ultimate Strength for Clad 2024-T3

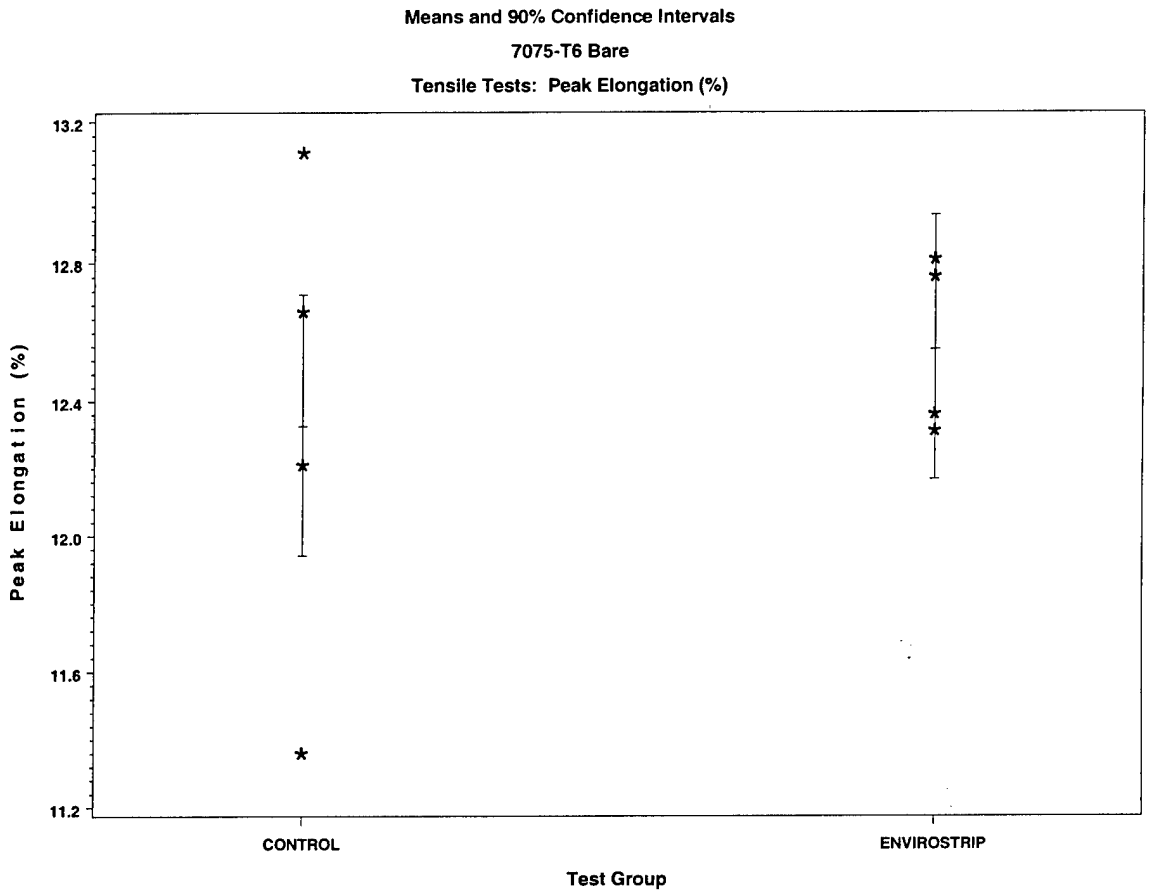

Figure 3.9 Scatter, Mean, and 90 Percent Confidence Intervals of Peak Elongation for Bare 7075-T6

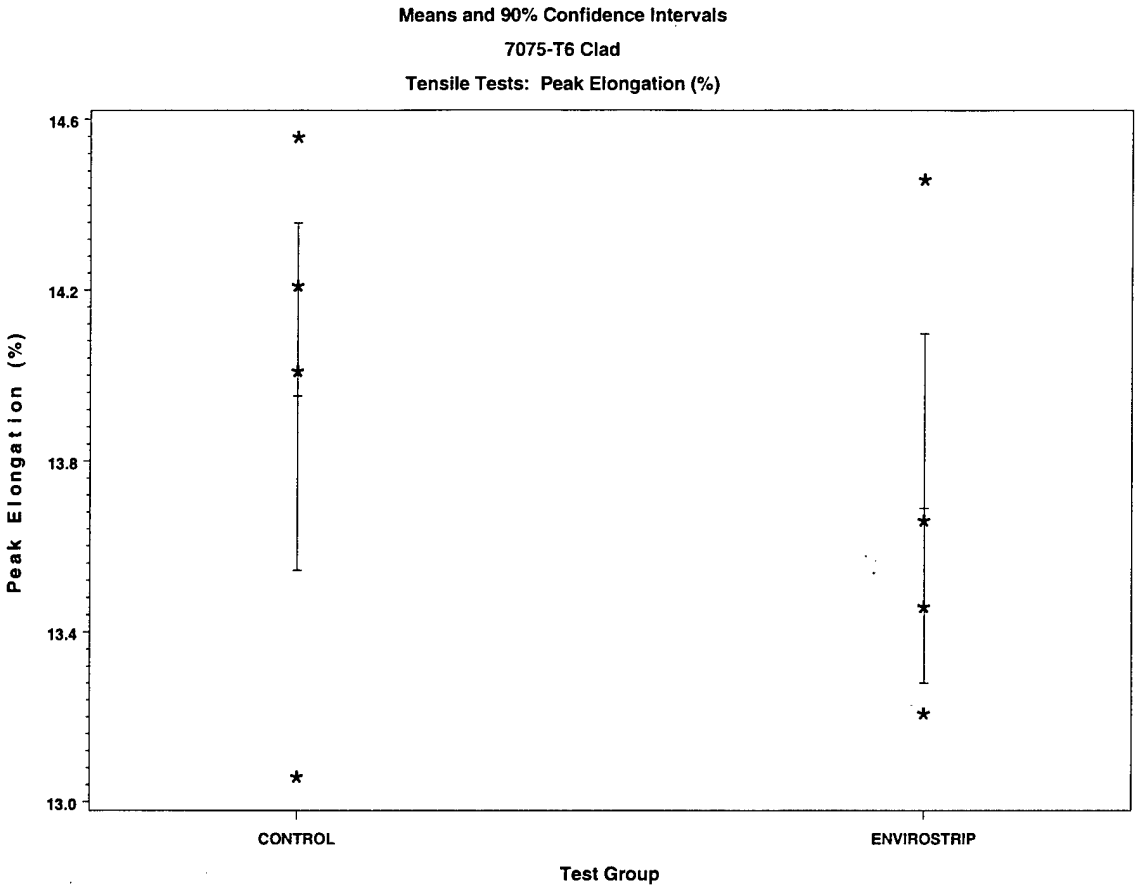

Figure 3.10 Scatter, Mean, and 90 Percent Confidence Intervals of Peak Elongation for Clad 7075-T6

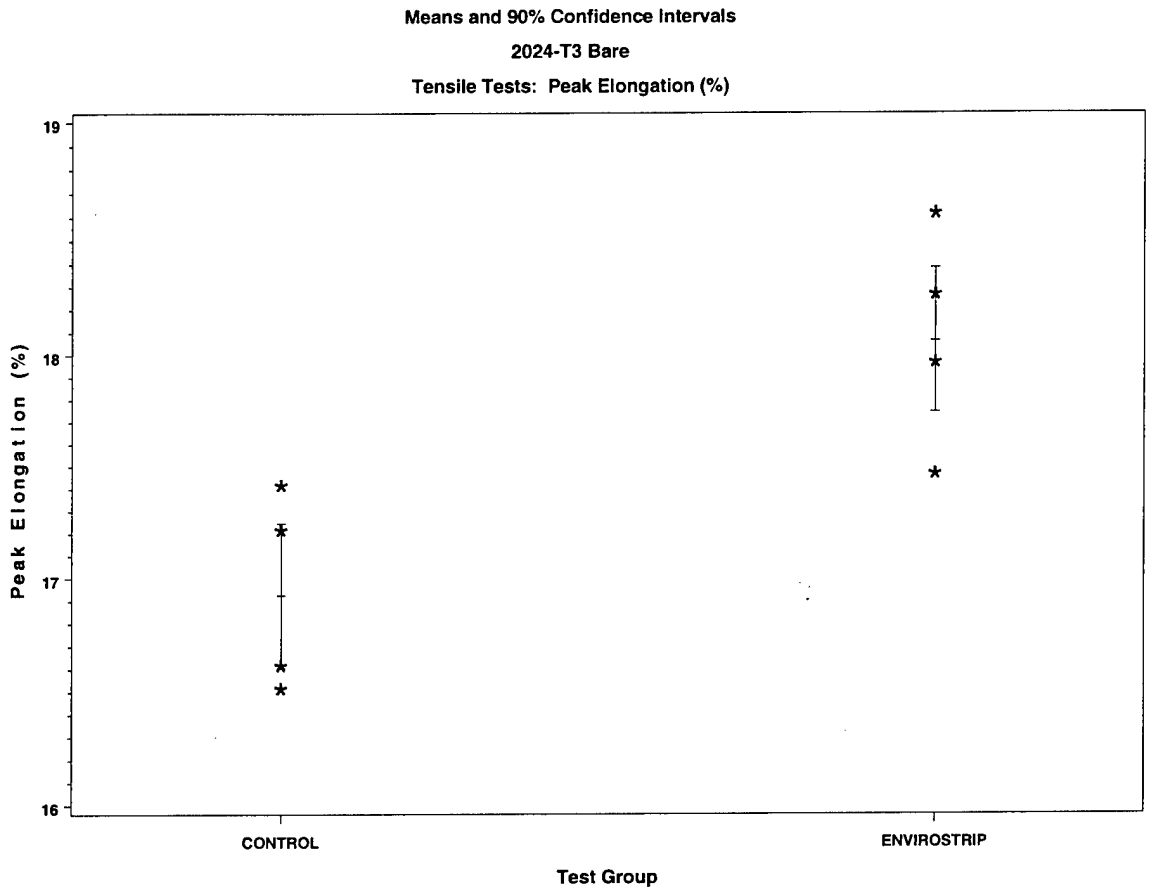

Figure 3.11 Scatter, Mean, and 90 Percent Confidence Intervals of Peak Elongation for Bare 2024-T3

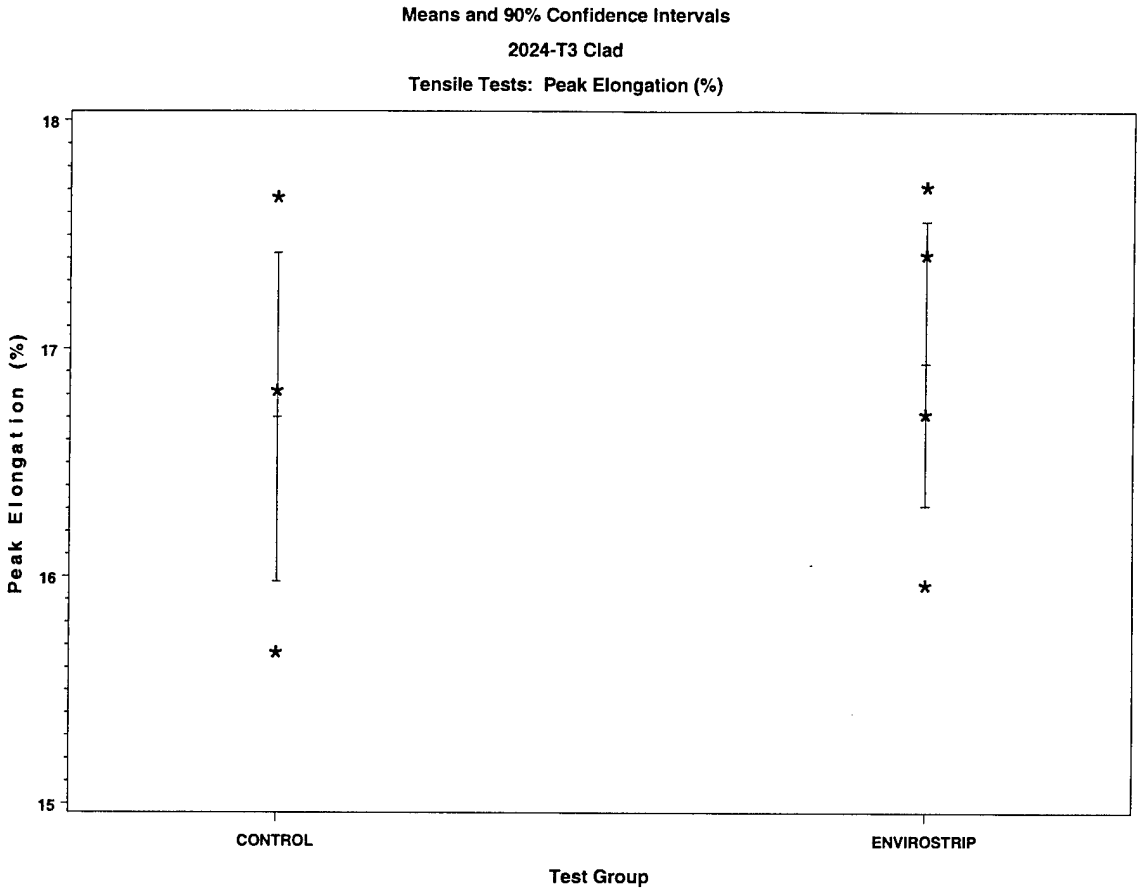

Figure 3.12 Scatter, Mean, and 90 Percent Confidence intervals of Peak Elongation for Clad 2024-T3

4. FATIGUE TEST RESULTS

The fatigue test results for bare and clad 7075-T6 are tabulated in Tables 4.1 and 4.2, respectively. The results for bare and clad 2024-T3 are given in Tables 4.3 and 4.4, respectively. The tables provide all pertinent test information such as test specimen number, temperature, relative humidity, specimen dimensions, maximum stress, and total cycles to failure. The comment section includes information with regard to crack initiation sites. The location of the crack initiation is either on the surface, edge, or corner of the blasted or unblasted side of the test specimen. The distance from the fracture to the mid-length of the specimen is also included. Distances greater than 2 inches were outside of the test section and were considered invalid.

A statistical summary of the data is given in Table 4.5. There was no statistically significant difference in the average fatigue lives from Control to Blasted specimens for bare 7075-T6. There were, however, statistically significant decreases in fatigue lives for clad 7075-T6, and for bare and clad 2024-T3. Figure 4.1 shows the scatter of the cycles to failure for Control and Blasted tests for bare 7075-T6, the means of each group, and the 90% confidence intervals about the mean computed from the ANOVA for each group. The confidence intervals for bare 7075-T6 overlap, and one can state that there is not a statistically significant difference in the average fatigue lives from Control and Blasted for bare 7075-T6. Similar plots for clad 7075-T6, bare 2024-T3, and clad 2024-T3 are given in Figures 4.2, 4.3, and 4.4, respectively. The confidence intervals do not overlap, and one can state that there are statistically significant decreases in the average fatigue lives from Control and Blasted for these three materials.

Unlike the tensile test results in Section 3.0, the debits in the fatigue lives of clad 7075-T6 and bare and clad 2024-T3 are significant from both statistical and engineering points of view. Examining the coefficients of variation (COV) for each group in Tables 4.1 – 4.4, it is seen that the scatter in the Control and Blasted groups for clad 7075-T6 and bare and clad 2024-T3 are small in comparison to the scatter for bare 7075-T6. The COV's are evidence of the reproducibility of the experimental results over the ten test samples within each group. (The larger scatter in the bare 7075-T6 groups may have contributed to lack of statistical significance between the data sets.) The substantial decreases in fatigue lives prompted further investigations to explore why the debits were observed for the Envirostrip process. Brief, exploratory investigations, which are described in Appendix B, led to formulations of simple hypotheses for the observed behavior. Historical fatigue life data from Type V and Polymedia-Lite™, surface roughness, and residual stress measurements (described in Section 6.0) were considered in the formulation of the hypotheses.

To summarize for completeness the results of Appendix B, the fatigue life behavior of blasted surfaces can be understood in terms of the competing effects of beneficial compressive surface residual stresses and harmful surface roughness. The Envirostrip™ blasting process had the most shallow (least beneficial) compressive residual stresses than either Type V or Polymedia-Lite™, and the shallow residual stresses may have been more

susceptible to stress relaxation during fatigue cycling. In comparison to Polymedia-Lite™ and Type V, the Envirostrip™ process exhibited higher and more damaging levels of surface roughness than Polymedia-Lite™, but were significantly less than the roughness levels resulting from Type V. (The increased surface roughness resulting from Type V was apparently offset by the substantially deeper levels of compressive residual stress, resulting in no statistically significant loss in fatigue lives.) No definitive conclusions could be reached about the factors that affected fatigue performance of dry media blasted aluminum alloys, but the available information supported the hypothesis that fatigue performance was influenced by the beneficial effects of compressive residual stresses and the deleterious effects of surface roughness.

Table 4.1 Fatigue Test Results for Bare 7075-T6

Fatigue Test Results for Bare 7075-T6
Controls:

Specimen Number	Temp	RH	Width	Thickness	Area	Max Stress	Cycles to Failure	Comments (1)
KCF-1	78	44	0.999	0.032	0.032	47.8	37717	Surface: 0.10 in.
KCF-2	78	44	0.998	0.032	0.032	47.8	23978	Surface: 0.20 in.
KCF-3	78	44	0.999	0.032	0.032	47.8	48276	Surface: 1.99 in.
KCF-4	78	44	0.998	0.032	0.032	47.8	36624	Surface: 1.99 in.
KCF-5	78	44	0.997	0.032	0.032	47.8	36520	Edge: 0.65 in.
KCF-6	78	44	0.998	0.032	0.031	47.8	84053	Surface: 1.45 in.
KCF-7	78	44	0.995	0.032	0.031	47.8	43650	Surface: 0.35 in.
KCF-11	78	44	0.997	0.032	0.031	47.8	58284	Surface: 1.00 in.
KCF-12	78	44	0.997	0.032	0.031	47.8	68884	Surface: 0.95 in.
KCF-14	76	42	0.999	0.032	0.031	47.8	51386	Surface: 0.80 in.
Average							48937	
Std Dev							17662	
COV							0.36	

Comments:
1. Fracture initiation site and distance from centerline.

Fatigue Test Results for Bare 7075-T6
Envirostrip: Fourth Cycle

Specimen Number	Temp	RH	Width	Thickness	Area	Max Stress	Cycles to Failure	Comments (1)
	(F)	(%)	(in)	(in)	(sq in)	(ksi)		
KWBF-1	72	47	0.997	0.032	0.0319	47.8	25440	Blasted, Surface: 0.60 in
KWBF-2	71	45	0.998	0.032	0.0319	47.8	52318	Unblasted, Surface: 0.10 in.
KWBF-3	71	45	0.996	0.032	0.0319	47.8	18229	Unblasted, Surface: 1.95 in.
KWBF-4	70	47	0.995	0.032	0.0318	47.8	30095	Unblasted, Surface: 0.05 in.
KWBF-5	70	47	0.995	0.032	0.0318	47.8	25208	Blasted, Surface: 1.70 in.
KWBF-6	70	47	0.992	0.032	0.0317	47.8	67840	Blasted, Surface: 1.95 in.
KWBF-7	70	47	0.992	0.032	0.0317	47.8	54496	Blasted, Surface: 1.90 in.
KWBF-8	70	47	0.994	0.032	0.0318	47.8	62798	Unblasted, Surface: 1.95 in.
KWBF-10	70	42	0.995	0.032	0.0318	47.8	34390	Edge: 0.75 in.
KWBF-11	70	42	0.997	0.032	0.0319	47.8	32187	Blasted, Surface: 1.70 in.
Average							40300	
Std Dev							17484	
COV							0.43	

COMMENTS:
1. Fracture initiation site and distance from centerline

Table 4.2 Fatigue Test Results for Clad 7075-T6

Fatigue Test Results for Clad 7075-T6
Controls:

Specimen Number	Temp	RH	Width	Thickness	Area	Max Stress	Cycles to Failure	Comments (1)
	(F)	(%)	(in)	(in)	(sq in)	(ksi)		
LCF-1	77	44	0.993	0.032	0.031	38.50	106089	Surface: 1.30 in.
LCF-3	77	44	0.995	0.032	0.031	38.50	112347	Edge: 0.40 in.
LCF-4	77	44	0.996	0.032	0.031	38.50	116691	Surface: 0.35 in.
LCF-6	77	44	0.998	0.032	0.031	38.50	121461	Edge: 0.25 in.
LCF-7	77	44	0.996	0.032	0.031	38.50	101632	Edge: 0.10 in.
LCF-8	77	44	0.994	0.032	0.031	38.50	85017	Edge: 1.05 in.
LCF-9	77	44	0.994	0.032	0.031	38.50	128301	Edge: 1.45 in.
LCF-10	77	44	0.994	0.032	0.031	38.50	109347	Edge: 0.60 in.
LCF-11	77	44	0.991	0.032	0.031	38.50	100146	Surface: 0.15 in.
LCF-13	77	44	0.996	0.032	0.031	38.50	88192	Surface: 0.35 in.
Average							106922	
Std Dev							13762	
COV							0.13	

Comments:
1. Fracture initiation site and distance from centerline.

Fatigue Test Results for Clad 7075-T6
Envirostrip: Fourth Cycle

Specimen Number	Temp	RH	Width	Thickness	Area	Max Stress	Cycles to Failure	Comments (1)
	(F)	(%)	(in)	(in)	(sq in)	(ksi)		
LWBF-1	71	40	0.996	0.032	0.032	38.5	99859	Unblasted, Surface: 1.85 in
LWBF-2	71	41	0.997	0.032	0.032	38.5	122813	Unblasted, Surface: 0.10 in.
LWBF-3	71	40	0.998	0.032	0.032	38.5	82284	Unblasted, Surface: 0.30 in.
LWBF-4	72	50	0.998	0.032	0.032	38.5	113881	Unblasted, Surface: 1.10 in.
LWBF-5	72	50	0.996	0.032	0.032	38.5	88125	Unblasted, Surface: 1.90 in.
LWBF-6	72	49	0.996	0.032	0.032	38.5	86127	Blasted, Surface: 1.65 in.
LWBF-7	71	50	0.998	0.032	0.032	38.5	80788	Blasted, Surface: 0.30 in.
LWBF-10	70	49	0.997	0.032	0.032	38.5	91237	Unblasted, Surface: 1.60 in.
LWBF-12	70	50	0.997	0.032	0.032	38.5	92796	Blasted, Surface: 1.00 in.
LWBF-13	70	49	0.996	0.032	0.032	38.5	80612	Unblasted, Surface: 0.20 in.
Average							93852	
Std Dev							14361	
COV							0.15	

COMMENTS:
1. Fracture initiation site and distance from centerline

Table 4.3 Fatigue Test Results for Bare 2024-T3

Fatigue Test Results for Bare 2024-T3
Controls:

Specimen Number	Temp	RH	Width	Thickness	Area	Max Stress	Cycles to Failure	Comments (1)
	(F)	(%)	(in)	(in)	(sq in)	(ksi)		
MCF-3	76	44	0.997	0.033	0.032	49.4	84890	Surface: 0.65 in.
MCF-4	76	44	0.997	0.033	0.032	49.4	83699	Surface: 0..81 in.
MCF-6	76	44	0.998	0.032	0.032	49.4	76556	Surface: 1.20 in.
MCF-7	76	44	0.999	0.032	0.032	49.4	89636	Edge: 1.20 in.
MCF-8	76	44	0.998	0.032	0.032	49.4	92419	Surface: 0.85 in.
MCF-9	76	42	0.998	0.032	0.032	49.4	77399	Surface: 1.65 in.
MCF-10	76	42	0.998	0.032	0.032	49.4	91516	Surface: 0.55 in.
MCF-11	76	42	0.998	0.032	0.032	49.4	72801	Edge: 1.55 in.
MCF-12	76	42	0.998	0.032	0.032	49.4	79889	Surface: 0.35 in.
MCF-15	76	42	0.997	0.032	0.032	49.4	83236	Surface: 1.95 in.
Average							83204	
Std Dev							6630	
COV							0.08	

Comments:
1. Fracture initiation site and distance from centerline.

Fatigue Test Results for Bare 2024-T3
Envirostrip: Fourth Cycle

Specimen Number	Temp	RH	Width	Thickness	Area	Max Stress	Cycles to Failure	Comments (1)
	(F)	(%)	(in)	(in)	(sq in)	(ksi)		
MWBF-1	72	48	0.995	0.032	0.032	49.4	98031	Blasted, Surface: 1.30 in
MWBF-2	70	50	0.995	0.032	0.032	49.4	53078	Blasted, Surface: 0.50 in.
MWBF-4	70	46	0.995	0.032	0.032	49.4	70188	Blasted, Surface: 1.05 in.
MWBF-7	72	44	0.997	0.032	0.032	49.4	31117	Edge: 1.05 in.
MWBF-8	72	44	0.996	0.032	0.032	49.4	35330	Blasted, Surface: 1.95 in.
MWBF-12	72	46	0.995	0.032	0.032	49.4	61886	Blasted, Surface: 1.95 in.
MWBF-14	71	47	0.998	0.032	0.032	49.4	55040	Blasted, Surface: 0.80 in.
MWBF-15	71	47	0.996	0.032	0.032	49.4	70385	Basted, Surface: 1.25 in.
MWBF-18	72	44	0.997	0.032	0.032	49.4	56470	Blasted, Surface: 1.87 in.
MWBF-19	72	44	0.997	0.032	0.032	49.4	72778	Edge: 0.91 in.
Average							60430	
Std Dev							19295	
COV							0.32	

COMMENTS:
1. Fracture initiation site and distance from centerline

Table 4.4 Fatigue Test Results for Clad 2024-T3

Fatigue Test Results for Clad 2024-T3
Controls:

Specimen Number	Temp	RH	Width	Thickness	Area	Max Stress	Cycles to Failure	Comments (1)
	(F)	(%)	(in)	(in)	(sq in)	(ksi)		
NCF-4	77	44	0.996	0.032	0.031	44.5	78349	Edge: 0.70 in.
NCF-5	77	44	0.995	0.032	0.031	44.5	99693	Edge: 0.45 in.
NCF-6	77	44	0.997	0.032	0.031	44.5	108326	Edge: 1.21 in.
NCF-7	77	44	0.994	0.032	0.031	44.5	116671	Edge: 0.50 in.
NCF-9	77	44	0.994	0.032	0.031	44.5	103442	Edge: 1.98 in.
NCF-10	77	44	0.993	0.032	0.031	44.5	107235	Surface: 1.10 in.
NCF-12	77	44	0.996	0.032	0.031	44.5	94272	Edge: 0.80 in.
NCF-13	77	44	0.997	0.032	0.031	44.5	104272	Edge: 1.80 in.
NCF-15	77	44	0.998	0.032	0.031	44.5	93469	Edge: 1.85 in.
NCF-16	77	44	0.994	0.032	0.031	44.5	95845	Edge: 0.45 in.
Average							100157	
Std Dev							10494	
COV							0.10	

Comments:
1. Fracture initiation site and distance from centerline.

Fatigue Test Results for Clad 2024-T3
Envirostrip: Fourth Cycle

Specimen Number	Temp	RH	Width	Thickness	Area	Max Stress	Cycles to Failure	Comments (1)
	(F)	(%)	(in)	(in)	(sq in)	(ksi)		
NWBF-1	71	45	0.995	0.032	0.032	44.5	72075	Blasted, Surface: 1.63 in
NWBF-2	71	45	0.995	0.032	0.032	44.5	62662	Blasted, Surface: 0.45 in.
NWBF-3	71	43	0.994	0.032	0.032	44.5	67498	Edge: 1.95 in.
NWBF-6	71	45	0.994	0.032	0.032	44.5	54812	Blasted, Surface: 1.10 in.
NWBF-7	71	44	0.994	0.032	0.032	44.5	70645	Blasted, Surface: 1.95 in.
NWBF-8	72	44	0.995	0.032	0.032	44.5	66327	Blasted, Surface: 1.00 in.
NWBF-10	72	45	0.995	0.032	0.032	44.5	69157	Edge: 0.80 in.
NWBF-11	71	45	0.994	0.032	0.032	44.5	42282	Basted, Surface: 1.37 in.
NWBF-12	71	47	0.993	0.032	0.032	44.5	80824	Blasted, Surface: 1.20 in.
NWBF-13	72	47	0.994	0.032	0.032	44.5	78584	Blasted, Surface: 0.75 in.
Average							66487	
Std Dev							11281	
COV							0.17	

COMMENTS:
1. Fracture initiation site and distance from centerline

Table 4.5 Fatigue Test Data and Statistical Summary for Envirostrip™

Material	Condition	Average Cycles to Failure	Statistical Significance
7075-T6 Bare	Control	48900	NS
	Blasted	40300	
7075-T6 Clad	Control	106900	S↓
	Blasted	93900	
2024-T3 Bare	Control	83200	S↓
	Blasted	60400	
2024-T3 Clad	Control	100200	S ↓
	Blasted	66500	

NS = No statistically significant difference in averages at a 10% level of significance.

S ↓ = Statistically significant decrease in the average ultimate strength from Control to Envirostrip™ specimens at the 10% level of significance.

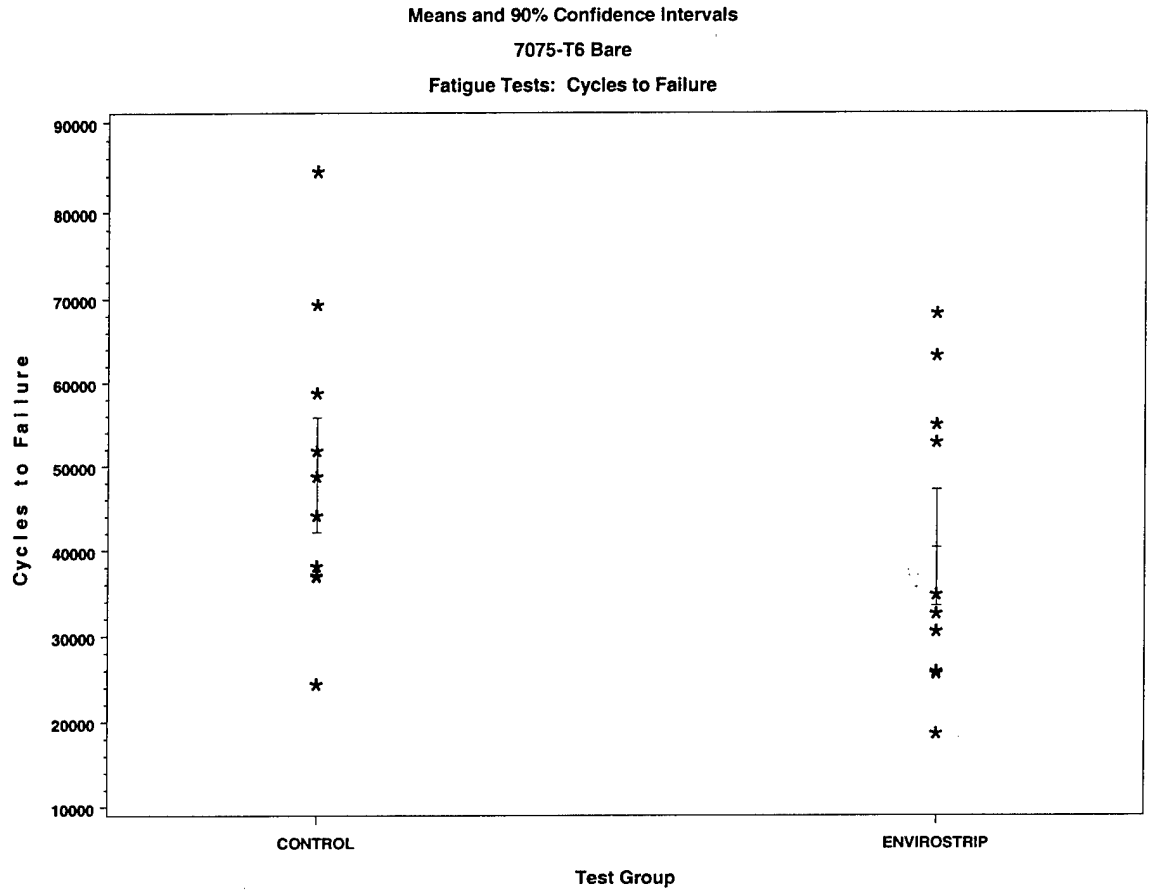

Figure 4.1 Scatter, Mean, and 90 Percent Confidence Intervals of Cycles to Failure for Bare 7075-T6

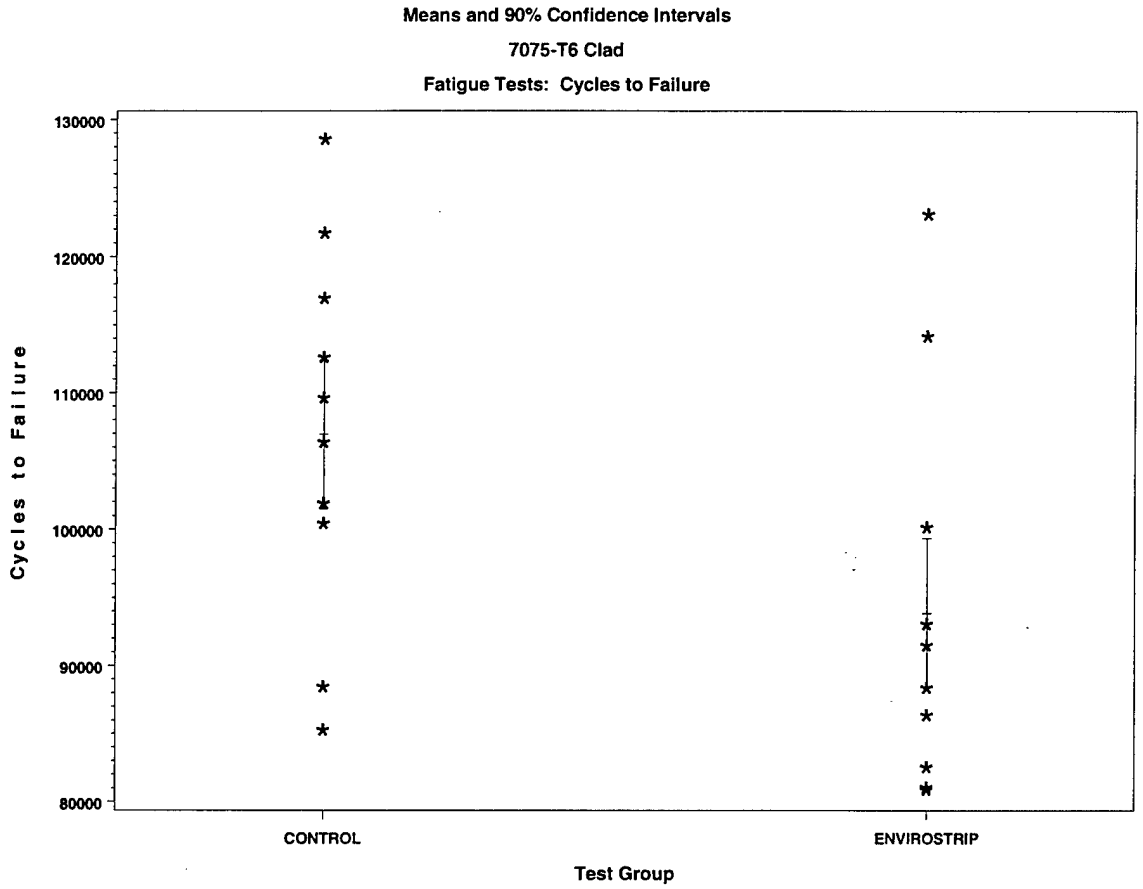

Figure 4.2 Scatter, Mean, and 90 Percent Confidence Intervals of Cycles to Failure for Clad 7075-T6

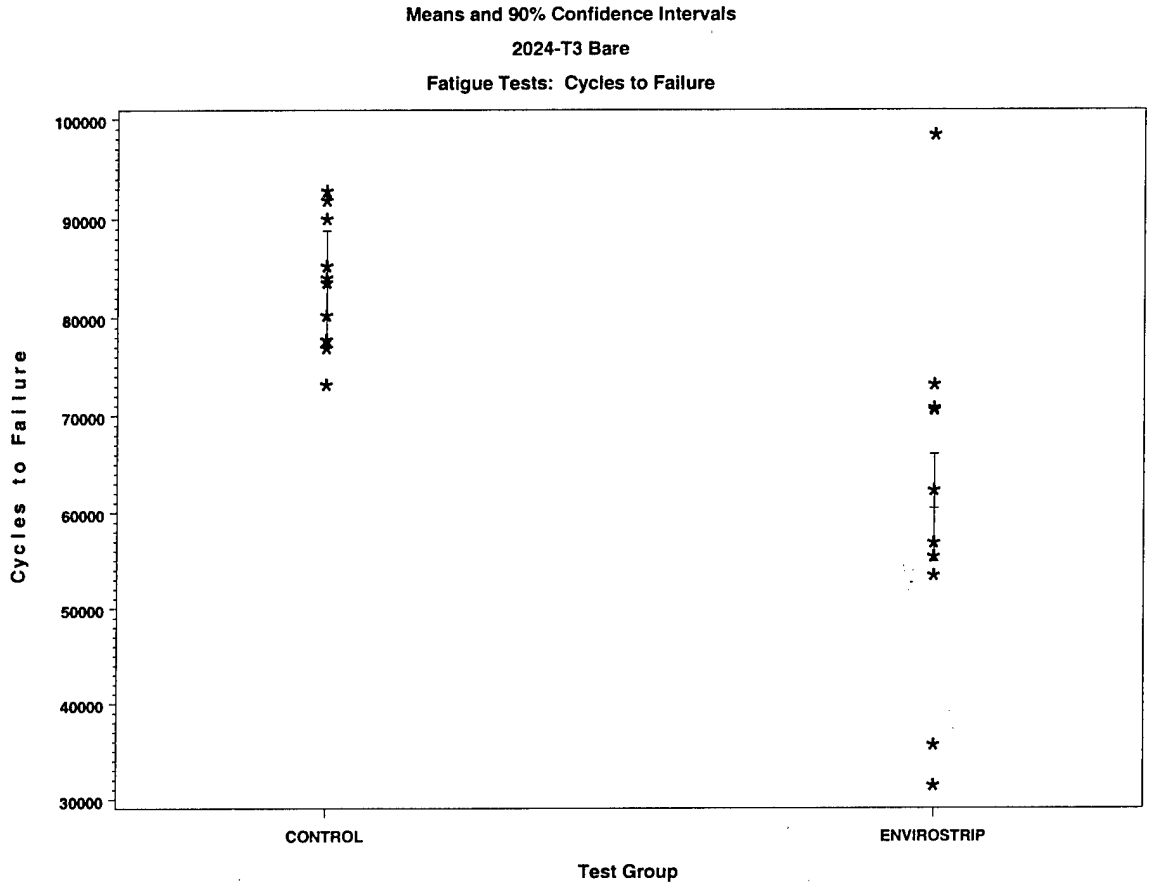

Figure 4.3 Scatter, Mean, and 90 Percent Confidence Intervals of Cycles to Failure for Bare 2024-T3

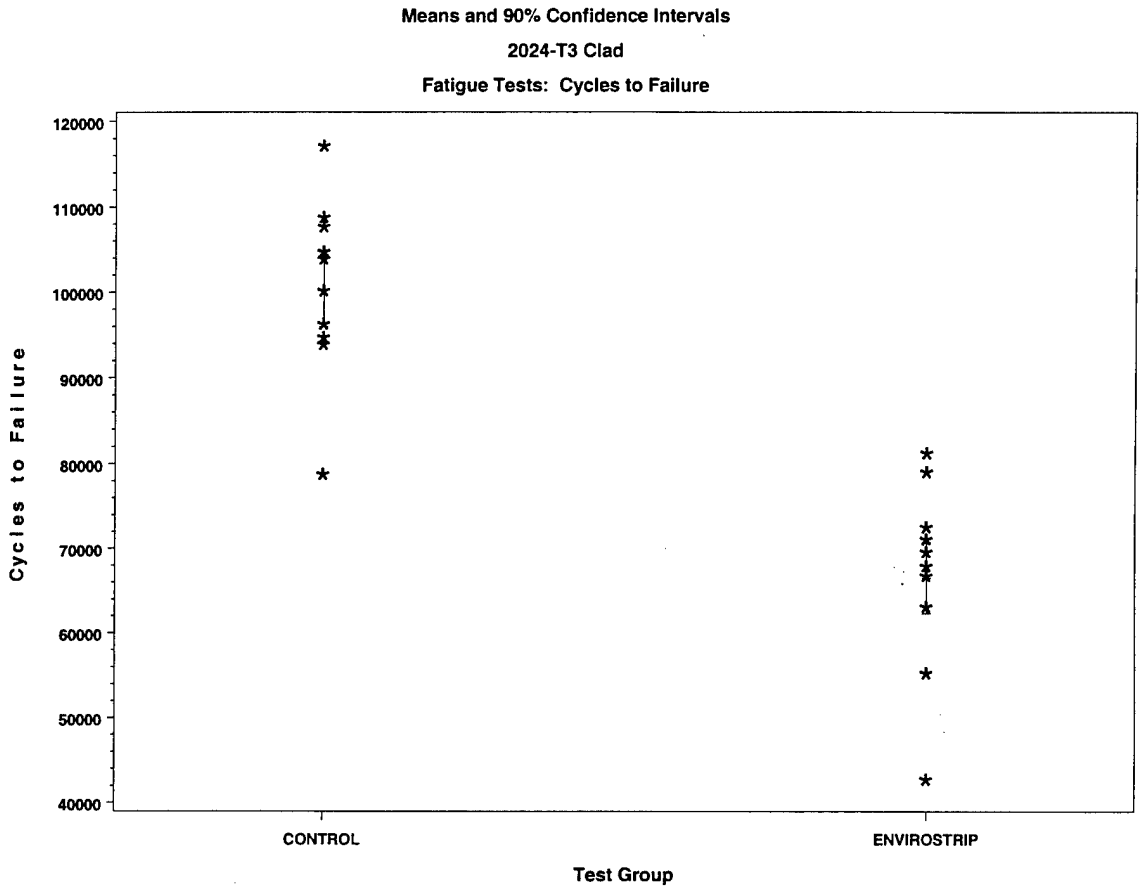

Figure 4.4 Scatter, Mean, and 90 Percent Confidence Intervals of Cycles to Failure for Clad 2024-T3

5. FATIGUE CRACK GROWTH RATE (FCGR) TEST RESULTS

Plots of crack growth rate (*da/dN*) versus stress intensity range (ΔK) for each set of Control and Blasted specimens of bare and clad 7075-T6, and bare and clad 2024-T3, are shown in Figures 5.1 through 5.8, respectively. There is very little scatter in the crack growth data in either the Control or Blasted groups. Each of the ten specimens within each group exhibited nearly identical fatigue crack growth rates throughout the ΔK range.

Figure 5.9 illustrates a third-order polynomial fit of the Control and Blasted bare 7075-T6 crack growth rate data, and Figure 5.10 is a polynomial fit of the Control and Blasted clad 7075-T6 data. For both the bare 7075-T6 and clad 7075-T6, the Control specimens appear to have a slightly slower crack growth rate than the Blasted specimens. The slopes of the curves are nearly the same. For the softer bare and clad 2024-T3 materials, the crack growth rates are virtually identical, as seen if Figures 5.11 and 5.12, respectively.

In order to compare the Control and Blasted specimens, the results were statistically analyzed by evaluating the FCGR for each specimen at a discrete stress intensity range. Outlier tests were performed on individual data points, and any identified outliers were deleted from the data set. For the tested specimens, the mean of the crack growth rate was calculated for the Control and Blasted specimens independently. ANOVA techniques were then used to compare the average crack growth rate of the Blasted specimens to the average crack growth rate of the Control specimens. All statistical tests were made at the 10% level of significance. The results of the statistical analyses are given in Tables 5.1 through 5.4. In general, there appears to be a statistically significant increase in the average crack growth rates from Control to Blasted specimens in at least three of the four materials, but, upon further analysis of the data sets, there is no engineering significance to this finding.

An assessment of the data was conducted because of the inherent variability in FCGR testing. With reference to ASTM E647, the precision in FCGR tests is a function of inherent material variability, as well as errors in crack measurement and the applied load. With the closed-loop electrohydraulic test equipment used in this study, a ±2% variation in the applied ΔK translates to a ±4% to ±10% variation in *da/dN* for a given ΔK above the near-threshold regime. In general, however, the crack length measurement error is a more significant contribution to the variation in *da/dN*. The ASTM standard states that this contribution is difficult to isolate since it is coupled with the analysis procedure of converting "a versus N" to "*da/dN*," and to the inherent material variability. In addition, an overall measure of variability in *da/dN* versus ΔK was available from the results of an ASTM interlaboratory test program involving 14 laboratories. Although the test data were obtained from a highly homogeneous material, the reproducibility in *da/dN* within a laboratory averaged ±27%, and ranged from ±13% to ±50%, depending on the particular laboratory. The repeatability between laboratories was ±32%. The cited variability in *da/dN* were believed to have arisen primarily from random crack length measurement errors. These

data are often used as a guideline for the kind of variability expected under ordinary circumstances.

Tables 5.1 through 5.4 list the coefficient of variation (COV) within each Control and Blasted group. With the bare and clad 7075-T6 materials, it is noted that the variability for the Blasted groups is nominally half that of the Control groups. For the bare and clad 2024-T3 materials, the variability of the Blasted groups is generally less than that of the Control groups, but certainly not to the extent seen with the bare and clad 7075-T6 materials.

Tables 5.1 through 5.4 also list the percentage deviation of the average of the Blasted group from the average of the Control group. In general, the percentage deviations from the Controls are on the order of 15-30% for the bare and clad 7075-T6, and 1-8% for the bare and clad 2024-T3. (It is noted that the percentage deviation between the Control and Blasted groups of clad 7075-T6's is 37% at ΔK=15. But there is generally more variability within data sets at higher levels of ΔK as the rate of crack growth begins to accelerate.) The variability in the 7075-T6 and 2024-T3 materials are generally below the average of the ASTM guidelines on reproducibility, and one cannot readily distinguish any differences in crack growth between Control and Blasted data sets.

An engineering summary of the FCGR data is given in Table 5.5. Table 5.5 also compares the engineering FCGR results for Envirostrip™ to the results for Type V and Polymedia-Lite™[1,2]. (The results for Type V blasting are different than what was reported in Reference 1. At that time, there was no consideration given to the inherent variability in the FCGR tests, and the statistical results were taken on face value. However, re-examination of the data revealed that the percentage deviations from Control at all levels of ΔK were well below the ASTM guidelines.) For the three different media, it was difficult to distinguish any differences in crack growth between Control and Blasted data sets for any of the aluminum alloys.

Table 5.1 Fatigue Crack Growth Rate Data and Statistical Analysis Results for 7075-T6 Bare

ΔK	Condition	Number of Tests	Average	Std Deviation	COV (%)	% Deviation from Control	Statistical Summary	Engineering Summary
	Control	10	4.347	0.568	13.1			
6	Envirostrip™	10	4.210	0.193	4.6	-3.2	NS	NPS
	Control	10	6.888	0.603	8.8			
7	Envirostrip™	10	6.248	0.366	5.9	-9.3	S ↓	NPS
	Control	10	8.640	0.725	8.4			
8	Envirostrip™	10	9.713	0.421	4.3	12.4	S ↑	NPS
	Control	10	11.225	0.969	8.6			
9	Envirostrip™	10	12.836	0.710	5.5	14.4	S ↑	NPS
	Control	10	14.319	1.349	9.4			
10	Envirostrip™	10	16.594	0.879	5.3	15.9	S ↑	NPS
	Control	10	17.473	1.635	9.4			
11	Envirostrip™	10	20.400	1.104	5.4	16.8	S ↑	NPS
	Control	10	20.614	2.496	12.1			
12	Envirostrip™	10	24.716	1.458	5.9	19.9	S ↑	NPS
	Control	10	24.542	3.448	14.0			
13	Envirostrip™	10	29.625	1.471	5.0	20.7	S ↑	NPS
	Control	9	29.329	3.012	10.3			
14	Envirostrip™	10	36.831	2.301	6.2	25.6	S ↑	NPS
	Control	7	37.590	3.154	8.4			
15	Envirostrip™	10	44.383	3.490	7.9	18.1	S ↑	NPS

NPS = Statistically significant difference in the average crack growth rate, but not practically significant.

NS = No statistically significant difference in the average crack growth rate between the Control specimens and the Envirostrip™ Specimens at the 10% level of significance.

S ↑ = Statistically significant increase in the average crack growth rate from Control to Envirostrip™ specimens at the 10% level of significance.

S ↓ = Statistically significant decrease in the average crack growth rate from Control to Envirostrip™ specimens at the 10% level of significance.

Table 5.2 Fatigue Crack Growth Rate Data and Statistical Analysis Results for 7075-T6 Clad

ΔK	Condition	No. Tests	Average	Std Deviation	COV (%)	% Deviation from Control	Statistical Summary	Engineering Summary
	Control	10	3.965	0.925	23.3			
6	Envirostrip™	10	4.158	0.178	4.3	4.9	NS	NPS
	Control	10	6.089	0.607	10.0			
7	Envirostrip™	10	6.852	0.226	3.3	12.5	S ↑	NPS
	Control	10	8.712	0.646	7.4			
8	Envirostrip™	10	9.773	0.266	2.7	12.2	S ↑	NPS
	Control	10	11.215	0.754	6.7			
9	Envirostrip™	10	13.307	0.573	4.3	18.7	S ↑	NPS
	Control	10	15.071	0.722	4.8			
10	Envirostrip™	10	16.767	0.695	4.1	11.3	S ↑	NPS
	Control	10	18.058	1.196	6.6			
11	Envirostrip™	10	20.861	1.025	4.9	15.5	S ↑	NPS
	Control	10	20.838	1.823	8.7			
12	Envirostrip™	10	25.427	1.139	4.5	22.0	S ↑	NPS
	Control	10	24.043	2.062	8.6			
13	Envirostrip™	10	31.245	1.559	5.0	30.0	S ↑	NPS
	Control	10	28.907	3.495	12.1			
14	Envirostrip™	10	38.037	3.435	9.3	31.6	S ↑	NPS
	Control	10	35.244	3.909	11.1			
15	Envirostrip™	10	48.402	3.854	8.0	37.3	S ↑	NPS

NPS = Statistically significant difference in the average crack growth rate, but not practically significant.

NS = No statistically significant difference in the average crack growth rate between the Control specimens and the Envirostrip™ Specimens at the 10% level of significance.

S ↑ = Statistically significant increase in the average crack growth rate from Control to Envirostrip™ specimens at the 10% level of significance.

Table 5.3 Fatigue Crack Growth Rate Data and Statistical Analysis Results for 2024-T3 Bare

ΔK	Condition	No. Tests	Average	Std Deviation	COV (%)	% Deviation from Control	Statistical Summary	Engineering Summary
	Control	10	1.292	0.113	8.7			
7	Envirostrip™	10	1.333	0.052	3.9	3.2	NS	NPS
	Control	10	1.837	0.079	4.3			
8	Envirostrip™	10	1.871	0.489	26.1	1.9	NS	NPS
	Control	10	2.553	0.113	27.4			
9	Envirostrip™	10	2.563	0.090	3.5	0.4	NS	NPS
	Control	10	3.373	0.164	4.9			
10	Envirostrip™	10	3.298	0.199	6.0	-2.2	NS	NPS
	Control	10	4.333	0.239	5.5			
11	Envirostrip™	10	4.272	0.153	3.6	-1.4	NS	NPS
	Control	10	5.097	0.855	16.8			
12	Envirostrip™	10	5.259	0.275	5.2	3.2	NS	NPS
	Control	10	6.791	0.376	5.5			
13	Envirostrip™	10	6.571	0.535	8.1	-3.2	NS	NPS
	Control	10	8.688	0.350	4.0			
14	Envirostrip™	10	7.958	0.314	3.9	-8.4	S ↓	NPS
	Control	10	10.437	0.746	7.1			
15	Envirostrip™	10	10.062	0.574	5.7	-3.6	NS	NPS

NPS = Statistically significant difference in the average crack growth rate, but not practically significant.

NS = No statistically significant difference in the average crack growth rate between the Control specimens and the Envirostrip™ Specimens at the 10% level of significance.

S ↓ = Statistically significant decrease in the average crack growth rate from Control to Envirostrip™ specimens at the 10% level of significance.

Table 5.4 Fatigue Crack Growth Rate Data and Statistical Analysis Results for 2024-T3 Clad

ΔK	Condition	No. Tests	Average	Std Deviation	COV (%)	% Deviation from Control	Statistical Summary	Engineering Summary
	Control	10	1.205	0.072	6.0			
7	Envirostrip™	10	1.260	0.044	3.5	4.6	S ↑	NPS
	Control	10	1.566	0.126	8.0			
8	Envirostrip™	10	1.699	0.067	3.9	8.5	S ↑	NPS
	Control	10	2.080	0.215	10.3			
9	Envirostrip™	10	2.258	0.153	6.8	8.6	S ↑	NPS
	Control	10	2.899	0.403	13.9			
10	Envirostrip™	10	3.054	0.202	6.6	5.3	NS	NPS
	Control	10	3.893	0.169	4.3			
11	Envirostrip™	10	4.136	0.219	5.3	6.2	S ↑	NPS
	Control	10	5.161	0.524	10.1			
12	Envirostrip™	10	5.455	0.267	4.9	5.7	NS	NPS
	Control	10	6.506	0.559	8.6			
13	Envirostrip™	10	6.935	0.455	6.6	6.6	S ↑	NPS
	Control	10	8.405	0.396	4.7			
14	Envirostrip™	10	8.957	1.042	11.6	6.6	NS	NPS
	Control	10	11.111	1.766	15.9			
15	Envirostrip™	10	11.158	1.009	9.0	0.4	NS	NPS

NPS = Statistically significant difference in the average crack growth rate, but not practically significant.

NS = No statistically significant difference in the average crack growth rate between the Control specimens and the Envirostrip™ Specimens at the 10% level of significance.

S ↑ = Statistically significant increase in the average crack growth rate from Control to Envirostrip™ specimens at the 10% level of significance

Table 5.5 FCGR Engineering Summary for Envirostrip™, Polymedia-Lite™, and Type V

Material	FCGR (1)		
	Envirostrip™	Polymedia-Lite™	Type V
7075-T6 Bare	NPS	NPS	NS
7075-T6 Clad	NPS	NPS	NPS
2024-T3 Bare	NPS	NPS	NPS
2024-T3 Clad	NPS	NPS	NPS

Notes:

1. NPS = Statistically significant difference in the average crack growth rate, but not practically significant.

NS = No statistically significant difference in the average crack growth rate between the Control specimens and the Blasted specimens at the 10% level of significance.

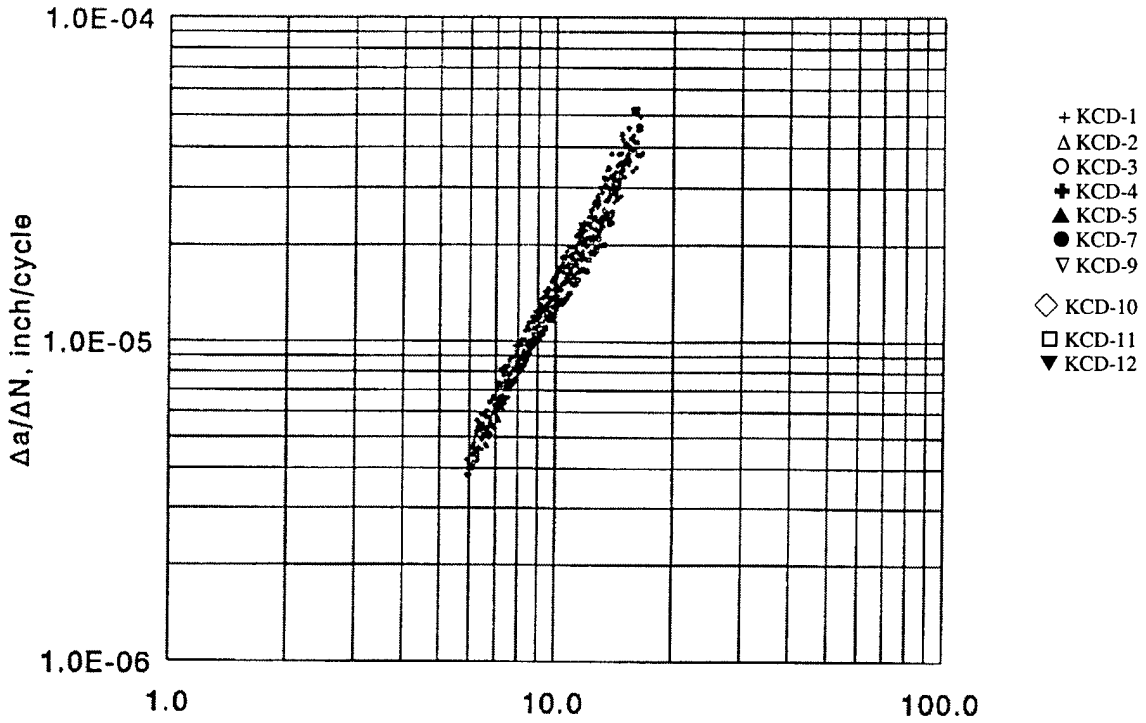

Figure 5.1 FCGR Test Results for Bare 7075-T6 Control Specimens

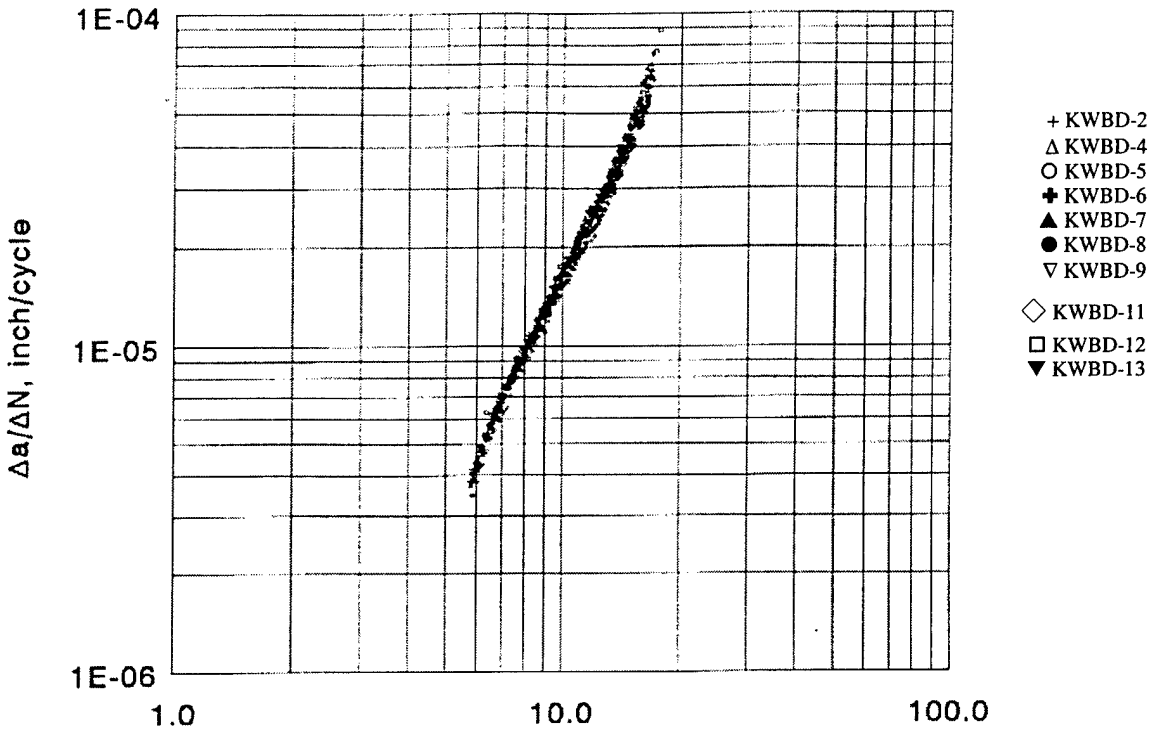

Figure 5.2 FCGR Test Results for Bare 7075-T6 Blasted Specimens

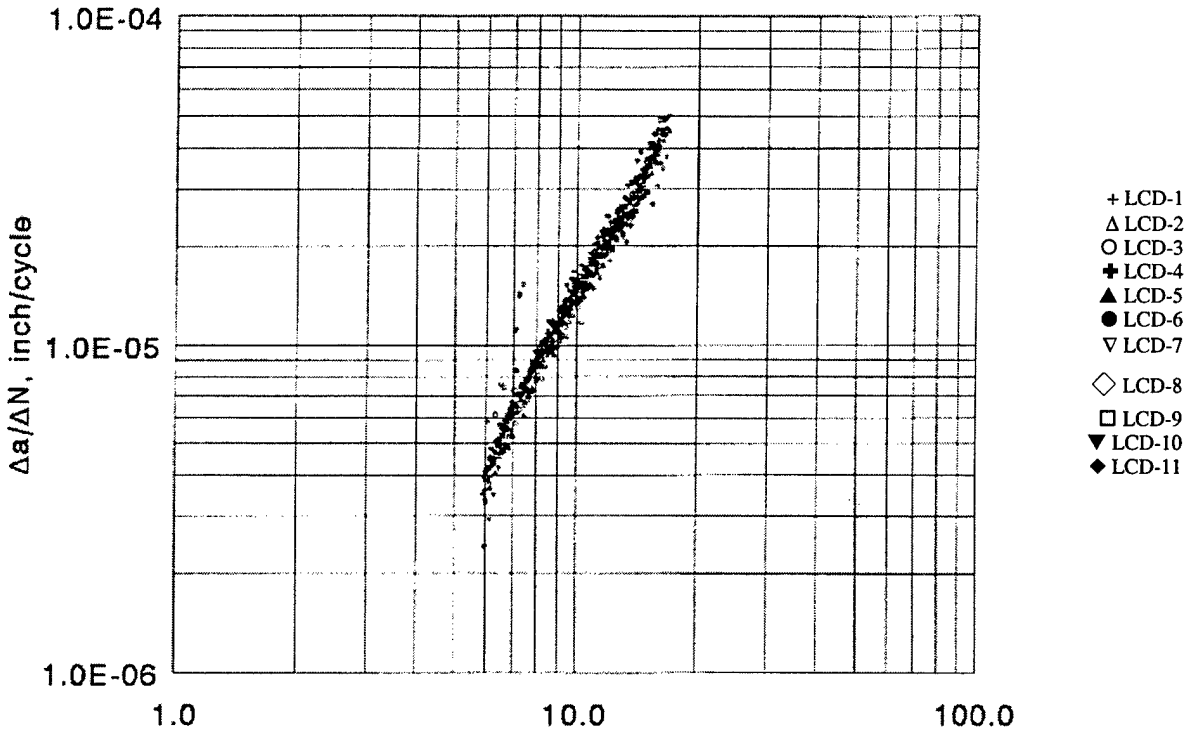

Figure 5.3 FCGR Test Results for Clad 7075-T6 Control Specimens

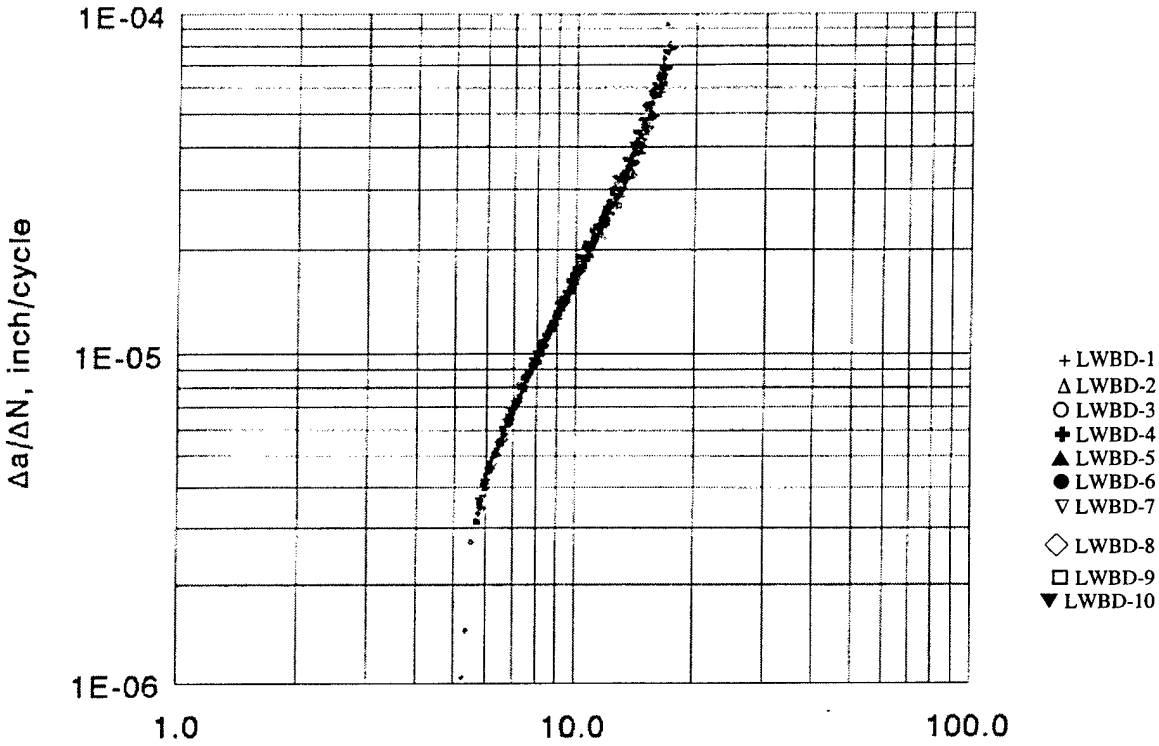

Figure 5.4 FCGR Test Results for Clad 7075-T6 Blasted Specimens

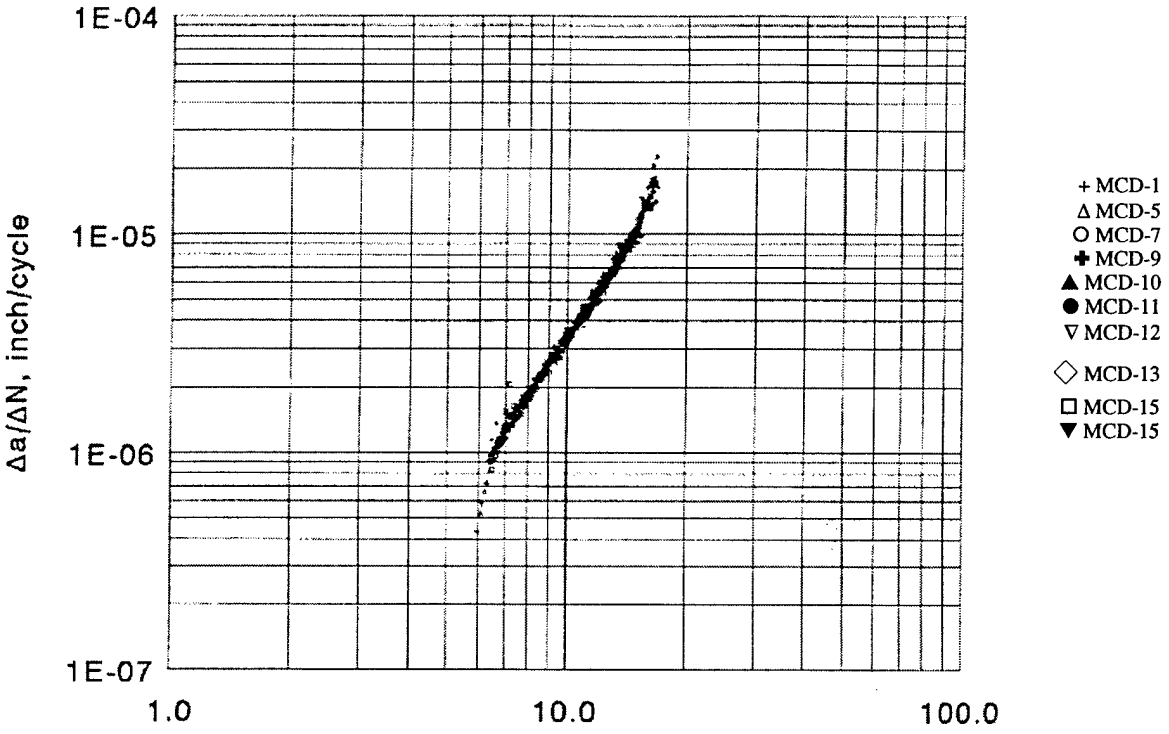

Figure 5.5 FCGR Test Results for Bare 2024-T3 Control Specimens

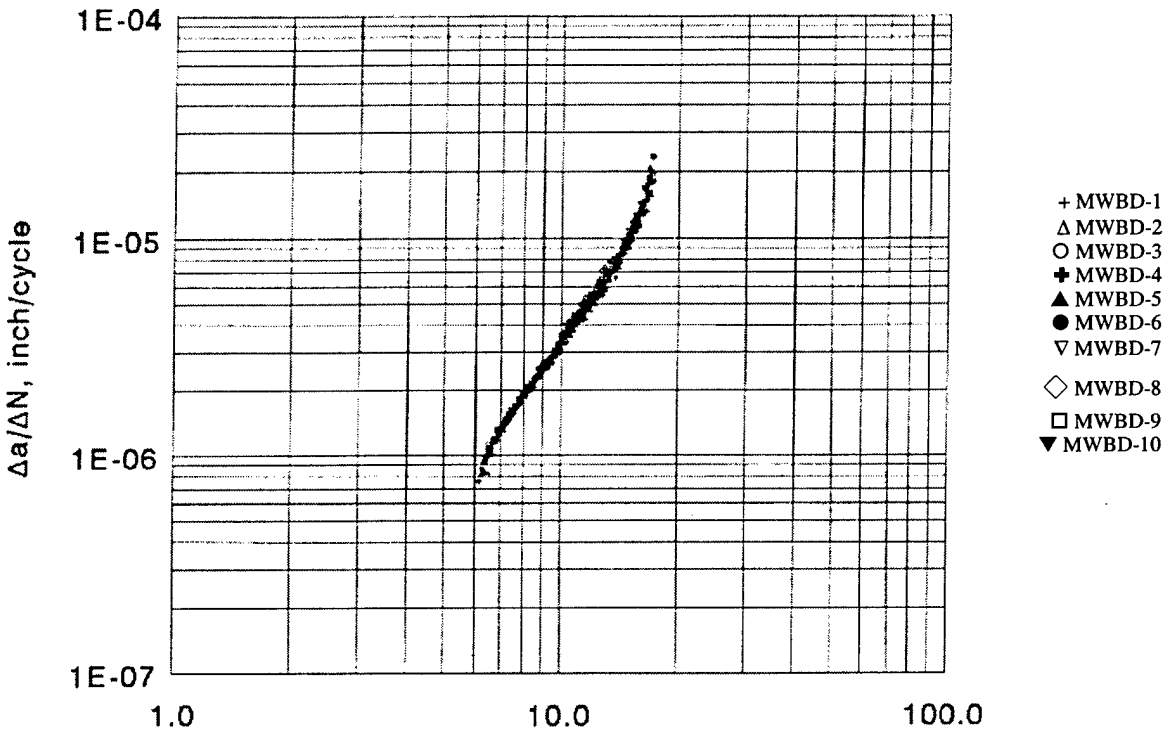

Figure 5.6 FCGR Test Results for Bare 2024-T3 Blasted Specimens

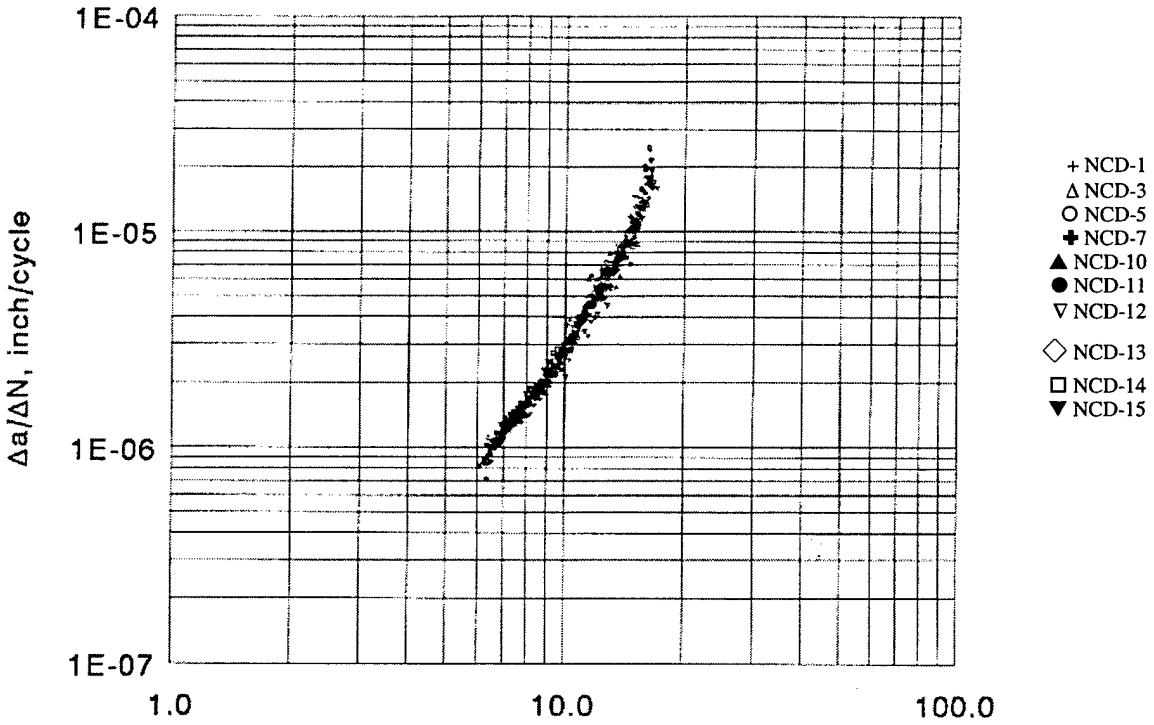

Figure 5.7 FCGR Test Results for Clad 2024-T3 Control Specimens

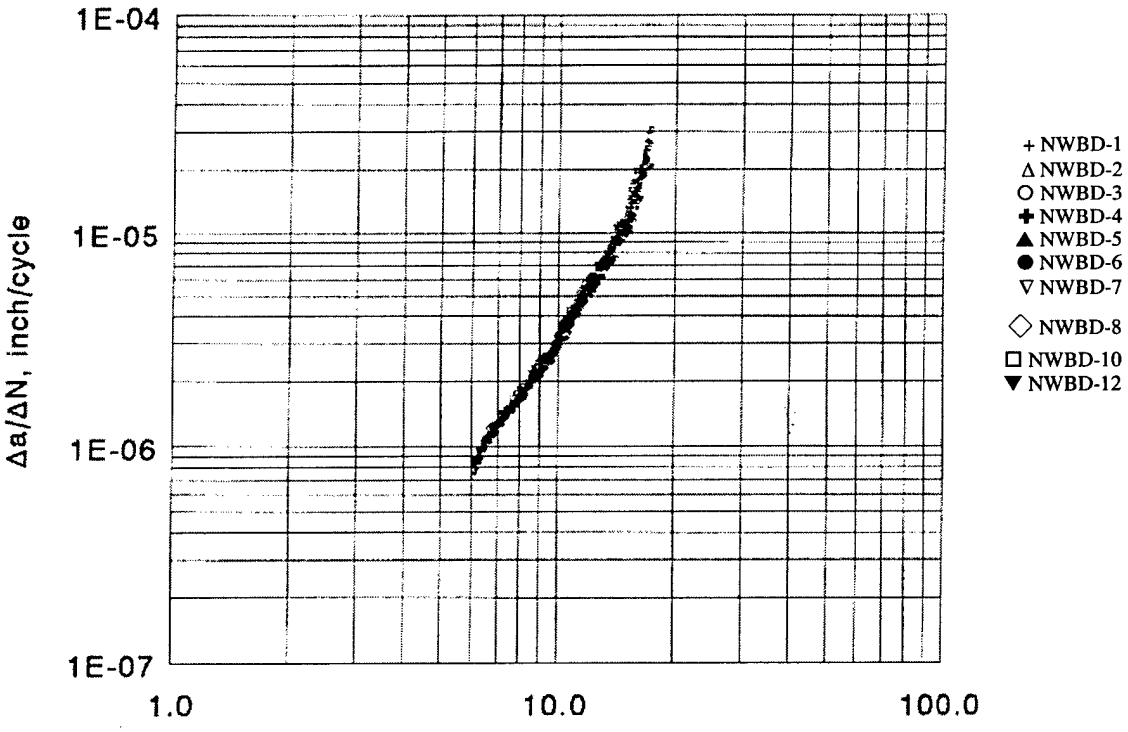

Figure 5.8 FCGR Test Results for Clad 2024-T3 Blasted Specimens

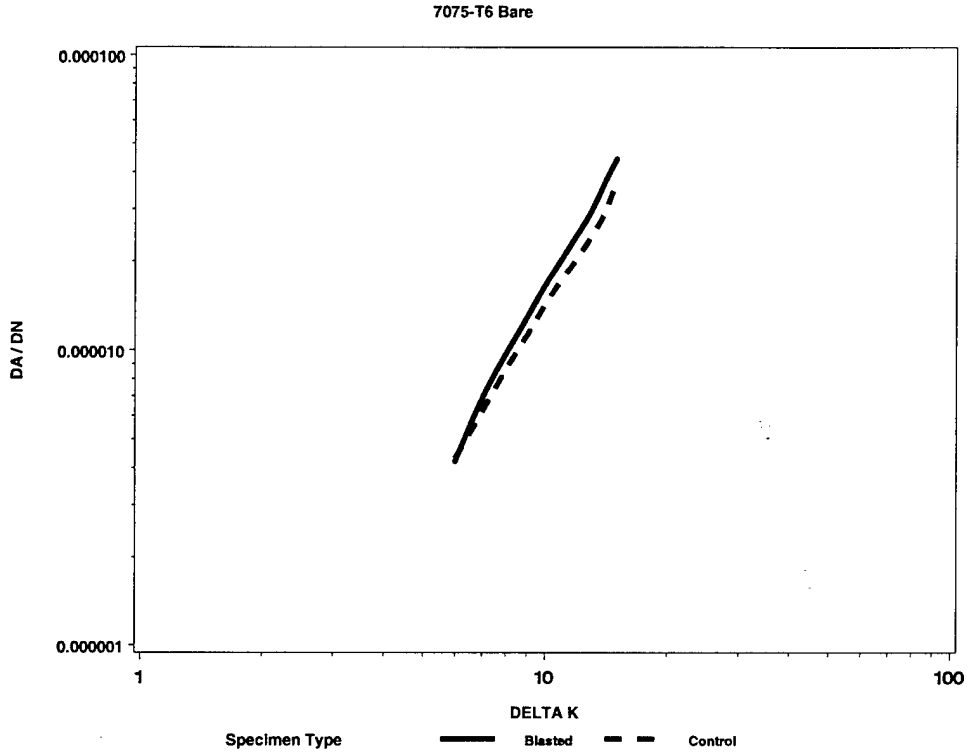

Figure 5.9 Comparison of Control and Blasted FCGR Curves for Bare 7075-T6

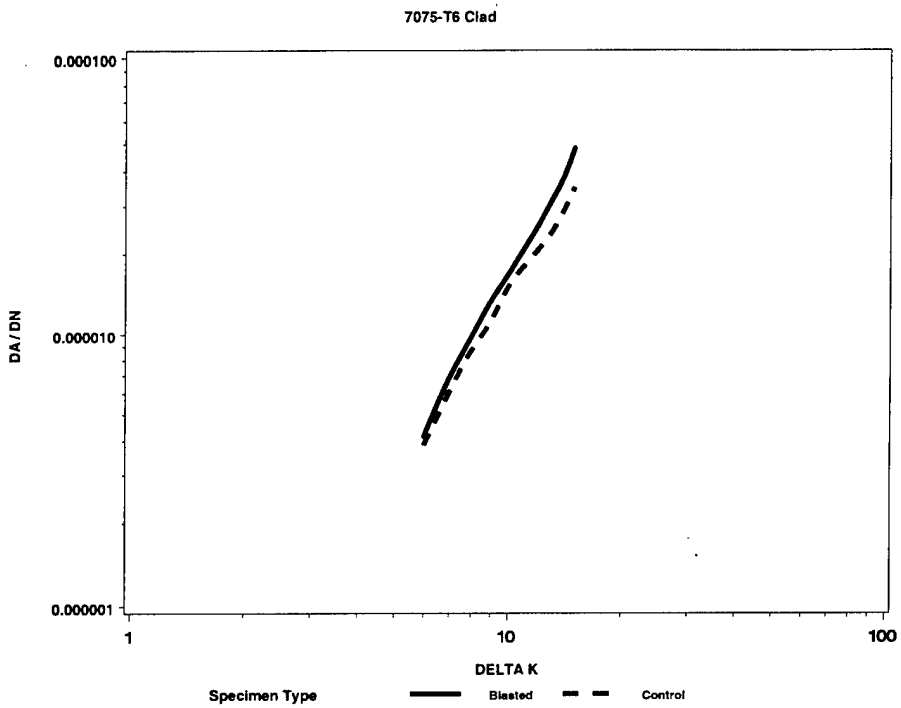

Figure 5.10 Comparison of Control and Blasted FCGR Curves for Clad 7075-T6

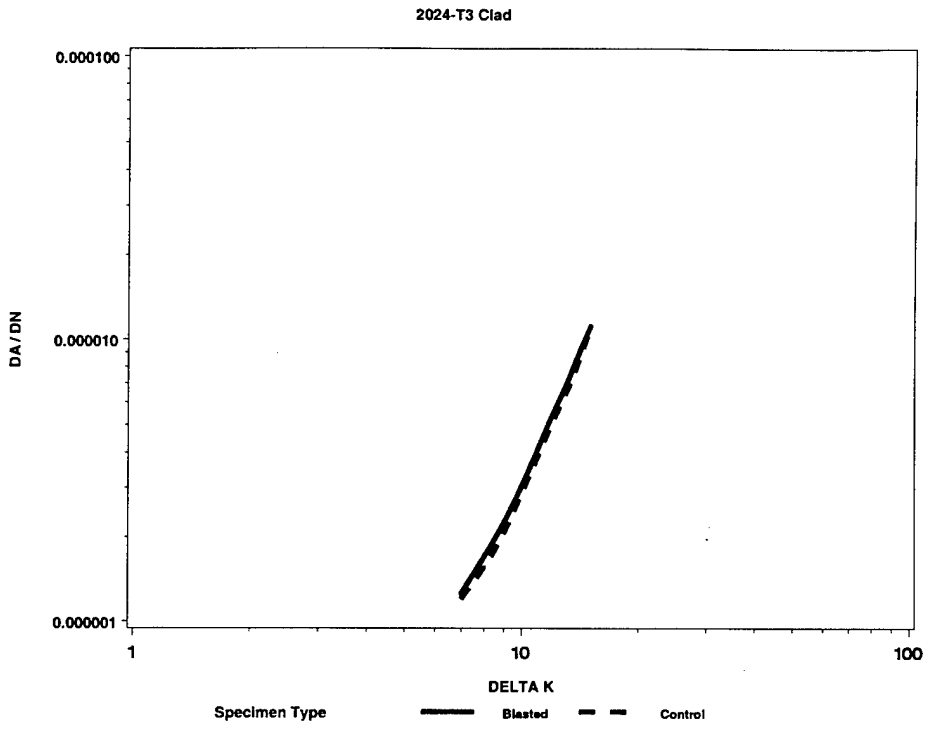

Figure 5.11 Comparison of Control and Blasted FCGR Curves for Bare 2024-T3

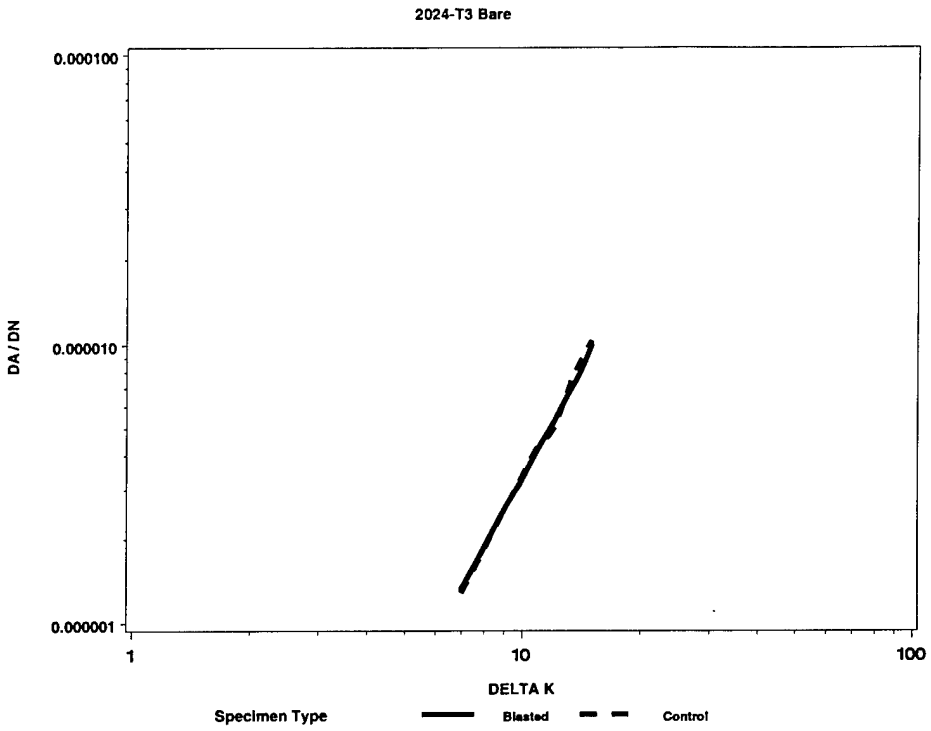

Figure 5.12 Comparison of Control and Blasted FCGR Curves for Clad 2024-T3

6. DAMAGE ASSESSMENT TEST RESULTS

Dry media blasting may to impart a layer of compressive residual stresses to the blasted surface of the aluminum material, while simultaneously causing an increase in the surface roughness. The compressive stresses may enhance the fatigue resistance of the part, while the increased surface roughness may diminish the fatigue resistance. These competing effects may or may not have a significant net effect on the fatigue life. The development of residual stresses in bare 2024-T3 were evaluated to determine how the effects of Envirostrip™ compare to Type V and Polymedia-Lite™, and to determine if the residual stresses could have influenced the fatigue test results presented in Section 4.0. In addition, once the fatigue test results indicated statistically significant decreases in the material properties, SwRI conducted surface roughness measurements on all four of the aluminum alloys to determine if the surface roughness may have influenced the test results. The reader is also referred to Appendix B for a thorough discussion of how residual compressive stresses and surface roughness may affect fatigue lives.

6.1 Residual Stress Saturation

Blast peak or saturation data were developed to indicate the degree of residual stress saturation for a given material, and at what point, in terms of strip cycle, this cumulative effect was thought to be a maximum. Measuring the change in height of blasted specimens was not a direct measurement of the blast-induced cold work strains, but rather a change in the bending moment of the unrestrained specimen produced by the residual stresses associated with the cold work process. As such, delta height measurements offered a relative gauge of the degree of blast-imparted residual stresses. The specimens used for this characterization were modified Almen specimens fabricated from unpainted bare 2024-T3 aluminum. The specimens were rectangular strips, 3 inches long and 0.75 inch wide. The thickness of the Almen strips was 0.032 inch. For each blast cycle, three Almen specimens were blasted with Envirostrip™ and the height of the strips was recorded for each strip cycle as the arithmetic mean of the three different specimens. For this test effort, a total of thirty Almen specimens were required to determine the Almen arc height for each of the ten blast cycles. All stripping parameters were identical to those used for the mechanical property tests.

The saturation data are given in Table 6.1 and plotted as a function of Almen arc height versus blast cycles in Figure 6.1, which also compares the Envirostrip results with Type V and Polymedia-Lite™ [1,2]. The Almen specimens blasted with Envirostrip™ reached saturation after seven blast cycles at an arc height of approximately 0.0058 inch (averaged over cycles 7 through 10). Almen specimens blasted with Polymedia-Lite reached saturation after four blast cycles at an arc height of approximately 0.0050 inch, although that

number rose slightly to 0.0057 inch after the eighth blast cycle (averaged over cycles 7 through 10). The final arc heights of bare 2024-T3 blasted with Envirostrip™ and Polymedia-Lite™ were nearly identical, although Almen specimens blasted with Polymedia-Lite™ reached a saturation level earlier in the blast cycle process. As seen in Figure 6.1, saturation with Type V media occurred after the fourth blast cycle, though the measured saturation Almen arc height was significantly higher at 0.0080 inch (averaged over Cycles 7 through 10).

6.2 Surface Profile Roughness

It was not originally intended to measure the surface roughness of aluminum alloys blasted with Envirostrip™ because the surface roughness had been measured previously in Reference 3. However, the statistically significant decreases in the tensile properties and fatigue lives prompted SwRI to undertake this additional effort. It was believed that the surface roughness data could help determine whether the trends in the mechanical property data were a real effect of the blasting operation, or were just a figment of the statistical analysis and had no true practical significance.

In the Reference 3 study, evaluation of the surface profile roughness on unpainted modified Almen specimens was done on both bare and clad 2024-T3 using Envirostrip™ media. The thickness of the test specimens was 0.025 inch and not the 0.032 inch used in this current study. Table 6.2 lists the surface profile roughness measurements for bare 2024-T3. The average and standard deviation were determined from five measurements on each specimen. It is noted that after four blast cycles, the average surface roughness of 0.025-inch-thick bare 2024-T3 blasted with Envirostrip™ was 11μin. The surface roughness measurement taken on unblasted material (Cycle 0) was 12μin. (Obviously, since one would not expect the roughness of the surface after four blast cycles to be less than the roughness of the unblasted surface, there is some variability in these measurements due to the nature of the variability of the material's surface and the precision of the surface roughness measurements as well.) This data indicates that the Envirostrip™ did not change the surface roughness of the bare 2024-T3.

Table 6.2 also lists the surface roughness values for 0.032-inch-thick bare 2024-T3 that was blasted with Type V and Polymedia-Lite™ [1,2], which after four blast cycles, were 23μin and 22μin, respectively. Figure 6.3 compares the surface roughness per blast cycle for all three media. The Type V and Polymedia-Lite™ did slightly roughen the surface of the bare 2024-T3, though the 10μin is not considered to be much of a difference.

Table 6.3 lists the surface profile roughness measurements on clad 2024-T3 blasted with Type V, Polymedia-Lite™, and Envirostrip™. After four blast cycles, these measurements were 149μin, 70μin, and 76μin, respectively, for the three media. It is noted that the first cycle roughness for the Type V was nominally 210μin, and that the drop in roughness during the latter cycles was attributed to a smoothing effect from the slight erosion of the clad. Figure 6.4 compares the average surface roughness per blast cycle for the clad

material. The roughness measurements for the clad 2024-T3 blasted with Polymedia-Lite™ and Envirostrip™ stayed relatively constant around 70μin. Both media were much less erosive to the clad than the Type V.

For the current study, strips of 0.032-inch-thick bare and clad 7075-T6 and bare and clad 2024-T3 were removed from the mechanical property test panels that had already been exposed to four blast cycles. These strips were extra material located near the edges of the panels. The strips were 16 inches long and at least 1.5 inches wide; they were not the size of modified Almen test specimens used in Reference 3. Measurements of the surface roughness were made using a MicroAnalyzer 2000 from Precision Devices, Inc. Measurements were taken in six locations along the midline of the strip and were one inch away from each other. In addition, the tip of the MicroAnalyzer averaged the surface roughness along a one-inch path at each location. In this manner, the surface roughness for each material was averaged from six different passes of the blast nozzle along one-inch distances within each pass. It is noted that the strips were not subjected to overblast since the X-Y positioner (see Section 2.4) moved beyond the test panel before traversing in the Y-direction in preparation for the next horizontal pass. Surface roughness measurements of the unblasted surfaces were also taken from the opposite side of the test strips. This provided a comparison of the change in surface roughness between the as-received and blasted surfaces.

Table 6.4 lists the surface roughness measurements for the four aluminum alloys at each of the six locations. The average surface roughness of the bare 7075-T6 rose from 17μin on the unblasted surface to 22μin on the blasted surface, which was an insignificant increase after four blast cycles. The surface roughness of the bare 2024-T3 behaved in a similar manner; the roughness increased from the as-received 12μin to 15μin after blasting. These data compared favorably to the surface roughness of 11μin measured on the 0.025-inch-thick bare 2024-T3. These small differences were also indicative of the consistency of the Envirostrip™ media and the reproducibility of the blast process using the robotic X-Y positioner.

Identical behaviors were seen when comparing the clad materials. From Table 6.4, the average surface roughness of the clad 7075-T6 rose from 5μin on the unblasted surface to 80μin on the blasted surface. Similarly, the surface roughness of the clad 2024-T3 rose from 4μin to 90μin. These numbers were slightly higher than the average surface roughness 76μin measured on the 0.025-inch-thick clad 2024-T3.

It is noted that there is a difference in the thickness of the clad layer on the 0.032-inch-thick and 0.025-inch-thick alloys. The clad layer is nominally 2-5% of the total sheet thickness. Assuming that the clad layer was 5% of the thickness, then the clad had a thickness of 0.0016 inch on the 0.032-inch panels and 0.0013 inch on the 0.025-inch panels.

The data for the bare and clad 2024-T3 from the current study is superimposed on Figures 6.2 and 6.3. The spread in the data is shown at the fourth blast cycle. It is evident that there is little difference in surface roughness between the 0.025-inch-thick 2024-T3 blasted with Envirostrip™, the 0.032-inch-thick 2024-T3 blasted with Envirostrip™, and the

0.032-inch-thick 2024-T3 blasted with Polymedia-Lite™. The only distinction that can be made is between the 0.032-inch-thick clad 2024-T3 blasted with Type V and all of the other dry media.

The surface roughness does not appear to be the sole reason for causing the statistically significant decreases in tensile properties and fatigue lives. There is little change in the average roughness of the bare materials, and thus the roughness alone can not account for the decreases in the material properties. It is also doubtful that the change in surface roughness affected the material properties of the clad materials. The similarities between the average roughness measurements for Polymedia-Lite™ and Envirostrip™ would suggest that the tensile and fatigue tests conducted with Polymedia-Lite™ would show the same statistically significant decreasing trend in material properties that were seen with Envirostrip™. This was not the case; in fact, there was no consistent trend in the Polymedia-Lite™ tensile test results (See Section 3.0) nor in the fatigue test results. (Although there was a statistically significant decrease in the fatigue life of bare 7075-T6 blasted with Polymedia-Lite™, this was attributed to scatter in the test results and additional testing was suggested to substantiate or repudiate this result.) Nonetheless, since there was no overall trend in the Polymedia-Lite™ tensile and fatigue test results despite having the same surface roughness values as Envirostrip™, it is inadvisable to claim that the surface roughness alone caused the statistically significant decreasing trend in the Envirostrip™-blasted materials. Rather, residual stress states in the materials may have also influenced the material property test results.

Table 6.1 Residual Stress Arc Heights of 0.032-inch-thick Bare 2024-T3 After Blasting with Dry Media

Blast Cycle	Dry Media		
	Type V	Polymedia-Lite™	Envirostrip™
1	0.0053	0.0024	0.0017
2	0.0062	0.0044	0.0028
3	0.0070	0.0046	0.0035
4	0.0075	0.0053	0.0045
5	0.0079	0.0052	0.0039
6	0.0076	0.0056	0.0048
7	0.0077	0.0051	0.0060
8	0.0076	0.0058	0.0058
9	0.0085	0.0055	0.0052
10	0.0083	0.0062	0.0063

Table 6.2 Surface Profile Roughness Measurements for Bare 2024-T3 Using Type V, Polymedia-Lite™, and Envirostrip

Blast Cycle	Surface Roughness (μin)					
	Type V (1)		Polymedia-Lite™ (1)		Envirostrip™ (1)	
	Average	Standard Deviation	Average	Standard Deviation	Average	Standard Deviation
0	8.1	-	-	-	12.1 (2)	-
1	9.7	-	14.4	2.9	9.8	1.6
2	9.8	-	17.0	1.7	9.3	0.6
3	14.0	-	20.8	1.6	10.8	1.7
4	22.1	-	22.8	1.9	11.3	2.0

Notes:

1. The thickness of the Type V and Polymedia-Lite™ test specimens was 0.032 inch. The thickness of the Envirostrip test specimens was 0.025 inch. Type V data is from Reference 1, Polymedia-Lite™ data is from Reference 2, and Envirostrip data is from Reference 3.

2. Blast Cycle 0 data for Envirostrip™ is from this current study. See also Table 6.4.

Table 6.3 Surface Profile Roughness Measurements for Clad 2024-T3 Using Type V, Polymedia-Lite™, and Envirostrip

Blast Cycle	Surface Roughness (µin)					
	Type V (1)		Polymedia-Lite™ (1)		Envirostrip™ (1)	
	Average	Standard Deviation	Average	Standard Deviation	Average	Standard Deviation
0	5.1	-	-	-	4.3 (2)	-
1	212.1	-	66.7	2.6	76.4	13.7
2	207.5	-	68.6	3.5	73.0	8.0
3	128.5	-	71.2	3.4	69.7	11.9
4	149.3	-	70.0	2.7	76.0	8.4

Notes:

1. Type V data is from Reference 1, Polymedia-Lite™ data is from Reference 2, and Envirostrip data is from Reference 3.

2. Blast Cycle 0 data for Envirostrip™ is from this current study. See also Table 6.4.

Table 6.4 Surface Roughness of 0.032-inch Panels Blasted with Envirostrip™

7075-T6 BARE				7075-T6 CLAD		
	Ra (uin)				Ra (uin)	
Location	Unblasted Surface (A)	Blasted Surface (B)		Location	Unblasted Surface (A)	Blasted Surface (B)
1	17.3	22.7		1	4.8	80.7
2	16.9	19.9		2	4.8	84.2
3	17.0	22.8		3	4.8	80.9
4	18.2	20.2		4	4.6	79.9
5	17.6	24.4		5	5.2	76.6
6	17.4	20.0		6	5.0	79.1
Average	17.4	21.7		Average	4.9	80.2
Std Dev	0.47	1.89		Std Dev	0.21	2.49
2024-T3 BARE				**2024-T3 CLAD**		
	Ra (uin)				Ra (uin)	
Location	Unblasted Surface (A)	Blasted Surface (B)		Location	Unblasted Surface (A)	Blasted Surface (B)
1	12.5	17.5		1	4.4	90.1
2	11.8	13.6		2	4.3	95.3
3	11.9	18.7		3	4.3	89.6
4	12.2	13.4		4	4.4	87.8
5	12.6	16.7		5	4.4	93.1
6	11.8	12.3		6	4.1	85.0
Average	12.1	15.4		Average	4.3	90.2
Std Dev	0.36	2.60		Std Dev	0.12	3.68

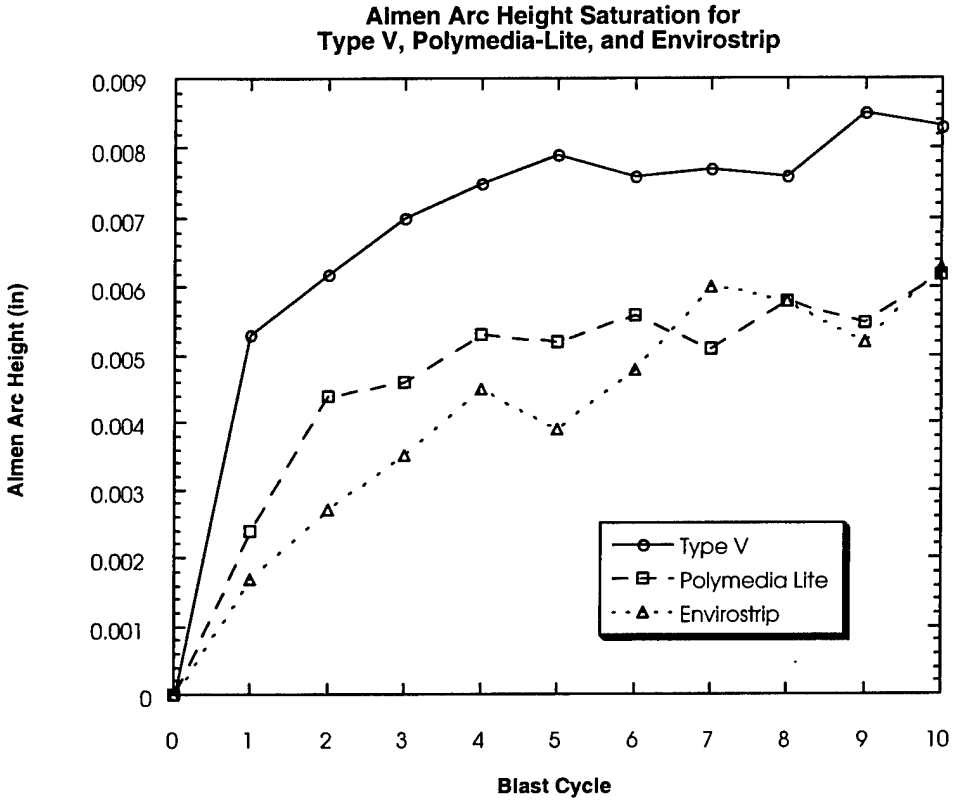

Figure 6.1 Almen Arc Height Saturation Curves for Type V, Polymedia-Lite™, and Envirostrip™ on 0.032-inch Bare 2024-T3

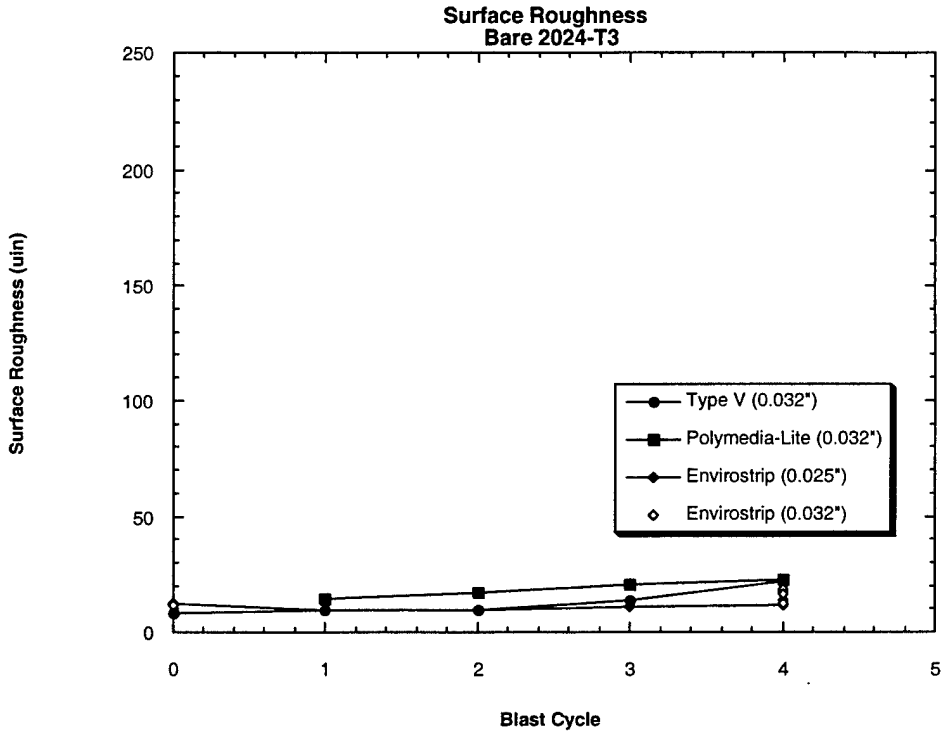

Figure 6.2 Surface Roughness Per Blast Cycle for Type V, Polymedia-Lite™, and Envirostrip™ on Bare 2024-T3

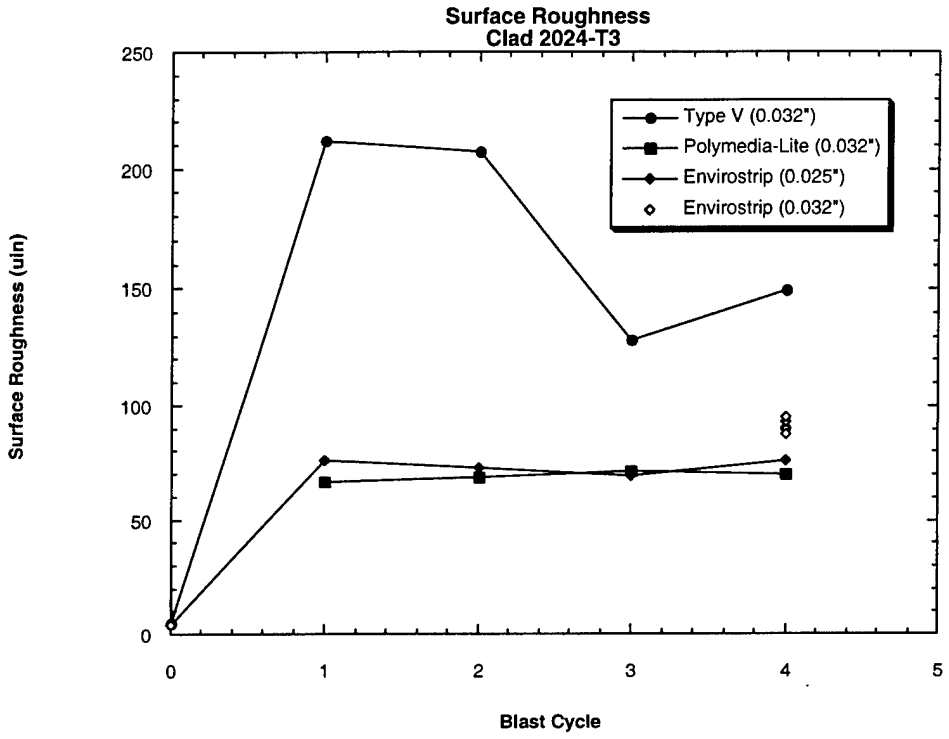

Figure 6.3 Surface Roughness Per Blast Cycle for Type V, Polymedia-Lite™, and Envirostrip™ on Clad 2024-T3

7. CONCLUSIONS/RECOMMENDATIONS

Southwest Research Institute has developed baseline data for assessing an Envirostrip™ media DMB process for use on 0.032-inch-thick 7075-T6 and 2024-T3 aluminum sheet panels. For both alloys, bare and clad panels were tested. The material property tests included static tensile tests, constant amplitude fatigue tests, and constant amplitude fatigue crack growth rate tests. In addition, material damage assessment tests were conducted. These tests included an assessment of surface profile roughness and residual stress peak/saturation data development.

The blasting parameters were determined by the media vendor, who demonstrated a coating removal rate of 0.83 square feet/minute on bare aluminum and 0.75 square feet/minute on clad aluminum using a nozzle pressure of 40 psi and a stand-off distance of 3 inches. The 0.5-inch round nozzle was oriented at 45 degrees to the panel, and the media flow rate was 12 lb/minute. Since the panels were not painted or prepared in any way, SwRI was unable to verify the strip rates.

The tensile test data indicated no degradation of material properties due to stripping with the Envirostrip™ process. The tensile yield stress and ultimate strength data were very precise; a difference of 3 ksi (or less than 4%) in the average measured properties resulted in a statistically significant effect. This difference was within accepted test variation due to experimental error and material variability, and for these reasons may not be of practical significance. There were no statistically significant differences in the average elongation for bare and clad 7075-T6 and clad 2024-T3. There was a statistically significant increase in the elongation for bare 2024-T3, but the difference was only 1%. This was also within accepted test variation and may not be of practical significance.

The majority of statistical results for fatigue crack growth rates indicated differences between the Control and Blasted groups. However, the variability in the 7075-T6 and 2024-T3 materials were generally below the average of the ASTM guidelines on reproducibility, and it was difficult to distinguish any differences in crack growth between Control and Blasted data sets.

The damage assessment test results were: (1) Test specimens blasted with Envirostrip™ reached saturated stress levels after seven blast cycles. The Almen arc height was approximately 0.0058 inch. In contrast, specimens blasted with Polymedia-Lite™ reached saturation after four blast cycles at an arc height of 0.0050 inch, although the number rose slightly to 0.0057 inch after the seventh blast cycle. Specimens blasted with Type V reached saturation after four blast cycles at an arc height of 0.0080 inch. (2) Experimental data indicated that Envirostrip™ did not change the surface roughness of bare 7075-T6 or bare 2024-T3. The roughness on clad 2024-T3 was approximately 70µin after four blast cycles, which was comparable to earlier results with Polymedia-Lite™. Tests on clad 7075-T6 yielded similar results, with the roughness after four blast cycles reaching 80µin.

There was no statistically significant difference in the average fatigue lives from Control to Blasted specimens for bare 7075-T6. There were, however, statistically significant decreases in fatigue lives for clad 7075-T6, and for bare and clad 2024-T3. Unlike the tensile test results, the debits in the fatigue lives were significant from both statistical and engineering points of view. The substantial decreases in fatigue lives prompted further investigations to explore why the debits were observed for the Envirostrip process. Brief, exploratory investigations led to formulations of simple hypotheses that may lead to a better understanding of the observed behavior. Historical fatigue life data from Type V and Polymedia-Lite™, surface roughness, and residual stress measurements were considered in the formulation of the hypotheses.

It was hypothesized that the fatigue life behavior of blasted surfaces can be understood in terms of the competing effects of beneficial compressive surface residual stresses and harmful surface roughness. The Envirostrip™ blasting process had the most shallow (least beneficial) compressive residual stresses than either Type V or Polymedia-Lite™ (based on test results from previous studies), and the shallow residual stresses may have been more susceptible to stress relaxation during fatigue cycling. The Envirostrip™ process exhibited higher and more damaging levels of surface roughness than Polymedia-Lite™, but were significantly less than the roughness levels resulting from Type V. (The increased surface roughness resulting from Type V was apparently offset by the substantially deeper levels of compressive residual stress, resulting in no statistically significant loss in fatigue lives.) No definitive conclusions could be reached about the fatigue performance of dry media blasted aluminum alloys, but the available information supported the hypothesis that fatigue performance was influenced by the beneficial effects of compressive residual stresses and the deleterious effects of surface roughness.

This hypothesis indicated that the effects of blasting on fatigue performance were inherently *surface* effects, and they led to changes in the fatigue performance because fatigue life (as measured in the DMB test programs) is predominantly driven by surface behavior. It would not be surprising, then, that blasting had relatively little effect on tensile strength or on fatigue crack growth properties, since these behaviors were predominantly controlled by the *bulk* response of the material. The bulk condition or response of the material was not substantially impacted by blasting processes.

Further work would be required to confirm or deny the fatigue life hypothesis, or, if desired, to develop a more fundamental understanding of the problem. No Almen strip deflection/residual stress tests were conducted with either clad 2024-T3 material or bare or clad 7075-T6, and these would be useful to characterize the residual stresses in the clad layer. It could be particularly interesting to evaluate the residual stresses before and after fatigue cycling, perhaps with Almen strip tests, to make some assessment of the residual stress relaxation due to cycling. A more systematic treatment of the problem comparing the residual stresses and the fatigue performance of clad material in the as-blasted condition with blasted material that has been stress relieved (to remove residual stresses) or electropolished (to remove surface roughness). Related to this is the potential impact of the sanding, priming, and repainting operation on the surface roughness of blasted material, and hence on the fatigue performance. Finally, just as shot-peening parameters can be

adjusted to optimize the depth and magnitude of the beneficial residual stresses while minimizing surface damage, it may be possible to optimize the blasting parameters in such a way as to improve their post-blast fatigue performance.

8. REFERENCES

1. Fitzgerald, J., Sharron, T., Spigel, B., Whitney, T., and Buckingham, J., "Plastic Media Blasting Material Characterization Study for Use on Thin-Skinned Substrate, Volume I – Evaluation of Aluminum Substrates," Final Report, San Antonio Air Logistics Center, Kelly AFB, TX, July 1995.

   Also in: Spigel, B., and Whitney, T., "Material Characteristic of Plastic Media Blasting (PMB) of Thin-Skinned Aluminum Substrates," Proceedings of the 1995 DoD/Industry Advanced Coatings Removal Conference, Albuquerque, NM, May 1995.

2. Spigel, B., and Buckingham, J., "Material Characteristic Study for Polymedia-Lite™ Blasting Media," Final Report, Coatings Technology Integration Office, Wright-Patterson AFB, OH, September 1996

3. Spigel, B., Buckingham, J., and McClung, C., "Evaluation of Type V, Polymedia-Lite™, and Envirostrip™ for Depainting 0.025-Inch 2024-T3 Aluminum Alloy," Draft Final Report, Coatings Technology Integration Office, Wright-Patterson AFB, OH, January 1999.

APPENDIX A

Letter from CAE to CTIO Specifying the Envirostrip™ Blast Process Parameters

CAE

CAE Electronics Ltd.
Advanced Aircraft Maintenance Systems
5838 Cypihot Street
Ville St-Laurent
Quebec, Canada H4S 1Y5

Tel (514) 333-6300
Fax (514) 734-5740

October 21, 1997

Mr. Chuck Cundiff
Southwest Research Institute
PO Box 7448
Warner Robins AFB, GA
31098 USA

by fax:
(912) 929-9354

Dear Chuck,

We completed our test verification yesterday at CAE's Test Center. As discussed in the attached notes, our approach was to establish blast parameters and x-y traverse speeds to effectively strip clad aluminum panels at a rate of 0.75 ft^2/min. We used a variety of mil-spec prepared and painted test panels (in accordance with T.O. 1-1-8) which were of very high quality (i.e. paint quality). Some of these panels date back to 1994.

Thus having stripped a number of these clad and bare aluminum panels, we are confident that the parameters recommended herein are effective for stripping mil-spec panels. I will bring samples of these panels along with me next week to review with you.

If you have any questions regarding the enclosed data, please contact me at (514) 333-6300 ext. 247.

Best regards.
CAE Electronics Ltd.

John Oestreich
Advanced Aircraft Maintenance Systems

cc: R. Lott Raytheon
C. Drake CAE
J. Contala CAE
P. Dicaire CAE

OCTAS 1991

Summary

The selection of process parameters for this CTIO study was based on previous studies performed by Southwest Research Institute (SWRI) for Type V PMB and Polymedia Lite. After discussions with SWRI personnel and Raytheon, we set our goal as follows: define blast parameters and x-y traverse speeds to strip at a rate of 0.75 ft^2/min on clad aluminum (0.032-inch 2024-T3) panels prepared to mil-spec requirements. Test parameters for bare aluminum panels were also then determined using the same blast parameters.

It is important to note that stripping of aluminum alloys thinner than 0.032-inch would require a different set of blast parameters. Specifically a lower pressure and higher media flow rates are recommended.

Clad Aluminum

To achieve a 0.75 ft^2/min strip rate on Alclad, we need to have, for example, the following X-Y automated stripping parameters:

Trace width	1.0 inch
x-axis:	108 inch/min (1.8 inch/sec)
y-axis:	60 inch/min (1.0 inch/sec)
Net strip rate:	0.75 ft^2/min

Note: These same automated parameters were used for testing Type V PMB (at a nozzle pressure of 30 psi). See Table 1.

Testing on various Alclad painted panels confirmed the blast parameters required to effectively strip paint using the above combination of travel speeds and trace width or path spacing. Thus, the recommended blast parameters to be used in this CTIO study for clad aluminum are:

Clad Aluminum Parameters:

Nozzle	1/2" venturi nozzle
Nozzle pressure	40 psi
Stand-off distance	3 inches
Media flow rate	12 lb/min
Blast angle	45°

Bare Aluminum

Although a target strip rate was not set for bare aluminum, we expected to achieve a faster strip rate on bare versus clad aluminum. Using the same blast parameters as stated above, the

following x-y traverse parameters were used:

Trace width	1.0 inch
x-axis:	120 inch/min (2.0 inch/sec)
y-axis:	60 inch/min (1.0 inch/sec)
Net strip rate:	0.83 ft^2/min

Testing on various bare aluminum painted panels confirmed that these parameters effectively strip paint mil-spec using the above combination of travel speeds and trace width. Thus, the recommended parameters for bare aluminum are:

Bare Aluminum Parameters:

Nozzle	1/2" venturi nozzle
Nozzle pressure	40 psi
Stand-off distance	3 inches
Media flow rate	12 lb/min
Blast angle	45°

Almen Arc Height Data

Almen arc height data were generated to verify the process intensity and residual stress inducement as measured with this method. The data is presented in Table 4. A set of eight Almen specimens (0.032-inch 2024-T3 bare aluminum) were mounted on a test block occupying a space 3-inch by 12-inch. The same automated parameters were used to completely strip these Almen specimens as if they were painted. Four blast cycles produced an average arc height of 2.8 mil, and at saturation (10 blast cycles), a 3.7 mil arc height was recorded.

Table I.

CTIO Southwest Research Institute (SWRI) Program cont'd
Previous Data (ref. 1995 DOD SWRI paper)

Type V: 30/40 — Bare Aluminum 0.032 inch 2024-T3

Parameters:	Nozzle pressure	30 psi
	Stand-off distance	21 inches
	Media flow rate	9 lb/min (assumed)
	Blast angle	60°
	1/2" Round Venturi Nozzle	
Data:	Trace width	1.125 inch
	x-axis:	144 inch/min (2.4 inch/sec)
	y-axis:	60 inch/min (1.0 inch/sec)
	Net strip rate:	1.125 ft^2/min

Type V: 30/40 — Clad Aluminum 0.032 inch 2024-T3

Parameters:	Nozzle pressure	30 psi
	Stand-off distance	21 inches
	Media flow rate	9 lb/min (assumed)
	Blast angle	60°
Data:	Trace width	1.0 inch
	x-axis:	108 inch/min (1.8 inch/sec)
	y-axis:	60 inch/min (1.0 inch/sec)
	Net strip rate:	0.75 ft^2/min

Almen Arc Height Data (avg. of 3 specimens):

1 cycle	5.3 mil
2 cycles	6.2 "
3 cycles	7.0 "
4 cycles	7.5 "
10 cycles	8.3 "

Surface Roughness R_a (on Alclad):

1 cycle	225 µinches
2 cycles	207 µinches
3 cycles	130 µinches
4 cycles	150 µinches

Table 2.

CTIO Southwest Research Institute (SWRI) Program
Previous Data (ref. 1996 DOD SWRI paper)

PML: 20/50 — Bare Aluminum 0.032 inch 2024-T3

Parameters:	Nozzle pressure	40 psi
	Stand-off distance	21 inches
	Media flow rate	500 lb/hr (8.33 lb/min ref. B.Spiegel)
	Blast angle	60°
	1/2" Round Venturi Nozzle	
Data:	Trace width	1.1 inch
	x-axis:	144 inch/min (2.4 inch/sec)
	y-axis:	30 inch/min (0.5 inch/sec)
	Net strip rate:	0.95 ft^2/min

PML: 20/50 — Clad Aluminum 0.032 inch 2024-T3

Parameters:	Nozzle pressure	40 psi
	Stand-off distance	21 inches
	Media flow rate	500 lb/hr (8.33 lb/min ref. B.Spiegel)
	Blast angle	60°
Data:	Trace width	1.0 inch
	x-axis:	115 inch/min (1.9 inch/sec)
	y-axis:	30 inch/min (0.5 inch/sec)
	Net strip rate:	0.75 ft^2/min

Almen Arc Height Data (avg. of 3 specimens):

1 cycle	2.4 mil
2 cycles	4.3 "
3 cycles	4.5 "
4 cycles	5.3 "
10 cycles	6.0 "

Surface Roughness R_a (on Alclad):

1 cycle	68 µinches
2 cycles	69 µinches
3 cycles	71 µinches
4 cycles	70 µinches

Table 3.

CTIO Southwest Research Institute (SWRI) Program cont'd
CAE Electronics Data - Oct. 21/97

Starch Media: Bare Aluminum 0.032 inch 2024-T3
12/100

Parameters:	Nozzle pressure	40 psi
	Stand-off distance	3 inches
	Media flow rate	12 lb/min
	Blast angle	45°
Data:	Trace width	1.0 inch
	x-axis:	120 inch/min (2.0 inch/sec)
	y-axis:	60 inch/min (1.0 inch/sec)
	Net strip rate:	0.83 ft^2/min

Starch Media: Clad Aluminum 0.032 inch 2024-T3
12/100

Parameters:	Nozzle pressure	40 psi
	Stand-off distance	3 inches
	Media flow rate	12 lb/min
	Blast angle	45°
Data:	Trace width	1.0 inch
	x-axis:	108 inch/min (1.8 inch/sec)
	y-axis:	60 inch/min (1.0 inch/sec)
	Net strip rate:	0.75 ft^2/min (target)

Almen Arc Height Data (avg. of 8 specimens):

1 cycle	1.7 mil
2 cycles	2.1 mil
3 cycles	2.4 mil
4 cycles	2.8 mil
10 cycles	3.7 mil

Surface Roughness R_a (on Alclad):

1 cycle	TBD µinches
2 cycles	TBD µinches
3 cycles	TBD µinches
4 cycles	TBD µinches

Table 4.

Blast Cycle	1	2	3	4	5	6	7	8	Average
1X	1.5	1.8	1.8	2.4	1.7	1.6	1.5	1.5	1.7
2X	2.0	2.4	2.2	2.5	2.0	1.8	2.0	2.0	2.1
3X	2.1	2.8	2.4	2.8	2.3	2.2	2.5	2.3	2.4
4X	2.3	3.1	2.5	2.9	2.8	2.8	2.8	3.0	2.8
10X	3.0	4.3	3.2	3.1	4.4	4.1	4.1	3.7	3.7

APPENDIX B

Discussion of the Fatigue Performance of Blasted 0.032-inch Thick Aluminum Alloys

APPENDIX B
DISCUSSION OF THE FATIGUE PERFORMANCE OF BLASTED 0.032-INCH-THICK ALUMINUM ALLOYS

B.1 Review of Fatigue Performance of Blasted 0.032-in and 0.025-in Aluminum Alloys

The fatigue performance of 0.032-inch aluminum alloys subjected to Envirostrip™ blasting was described in Section 4.0. For convenience, the key results are summarized in Table B-1. In this and the following tables, COV is the coefficient of variation, the ratio of the standard deviation to the mean value. The bare and clad 7075-T6 materials exhibited only small fatigue debits (blasted/control life ratios of 0.82 and 0.88). The bare 7075-T6 debit was within the test-to-test scatter and hence was not statistically significant. The clad 7075-T6 debit, although small, was larger than test-to-test scatter and hence was statistically significant. The somewhat larger debits for bare and clad 2024-T3, blasted/control life ratios of 0.73 and 0.66 respectively, were both statistically significant.

Results from previous fatigue testing of 0.032-inch bare and clad 7075-T6 and 2024-T3 aluminum alloys subjected to Type V [B1] and Polymedia-Lite™ [B2] blasting are summarized in Tables B-2 and B-3 for completeness. Blasting caused no statistically significant decreases in fatigue performance except for Type V-blasted clad 2024-T3 and Polymedia-Lite™-blasted bare 7075-T6.

A substantial fatigue debit associated with Envirostrip™ blasting of clad 2024-T3 was also observed previously [B3] in studies on 0.025-in sheets. These results are summarized in Table B-4, along with the results from fatigue testing of the same material subjected to Type V and Polymedia-Lite™ blasting. The Type V blasting caused a negligible fatigue debit (blasted/control life ratio of 0.96) that was not statistically significant. The Polymedia-Lite™ blasting caused a slightly larger debit (life ratio of 0.86) that was statistically significant, and the Envirostrip™ blasting caused a much more substantial fatigue debit (life ratio of 0.59) that was also statistically significant.

The substantial fatigue debits observed for Envirostrip™ blasting of 2024-T3 prompted further investigations to explore why debits were observed for some blasting processes and some materials, but not for other blasting processes or materials. These brief exploratory investigations have led to the formulation of simple hypotheses for the observed behavior. This appendix is written to summarize those investigations and the resulting hypotheses.

The appendix begins with a brief discussion of shot-peening. Shot-peening shares several important similarities with dry media blasting (DMB), and the fatigue credit or debit associated with shot-peening has been studied in some detail. This credit or debit appears to be primarily related to the competing effects of the residual stresses and the surface damage caused by the peening operation. By analogy, then, the same phenomena may be influencing the fatigue behavior of dry media blasted surfaces. The available information related to residual stresses and surface roughness caused by DMB is reviewed and analyzed in an attempt to explain the observed fatigue results.

Some portions of this appendix were originally published in an appendix to a previous SwRI report on DMB of 0.025-inch clad 2024-T3 [B3]. Those discussions are incorporated here for completeness and convenience, due to the limited distribution of that previous report.

B.2 Effects of Shot-peening on Fatigue Performance

Dry media blasting is analogous in many ways to shot-peening. Shot-peening [B4] is a cold working process in which the surface of a part is bombarded with small spherical media called shot. Each piece of shot striking the material acts as a tiny peening hammer, imparting to the surface a small indentation or dimple. In order for the dimple to be created, the surface layer of the material must be yielded in tension. Below the surface, the fibers try to restore the surface to its original shape, thereby below the dimple producing, a hemisphere of cold-worked material highly stressed in compression. Shot-peening is used primarily to impart this layer of compressive residual stresses in order to increase resistance to fatigue, corrosion, wear, and other damage mechanisms. Added benefits can result from an increase in surface hardness due to the cold working (strain hardening) effect of shot-peening. However, peening also causes damage to the surface associated with the indentation process that can have a deleterious effect on the fatigue life. Proper design of a particular shot-peening process for a particular application requires an optimization of shot-peening parameters (shot size, hardness, velocity, etc.) to maximize the distribution of beneficial compressive residual stresses while minimizing detrimental surface damage.

While the intensity of DMB is less than that of shot-peening, the effects are qualitatively similar. The media will impart a layer of *compressive residual stresses* to the blasted surface of the part, while also causing an increase in the *surface roughness* of the part. Both of these effects have been documented in this study and in previous studies of DMB. The compressive residual stresses will *enhance* the fatigue resistance of the part, while the increased surface roughness will *diminish* the fatigue resistance. These competing effects may or may not have a significant net effect on the fatigue life.

Residual Stresses

Extensive scientific studies of shot-peening (e.g., [B5]) have identified the general form of the residual stress distribution resulting from peening. An example is given in Figure B-1, showing calculated and experimentally measured residual stresses in a thick plate of Udimet 720, a nickel-base superalloy [B6]. The residual stresses have a maximum compressive value that is approximately constant over some distance below the surface, with a slight decrease at the surface itself, and an approximately linear decay in stress magnitude towards the interior of the part.

As noted earlier, compressive residual stresses will have a *beneficial* effect on fatigue performance. Although the amplitude of the fatigue stress cycles will not change, the mean stress and the maximum stress in the fatigue cycle will decrease by an amount equal to the compressive residual stress. The surface and near surface stresses (where the compressive residuals are generally highest) are of greatest significance. Since the maximum compressive residual stress can be on the order of half the material yield strength or greater, this can be a substantial change in maximum stress (or mean stress). This change can lead (in theory) to a substantial change in fatigue life. Although the compressive residual stresses may not have a significant impact on the nucleation of microcracks, they will likely retard the growth of these microcracks and hence lengthen the fatigue life [B7-B8].

However, the residual stresses induced by shot-peening or DMB will not be fully effective during fatigue cycling, because they will gradually relax to some degree as a result of the fatigue cycling. This relaxation behavior is well documented for shot-peened surfaces [B9-B12]. The rate and extent of the residual stress relaxation is affected in a complex manner by the magnitude and distribution of the original stress field, the magnitude and duration of the fatigue cycling, and the properties of the material. No method is currently available to predict relaxation behavior *a priori*. Iida [B10] observed in his shot-peening studies that a shallow distribution of residual stress relaxed more rapidly and more completely

than a deeper distribution of residual stress in the same material, even when the maximum stress in the two distributions was similar.

Oshida and Daly [B13] cite experimental evidence that the residual stress relaxation depends on the magnitude of the applied fatigue stress relative to the material yield strength. Their own tests on shot-peened Bl 7050-T7651 showed greater relaxation as maximum bending stresses increased from 40% to 70% of yield. Hammond and Meguid [B14] found little or no relaxation during fatigue of peened Al 7075-T351 when maximum stresses were 50% of yield.

Surface Roughness

The other significant influence of shot-peening on fatigue behavior is a negative one. Shot-peening, by its very nature, causes damage to the part surface that manifests itself as an increase in surface roughness. The roughened, irregular surface provides local stress concentrations and sometimes local microfissures that can serve as preferential initiation sites for fatigue cracks. This negative effect on fatigue performance is sometimes overlooked because the positive effect of the compressive residual stresses is typically a stronger effect (at least for properly specified peening).

Systematic research studies have clearly demonstrated the competing effects of residual stresses and surface roughness on fatigue performance. For example, Wagner and Mueller [B15] have investigated the effect of shot-peening on the fatigue behavior of bare 2024-T3. They compared the high cycle fatigue strength of material that was (1) electropolished (EP) and unpeened; (2) shot-peened (SP); (3) shot-peened and then electropolished (SP + EP) to remove the surface roughness but leave the residual stresses largely intact; (4) shot-peened and then stress relieved (SP + SR) via heat treatment to remove the residual stresses but leave the surface roughness intact; and (5) shot-peened and then stress relieved and electropolished (SP + SR + EP), removing the two principal effects of the peening operation. The 10^7 fatigue strength of the baseline EP condition in 2024-T6 was about 200 MPa. The SP fatigue strength increased to about 225 MPa, while the SP + EP fatigue strength increased more dramatically to about 250 MPa. On the other hand, the SP + SR fatigue strength decreased sharply to 150 MPa. Interestingly, the SP + SR + EP remained elevated at about 225 MPa. This effect was attributed to the measured increases in the dislocation density caused by peening that were unaffected by either SR or EP.

Softer materials generally exhibit more surface damage as a result of peening than hard materials. This is a general problem for all aluminum alloys [B7], in comparison to high strength steels, titanium alloys, and nickel-based alloys that are more routinely peened.

B.3 An Evaluation of the Effects of DMB on Residual Stresses and Surface Roughness

The effects of shot-peening on fatigue life have been explained in terms of the residual stresses and surface roughness imparted by the peening process. Can these same phenomena explain the observed effects of dry media blasting on fatigue life? Limited data are available on the residual stresses and surface roughness caused by DMB of thin aluminum sheets. In the sections that follow, these data are analyzed qualitatively and (where possible) quantitatively and compared with the fatigue life results.

Residual Stresses

Residual stress information for blasted aluminum sheets is available indirectly in the form of Almen strip test results. Almen results are available for 0.032-inch bare 2024-T3 sheet subjected to Type V, Polymedia-Lite™, and Envirostrip™ blasting (Section 6.1) and for 0.025-inch bare 2024-T3 subjected to Envirostrip™ blasting [B3]. Almen strip deflection measurements were performed after different numbers of blast cycles, ranging from 1 cycle up to 10 cycles. These measurements are summarized in Table B-5,

and the 0.032-inch measurements are also shown in Figure B-2. Almen strip deflections are not available for clad 2024-T3, or for bare or clad 7075-T6.

Deflections of the Almen strips are due to the residual stresses imparted by the blasting process. Although it is not possible to determine the complex distribution of residual stresses near the surface from a single-valued measurement of strip deflection, it is possible to conduct an approximate analysis of residual stresses in the blasted aluminum sheets by idealizing the residual stress profile. The general form of the residual stress profile is assumed to be similar to the well-known profiles established in extensive studies of shot-peened surfaces [B5-B6].

The idealized residual stress profile is shown in Figure B-3. Here the compressive residual stresses take a maximum constant value with magnitude σ_1 over a distance d_1 below the surface. For simplicity, the slight downturn at the surface itself is neglected. These compressive residual stresses then decrease linearly over a distance d_2. Since the stresses in the strip must satisfy equilibrium of forces, a small tensile stress σ_2 (assumed constant in this idealized model) must be generated in the remaining thickness of the strip. The magnitude of σ_2 is fixed by the values of σ_1, d_1, and d_2, and the equation of force equilibrium.

The stresses in Figure B-3 characterize the thin strip in its unbent configuration. Since the asymmetric stress distribution produces a nonzero bending moment, an unrestrained strip will bend into a curved shape. This type of behavior is often seen during blasting of the test panels. During the blasting process, the panels are externally constrained so that they cannot bend. When the clamps are released, the compressive residual stresses present in the panel cause the panel to bow. The panel or Almen strip will curve so that the linear stress distribution introduced by the bending gives an equal and opposite moment to the unbent residual stresses, and the strip (or panel) will be in equilibrium. A thinner panel or strip will bow more severely, not because the residual stresses are greater (they are likely the same), but because the thinner panel offers less inherent resistance to bending and hence must deflect more to equilibrate the bending moments. Since the bending stress distribution is directly related to the strip curvature by simple mechanics of materials theory, it is possible to calculate directly the resulting curvature in an unrestrained bent strip from the stress distribution in the restrained unbent strip.

The same equations can be solved in reverse to estimate the residual stress distribution from a measured strip curvature. Unfortunately, since the idealized residual stress distribution has three unknowns (σ_1, d_1, and d_2), a single curvature value can imply an infinite number of combinations of σ_1, d_1, and d_2. Further assumptions are therefore needed in order to interpret the curvature as a specific residual stress distribution.

In this analysis, the maximum value of the compressive stress, d_1, was assumed to be −12 ksi. This particular value corresponds to a single experimental measurement of maximum near-surface residual stress in bare 0.032-inch 2024-T3 following standard Type V blasting [B1]. This value is about 25 percent of the 52-ksi yield strength of this particular material. The implications of choosing a larger value of σ_1 are explored below.

An initial evaluation of the simple stress model was performed by calculating residual stress distributions from strip deflection measurements on two different thicknesses of bare 2024-T3 (0.032 and 0.025 inch), each subjected to four identical Envirostrip™ blast cycles. The deflection at the middle of a 3.0-inch span was taken as 0.0040 inch for the 0.032 inch strip and 0.0062 inch for the 0.025 inch strip (scatter in the experimental measurements was minimized by averaging the deflections corresponding to 3, 4, and 5 blast cycles). The resulting calculated values of d_1 and d_2 for an assumed $\sigma_1 = -12$ ksi are shown in Figure B-4. The lines in this figure show the locus of possible combinations of d_1 and d_2 that satisfy the equations of equilibrium for the specified bending displacement. If $d_2 = 0$ (all compressive residual stresses take a constant value), then d_1 is about 0.0005 inch. If $d_1 = 0$ (the entire compressive residual profile is linear), then this linear profile has a depth of about 0.001 inch. It is not possible to determine the

proportion of d_1 and d_2 from the limited information available, but the analysis does provide a reasonable set of bounds on the approximate depth of the total compressive residual stress field.

The key observation in this case is that the two residual stress distributions have approximately the same dimensions, which should be the case if the two strips were subjected to identical blasting processes (as they were). Since the total depth of the compressive residual stress fields is small in comparison to the total strip thickness (less than 4% of the thickness), the strip can still be regarded as "thick" from a mechanic's viewpoint, even though the physical dimensions are small. This agreement provides some measure of confidence in the simple mechanics model. When a larger value of the maximum compressive residual stress, $\sigma_1 = -25$ ksi, was assumed, the two residual stress distributions were still nearly identical, although the dimensions d_1 and d_2 both decreased by approximately a factor of two. Therefore, the observed agreement does not depend on the assumed magnitude of the stress field.

The simple model was then applied to evaluate the residual stress profiles for 0.032-inch bare 2024-T3 sheets subjected to three different blasting methods: Type V, Polymedia-Lite™, and Envirostrip™. Almen strip deflection measurements following four blast cycles were 0.0075 inch for Type V, 0.0050 inch for Polymedia-Lite™, and 0.0040 inch for Envirostrip™, again based on an average of measurements from 3, 4, and 5 blast cycles. The calculated values of d_1 and d_2 for these conditions are given in Figure B-5. The Type V residual stress profile is the deepest, consistent with the largest deflection value, and the Envirostrip™ profile is the shallowest. Again, it is not possible to draw more definitive quantitative conclusions about the dimensions of the residual stress profile, but to a first order it appears that the depth of the Type V residual stress profile is about twice as deep as the Envirostrip™ profile.

All of these analyses are for bare (unclad) materials, since no Almen strip deflection measurements were available for clad materials. However, the clad 2024-T3 is the material that exhibited the significant debit in fatigue life following blasting. Therefore, it is useful to explore the implications of the simple mechanics analysis for the blasted clad sheets.

The key difference between the clad layer and the core material for this problem is the strength. Whereas the yield strength of the core material is nominally 50 ksi, the yield strength of the cladding (typically Al 1230, a very high-purity Al) in the fully annealed condition is nominally about 4 ksi. Even with substantial work hardening, the clad yield strength is probably still in the range of 15-20 ksi.

This decreased yield strength has two significant implications for the development of compressive residual stresses. On one hand, a softer material will deform much more easily during the blasting process, tending to produce more substantial residual stresses (in the other extreme, a very hard material might deform little at all during blasting, leading to almost no residual stresses following blasting). On the other hand, the magnitude of the residual stresses will be limited to some degree by the strength of the material. Residual stresses generally will not exceed by any substantial margin the yield strength of the material in which they are found (unless other factors such as structural constraint are significant). Therefore, it is unlikely that the maximum value of the post-blast residual stresses in the clad layer will be greater than 15-20 ksi. To a first approximation, then, the assumed values of $\sigma_1 = -12$ to -25 ksi in the previous analysis of the bare sheet are probably reasonable for the clad sheet as well.

The depth of the clad layer is nominally 2% - 5% of the total sheet thickness [B16]. In a 0.025-inch sheet, this depth corresponds to about 0.0005 to 0.00125 inch, which is on the same order as the total depth of the residual stress profiles calculated above. Therefore, most or all the clad layer probably exhibits substantial compressive residual stresses, but the core material immediately below the clad layer may be relatively free of residual stresses. The possible exception is the deeper Type V profile, which could extend into the core material. Actually, the bimaterial system with such great contrast of yielding properties may well exhibit a more complex residual stress field, but the analysis of this more difficult problem is well beyond the scope of the current effort. The simple model employed here should still be sufficient as a general scoping of the problem.

It was previously noted that residual stresses in shot-peened surfaces will relax during fatigue cycling, and that this relaxation occurs more quickly and more completely for shallower residual stress distributions and under more severe fatigue cycling. By analogy, then, the residual stresses in the shallow Envirostrip™ distribution would be expected to relax more quickly and to a greater extent than the residual stresses in the deeper Type V distribution (see Figure B-5). Furthermore, it was observed that the deflection of the Almen strips had not reached saturation levels in bare 2024-T3 even after five or six blast cycles. This indicates that the residual stresses had not yet stabilized to maximum values and hence might be even more susceptible to relaxation during subsequent fatigue cycling. This behavior is in contrast to Type V and Polymedia-Lite™, where Almen deflections were approaching saturation after only four cycles [B1, B2].

In the present study, the maximum fatigue stress was 44.5 ksi, compared to a yield strength of about 50 ksi for the clad material, so maximum stresses were about 90% of yield. Under these conditions, significant residual stress relaxation is highly likely. It should be noted, however, that residual stress relaxation would be expected to be less severe if fatigue cycling were less severe. This could mean that the observed fatigue debit associated with some DMB processes might be less severe in a longer life regime. In other words, if the fatigue tests in this program were conducted at lower stresses and therefore longer average fatigue lives (e.g., 10^6 or 10^7 cycles rather than 10^5 cycles), the observed fatigue debits might have been less severe. Such a postulate is consistent with the observation of Sharp et al. [B7] that peening of aluminum alloys is most effective as protection against fatigue under low service stresses.

Before discussing the surface roughness issues, it is useful to offer two additional observations from the residual stress study. First of all, the compressive residual stresses in these thin blasted panels are found only in the very near-surface layer, perhaps down to a depth on the order of 0.0005 to 0.002 inch. Any attempts to measure these stresses experimentally must hence focus on very near-surface regions of the sheet. Second, the total depth of the residual stress profile is still very small compared to the sheet thickness, even for these particularly thin product forms. This suggests that the thinness of the 0.032-inch and 0.025-inch sheets from a mechanics perspective should not be a significant factor in their performance following blasting. It is clear that thin, unrestrained sheets will exhibit substantial bending deflection that, in turn, will affect the stresses in the sheets. However, if the aircraft structure (or the fatigue test machine) restrains the sheet so that bending does not occur, then the near-surface stresses will be approximately the same in thin or thick sheets.

The self-equilibrating residual tensile stress in the remaining thickness of the sheet (σ_2 in Figure B-3) is probably less than 1 ksi. Note that this residual tensile stress would be large if the compressive residual stress profile was very deep in comparison to sheet thickness, and could induce fatigue failure on the unblasted side of the sheets. As noted below, failure on the unblasted side was actually observed for some sheets where higher levels of compressive residual stress were likely present. This phenomenon inherently limits the maximum benefit that can be gained from compressive residual stresses due to blasting. The average fatigue life of a thin sheet blasted on one side will inevitably be the same as, or lower than, the average fatigue life of the equivalent unblasted sheet, due to crack nucleation on the unblasted side.

Surface Roughness

Measurements of surface roughness on 0.032-inch sheets blasted with Envirostrip™ (see Section 6.2) are summarized for convenience in Table B-6. Surface roughness of blasted bare 7075-T6 and 2024-T3 was only slightly higher than the roughness of unblasted bare sheets. Surface roughness of blasted clad 7075-T6 and 2024-T3 was substantially higher than the roughness of unblasted clad sheets.

Comparisons of the surface roughness of bare and clad 2024-T3 before and after blasting with the three different media [B3] are provided in Table B-7 (similar data are not available for 7075-T6). Note that slightly different measurement techniques were used to obtain the data in Table B-6, so these two tables cannot be directly compared. Average surface roughness for bare 2024-T3 after 4 blast cycles ranges from about 11 μin for Envirostrip™ to about 22 or 23 μin for Type V and Polymedia-Lite™. These are all relatively mild roughness values, compared to the unblasted conditions. For clad 2024-T3, the average surface roughness after four blast cycles ranges from 70 μin for Polymedia-Lite™ to 76 μin for Envirostrip™, and nearly 150 μin for Type V. Note that although the average roughness of clad 2024-T3 is only slightly higher for Envirostrip™ in comparison to Polymedia-Lite™, the scatter in the roughness is much higher for Envirostrip™, and so the "worst" roughness (e.g., mean + 3 sigma) would be noticeably higher for Envirostrip™ than for Polymedia-Lite™. Fatigue crack nucleation would likely occur at the most severe local conditions on the specimen surface.

Further evidence of the competing effects of the beneficial compressive residual stresses and detrimental surface roughness was evident from the failure locations for the 0.025-inch clad 2024-T3 specimens [B3], which are summarized in Table B-8. The majority of the Type V specimen failures initiated on the concave, unblasted surface. The residual compressive stresses due to the blasting were apparently sufficient to overcome the higher level of surface roughness, and the specimens failed on the surface with residual tensile stresses. Each of the Polymedia-Lite™ and Envirostrip™ specimens failed on the convex, blasted surface. Thus, despite the residual compressive stresses on the blasted surface and the residual tensile stresses on the opposite surface, the failure initiated on the blasted surface. This was most likely due to the surface roughness.

B.4 Hypothesis on the Fatigue Life Behavior

The fatigue life behavior of shot-peened surfaces can be understood in terms of the competing effects of (beneficial) compressive surface residual stresses and (harmful) surface roughness. It is reasonable to ask if the same explanation applies to the analogous dry media blasting process. The available information about fatigue life, residual stresses, and surface roughness in blasted aluminum sheets was reviewed above. Is this information consistent with the hypothesis? Unfortunately, the available information about residual stresses and surface roughness is incomplete; in particular, residual stress information is available only for bare 2024-T3. Nevertheless, it is useful to explore the extent to which the available residual stress and roughness information is consistent or inconsistent with the observed fatigue life behavior.

The Envirostrip™ blasting process (and particular blasting parameters) employed in these studies generally led to larger fatigue debits than either the Polymedia-Lite™ or Type V processes/parameters. See again Tables B-1 through B-3, where Envirostrip™ blasting gave the largest fatigue debits for 0.032-inch bare and clad 2024-T3 and clad 7075-T6, and all three of these debits were statistically significant. The only exception to this trend was 0.032-inch bare 7075-T6, where only Polymedia-Lite™ gave a statistically significant decrease in fatigue life, but this result was apparently influenced by considerable scatter in the control tests. Envirostrip™ also gave the largest fatigue debit for 0.025-inch clad 2024-T3 (see again Table B-4).

How do these fatigue results compare with residual stress and surface roughness information? Based on available Almen strip deflections for bare 2024-T3, Envirostrip™ had the most shallow (and therefore least beneficial) levels of compressive residual stress in comparison to Polymedia-Lite™ and Type V. This shallow, unsaturated residual stress distribution may also be more susceptible to relaxation during fatigue cycling. On the other hand, Envirostrip™ exhibited higher (more damaging) levels of surface roughness than Polymedia-Lite™. Type V surface roughness was higher still, but this increased roughness was apparently compensated by the substantially deeper levels of compressive residual stress with Type V.

In fact, for clad 2024-T3, the compressive residual stresses were significant enough that failure in 7 of 10 tests occurred on the unblasted side of the sheet.

A comparison among the different materials is more difficult due to the limited residual stress information available (bare 2024-T3 only). However, anecdotal observations of sheet bowing indicate that residual stresses in bare and clad 7075-T6 sheet are considerably smaller than in 2024-T3. These observations are consistent with the considerably higher yield stress in 7075-T6, such that more of the energy from the media blasting can be absorbed elastically. Statistically significant decreases in fatigue life were only observed twice in 7075-T6. One incidence was clad 7075-T6 blasted with Envirostrip™, where average surface roughness was measured as 80 μin (compared to a control average of 5 μin). The other incidence was bare 7075-T6, where (as noted previously) the fatigue debit may have been influenced by particularly large scatter in the control test results.

The greatest fatigue debits were observed in 2024-T3, which is considerably softer. The softest condition, clad 2024-T3, exhibited statistically significant fatigue debits for Envirostrip™ (both 0.032-inch and 0.025-inch thicknesses) and Type V, but not for Polymedia-Lite™. The bare 2024-T3 condition gave statistically significant debits for Envirostrip™ in both 0.032-inch and 0.025-inch thicknesses, but not for Type V or Polymedia-Lite™. It is difficult to interpret these behaviors without detailed residual stress information in bare vs. clad materials. As noted earlier, the residual stress profile is likely more complex in the clad bimaterial system. Certainly the surface roughness was greatest among all four materials for the clad 2024-T3.

No definitive conclusions can be drawn about the fatigue performance of dry media blasted aluminum alloys from this collection of models, observations, and analogies. However, it appears that the available information supports the hypothesis that fatigue performance is influenced by the beneficial effects of compressive residual stresses and the deleterious effects of surface roughness. Different blasting media and different aluminum sheet materials influence the residual stresses and surface roughness, leading to different fatigue performances.

Of course, this line of reasoning is missing many links of validating information. Further work would be required to confirm or deny this hypothesis or, if desired, to develop a more fundamental understanding of the problem. No Almen strip deflection/residual stress tests were conducted with either clad 2024-T3 material or bare or clad 7075-T6, and these would be useful to characterize the residual stresses in the clad layer (albeit harder to interpret analytically). It would be particularly interesting to evaluate the residual stresses before and after fatigue cycling, perhaps with Almen strip tests, to make some assessment of the residual stress relaxation due to cycling. Other, more direct, experimental measurements of residual stresses would be valuable, although it must be emphasized that any experimental technique must interrogate only a very shallow surface layer on the order of 0.001-inch-thick (or less) in order to capture the residual stresses of significance. A more systematic treatment of the problem might follow the general example of Wagner and Mueller [B15] by comparing the residual stresses and the fatigue performance of clad material in the as-blasted condition with blasted material that has been stress relieved (to remove residual stresses) or electropolished (to remove surface roughness). A related question is the potential impact of the sanding, priming, and repainting operation on the surface roughness of blasted material, and hence on the fatigue performance. Finally, just as shot-peening parameters can be adjusted to optimize the depth and magnitude of the beneficial residual stresses while minimizing surface damage, it may be possible to optimize the blasting parameters for clad materials in such a way as to improve their post-blast fatigue performance.

This hypothesis indicates that the effects of blasting on fatigue performance are inherently *surface* effects, and they lead to changes in the fatigue performance because fatigue life (as measured in the DMB test programs) is predominantly driven by surface behavior. It should not be surprising, then, that blasting has relatively little effect on tensile strength or on fatigue crack growth properties, since these

behaviors (as measured in the DMB test protocols) are predominantly controlled by the *bulk* response of the material. The bulk condition or response of the material is not substantially impacted by blasting processes.

Table B-1. Fatigue Behavior of 0.032-inch Panels Blasted with Envirostrip™

	0.032-inch 7075-T6		0.032-inch 2024-T3	
	Bare	Clad	Bare	Clad
Control				
Average Life	48937	106922	83204	100157
Standard Deviation	17662	13762	6630	10494
COV	0.36	0.13	0.08	0.10
Envirostrip™ Blasted				
Average Life	40300	93852	60430	66487
Standard Deviation	17484	14361	19295	11281
COV	0.43	0.15	0.32	0.17
Blasted/Control Life Ratio	0.82	0.88	0.73	0.66
Statistical Comparison	NS	S↓	S↓	S↓

Table B-2. Fatigue Behavior of 0.032-inch Panels Blasted with Type V

	0.032-inch 7075-T6		0.032-inch 2024-T3	
	Bare	Clad	Bare	Clad
Control				
Average Life	111011	118643	89148	92453
Standard Deviation	58345	18676	15895	7883
COV	0.53	0.16	0.18	0.09
Type V Blasted				
Average Life	79378	110210	95717	82103
Standard Deviation	26985	30828	11550	11274
COV	0.34	0.28	0.12	0.14
Blasted/Control Life Ratio	0.72	0.93	1.07	0.89
Statistical Comparison	NS	NS	NS	S↓

Table B-3. Fatigue Behavior of 0.032-inch Panels Blasted with Polymedia-Lite™

	0.032-inch 7075-T6		0.032-inch 2024-T3	
	Bare	Clad	Bare	Clad
Control				
Average Life	128595	89527	109163	83355
Standard Deviation	51004	11627	19082	14242
COV	0.40	0.13	0.17	0.17
Polymedia-Lite™ Blasted				
Average Life	59695	81947	96771	81027
Standard Deviation	18673	14651	21859	7452
COV	0.31	0.18	0.23	0.09
Blasted/Control Life Ratio	0.46	1.09	0.89	0.97
Statistical Comparison	S↓	NS	NS	NS

Table B-4. Fatigue Behavior of 0.025-inch Clad 2024-T3 Blasted with Different Media

	0.025-inch Clad 2024-T3
Control	
Average Life	90275
Standard Deviation	8393
COV	0.09
Type V Blasted	
Average Life	87459
Standard Deviation	14884
COV	0.17
Blasted/Control Life Ratio	0.96
Statistical Comparison	NS
Polymedia-Lite™ Blasted	
Average Life	77323
Standard Deviation	7991
COV	0.10
Blasted /Control Life Ratio	0.86
Statistical Comparison	S↓
Envirostrip™ Blasted	
Average Life	53003
Standard Deviation	5586
COV	0.11
Blasted/Control Life Ratio	0.59
Statistical Comparison	S↓

Table B-5. Almen Strip Deflections (in inches) for Blasted Bare 2024-T3

Blast Cycle	0.032-inch Type V	0.032-inch Polymedia-Lite™	0.032-inch Envirostrip™	0.025-inch Envirostrip™
1	0.0053	0.0024	0.0017	0.0037
2	0.0062	0.0044	0.0027	0.0044
3	0.0070	0.0046	0.0035	0.0058
4	0.0075	0.0053	0.0045	0.0063
5	0.0079	0.0052	0.0039	0.0066
6	0.0076	0.0056	0.0048	0.0080
7	0.0077	0.0051	0.0060	0.0070
8	0.0076	0.0058	0.0058	0.0088
9	0.0085	0.0055	0.0052	0.0084
10	0.0083	0.0062	0.0063	0.0089

Table B-6. Surface Roughness (in μin) of 0.032-inch Sheets Blasted with Envirostrip™

	Unblasted		Blasted	
	Average	Std Dev	Average	Std Dev
7075-T6 Bare	17.4	0.47	21.7	1.89
7075-T6 Clad	4.9	0.21	80.2	2.49
2024-T3 Bare	12.1	0.36	15.4	2.60
2024-T3 Clad	4.3	0.12	90.2	3.68

Table B-7. Surface Roughness (in μin) of 2024-T3 Sheets Blasted with Different Media

	Unblasted		Blasted	
	Average	Std Dev	Average	Std Dev
Bare 2024-T3				
0.032-inch, Type V	8.1	—	22.1	—
0.032-inch, Polymedia-Lite™	—	—	22.8	1.9
0.025-inch, Envirostrip™	—	—	11.3	2.0
Clad 2024-T3				
0.032-inch, Type V	5.1	—	149.3	—
0.032-inch, Polymedia-Lite™	—	—	70.0	2.7
0.025-inch, Envirostrip™	—	—	76.0	8.4

Table B-8. Summary of Fatigue Test Failure Locations for 0.025-inch, Clad 2024-T3

Media	Convex (Blasted)			Concave			Comments
	Surface	Corner	Edge	Surface	Corner	Edge	
Type V	3			7	1		1
Polymedia-Lite™	10						
Envirostrip™	10						
Controls	8		1				2

Notes: 1. One concave specimen failed at both surface and corner.
2. Five Control specimens failed very close to corners.

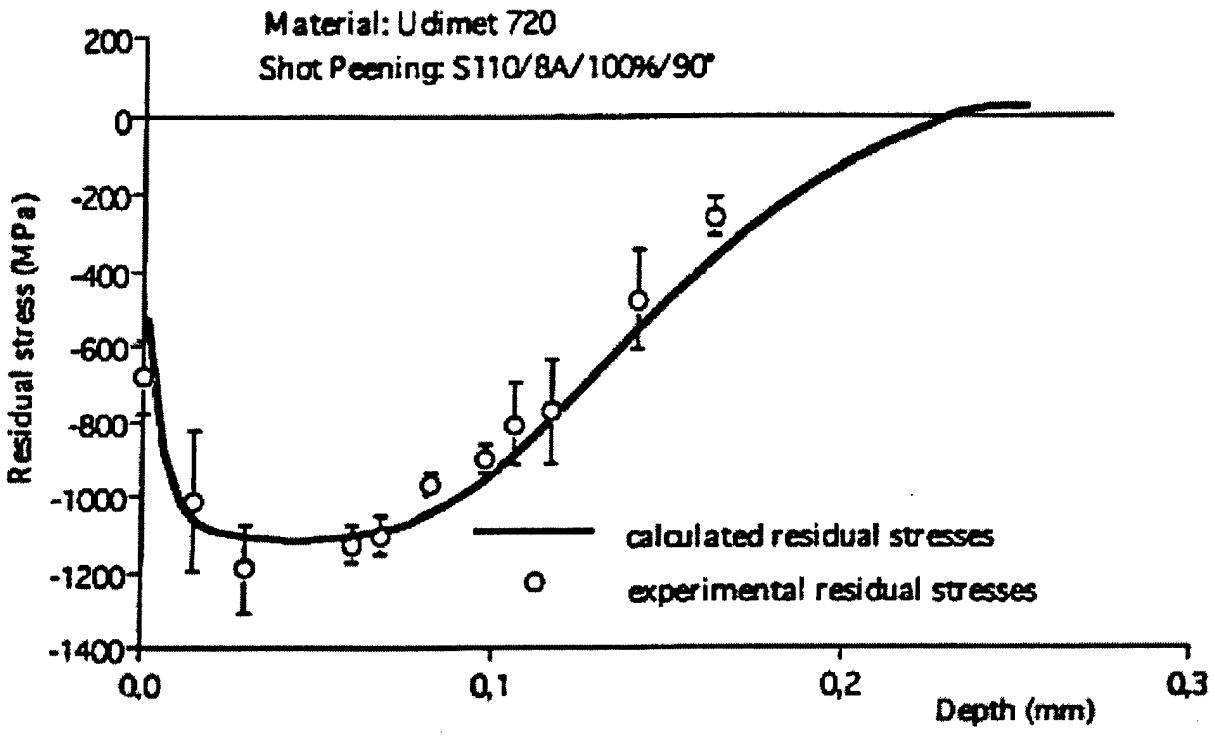

Figure B-1. Calculated and Measured Residual Stresses for Shot-Peened Udimet 720 [B6]

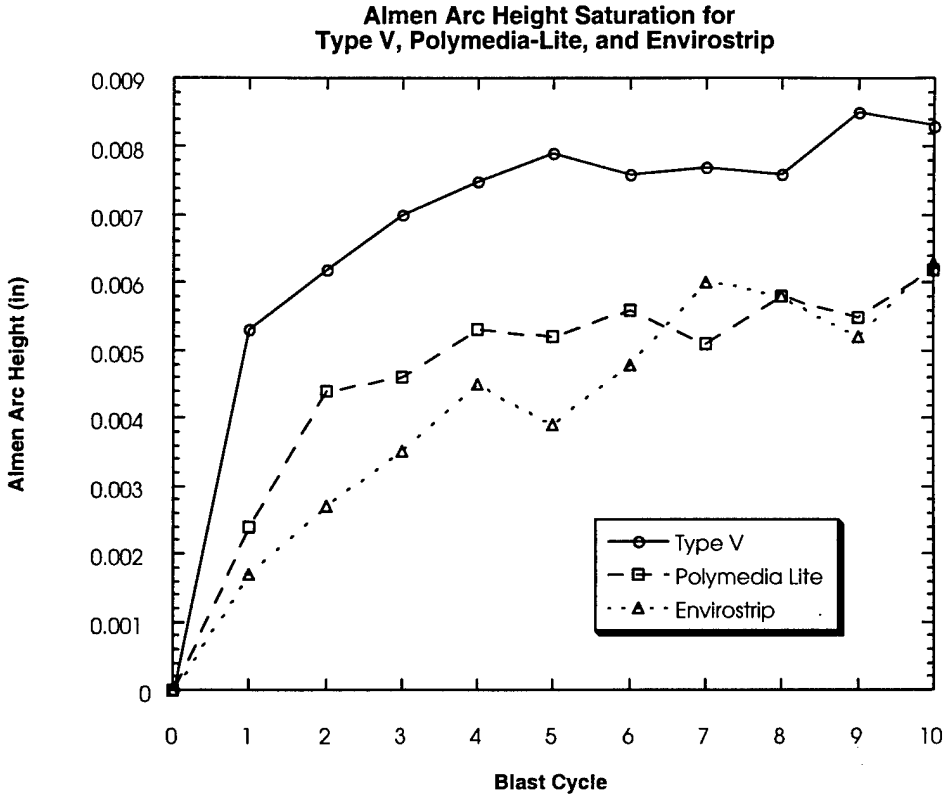

Figure B-2. Almen strip deflections for 0.032-inch bare 2024-T3 after different numbers of blast cycles for different blasting media

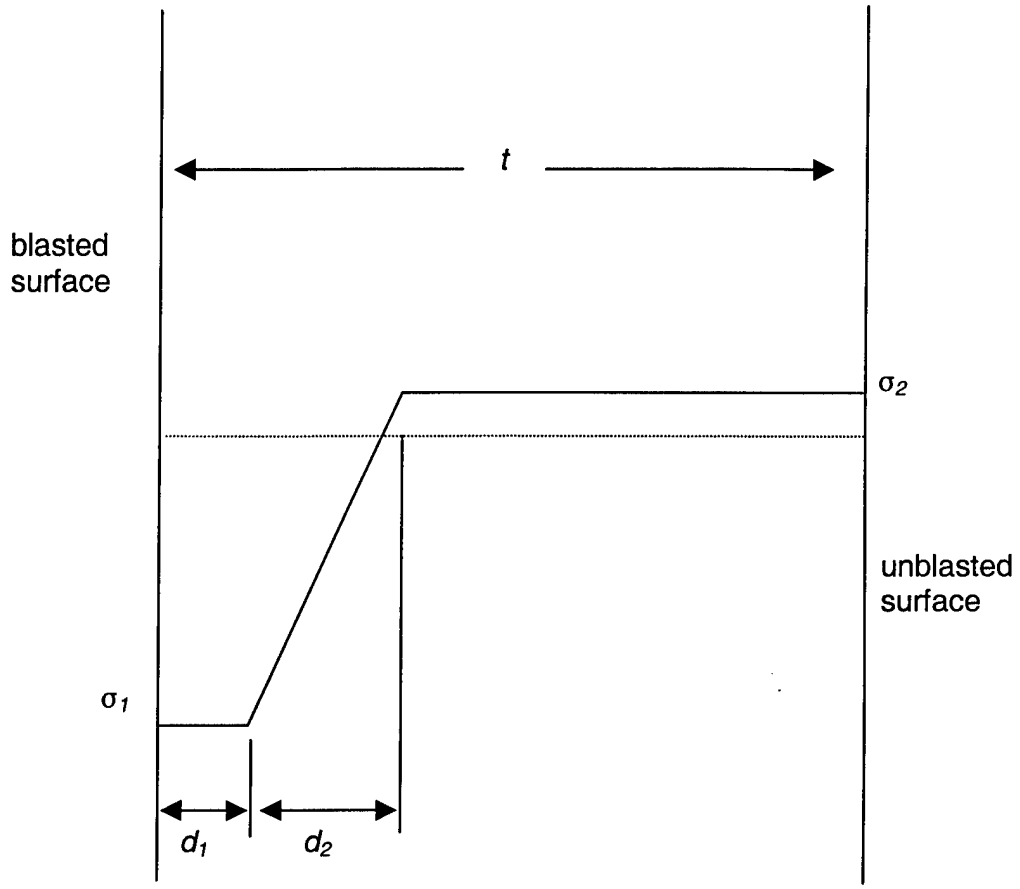

Figure B-3. Idealized Residual Stress Profile for Thin Aluminum Sheets Following Plastic Media Blasting.

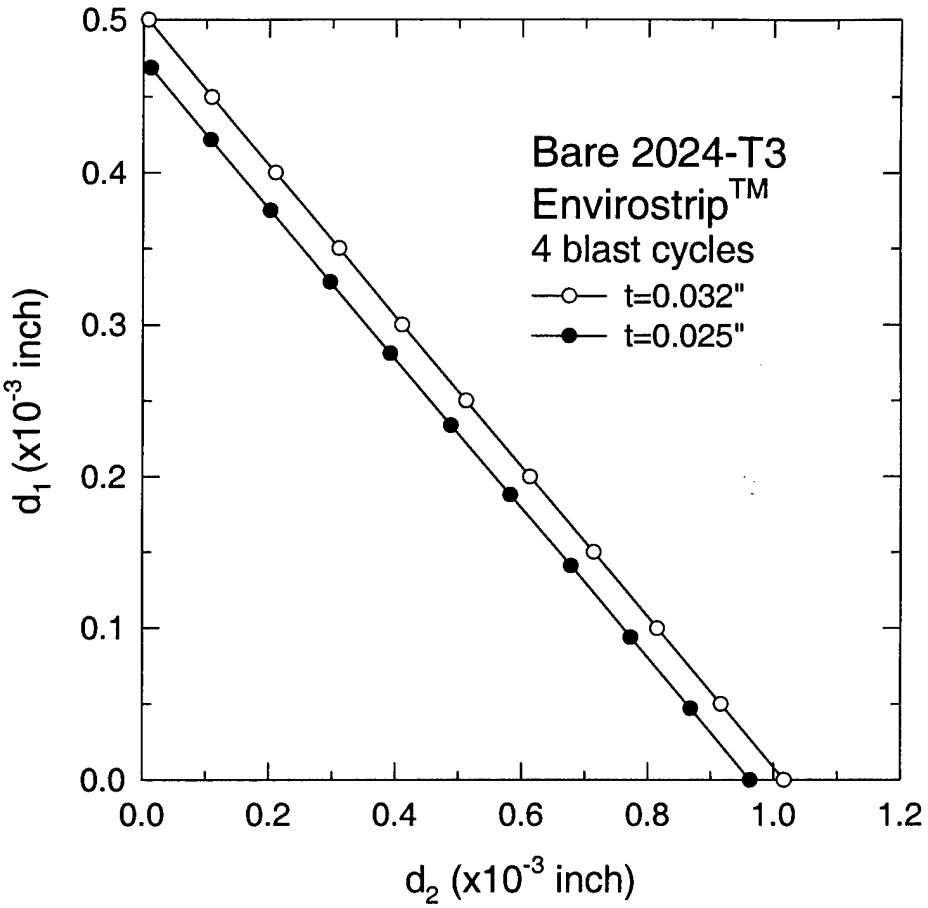

Figure B-4. Estimated Dimensions of Residual Stress Profile in Two Thicknesses **of A/ 2024-T3 Sheet Following Envirostrip™ Blasting**

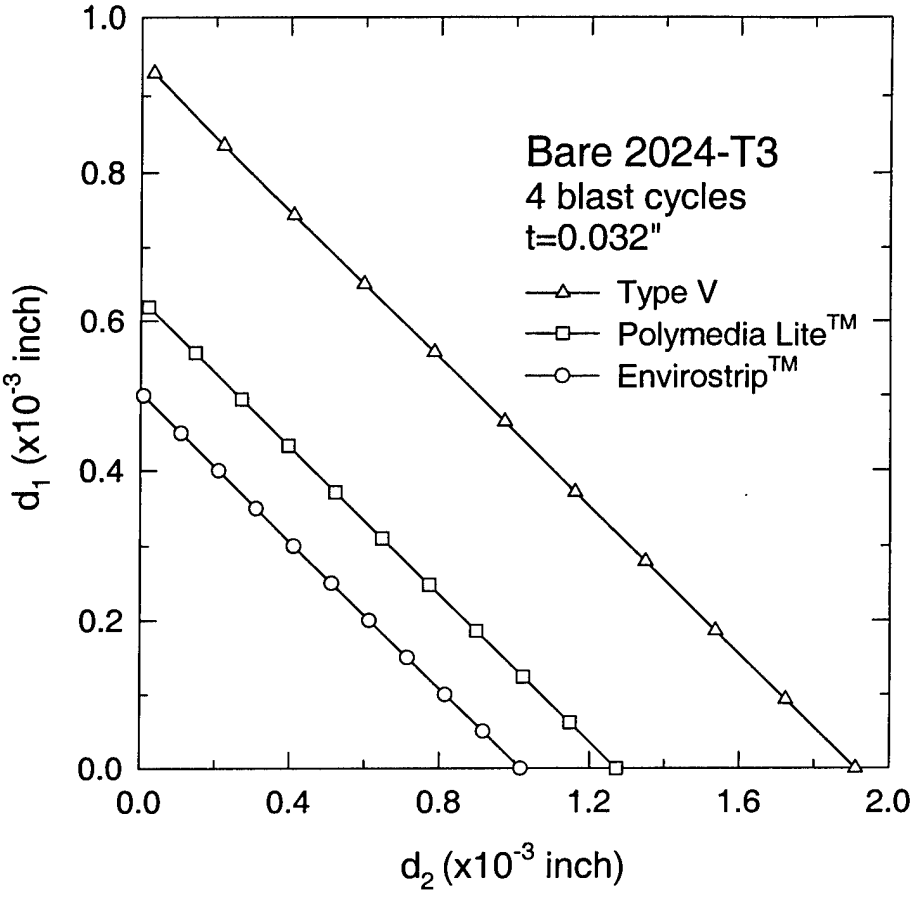

Figure B-5. Estimated Dimensions of Residual Stress in A/ 2024-T3 Sheet **Following Blasting by Three Different Media**

References

[B1] B. Spigel and T. Whitney, "Material Characteristics of Plastic Media Blasting (PMB) of Thin-Skinned Aluminum Substrates," *Proceedings of the 1995 DoD/Industry Advanced Coatings Removal Conference*, Albuquerque, NM, May 1995.

[B2] B. Spigel and J. Buckingham, "Material Characteristic Study for Polymedia-Lite™, Blasting Media," Coatings Technology Inegration Office, WPAFB, Ohio, September 1996.

[B3] B. Spigel, J. Buckingham, and C. McClung, "Evaluation of Type V, Polymedia-Lite, and Envirostrip for Depainting 0.025-inch 2024-T3 Aluminum Alloy," Draft Final Report, Coatings Technology Integration Office, January 1999.

[B4] *Shot-peening Applications*, 7th Edition, Metal Improvement Company, n.d.

[B5] *Proceedings, Sixth International Conference on Shot-peening*, San Francisco, California, J. Champaigne, Editor, 1996.

[B6] R. Fathallah, G. Inglebert, and L. Castex, "Modelling of Shot-peening Residual Stresses and Plastic Deformation Induced in Metallic Parts," Proc. 6th Int. Conf. Shot-peening, San Francisco, 1996, pp 464-473.

[B7] P. K. Sharp, J. Q. Clayton, and G. Clark, "The Fatigue Resistance of Peened 7050-T7451 Aluminum Alloy—Repair and Re-Treatment of a Component Surface," *Fatigue and Fracture of Engineering Materials and Structures*, Vol. 17, 1994, pp. 243-252.

[B8] Y. Mutoh, G. H. Fair, B. Noble, and R. B. Waterhouse, "The Effect of Residual Stresses Induced By Shot-Peening on Fatigue Crack Propagation in Two High Strength Aluminum Alloys," Fatigue and Fracture of Engineering Materials and Structures, Vol. 10, 1987, pp. 261-272.

[B9] U. Martin, I. Altenberger, B. Scholtes, K. Kremmer, and H. Oettel, 'Characterization of the Defect Depth Profile of Shot-peened Steels by Transmission Electron Microscopy," Proc. 6th Int. Conf. Shot-peening, San Francisco, 1996, pp. 142-153.

[B10] K. Iida and K. Taniguchi, "Relaxation of Residual Stress Distribution Produced by Shot-peening Under Fatigue Test," Proc. 6th Int. Conf. Shot-peening, San Francisco, 1996, pp. 397-402.

[B11] V. Schulze, K.-H. Lang, O. Vohringer, and E. Macherauch, "Relaxation of Shot-peening Induced Residual Stresses in Quenched and Tempered Steel AISI 4040 Due to Uniaxial Cyclic Deformation," Proc. 6th Int. Conf. Shot-peening, San Francisco, 1996, pp. 403-412.

[B12] H. Holzapfel, V. Schulze, O. Vohringer, and E. Macherauch, "Stability and Relaxation Behavior of Shot-peening Induced Residual Stresses in AISI 4040 During Bending Fatigue," Proc. 6th Int. Conf. Shot-peening, San Francisco, 1996, pp. 413-423.

[B13] Y. Oshida and J. Daly, "Fatigue Damage Evaluation of Shot-peened High Strength Aluminum Alloy," *Proc. Int. Conf. Surface Engineering*, Elsevier, 1990, pp. 404-416.

[B14] D. W. Hammond and S. A. Meguid, "Fatigue Fracture and Residual Stress Relaxation in Shot-Peened Components," *Proc. Int. Conf. Surface Engineering*, Elsevier, 1990, pp. 386-392.

[B15] L. Wagner and C. Mueller, "Effect of Shot-peening Behavior on Fatigue Behavior in Al-Alloys," *Materials and Manufacturing Processes*, Vol. 7, 1992, pp. 423-440.

[B16] J. E. Hatch, *Aluminum: Properties and Physical Metallurgy*, ASM International, 1984.